

# **Understanding novel aspects of bone metabolism and fracture healing**

Submitted by

**Rhys Brady**

B.Sc. Hons (Nutrition)

A thesis submitted in total fulfilment  
of the requirements for the degree of  
Doctor of Philosophy

College of Science, Health and Engineering

School of Life Sciences

Department of Physiology, Anatomy and Microbiology

La Trobe University  
Bundoora, Victoria 3086  
Australia  
September 2016

## Abstract

Long bone fractures and their associated complications are a major health issue. Although there are several molecular therapies currently used clinically to promote healing the development of safer and more effective interventions is an important goal. Thymosin beta 4 ( $T\beta_4$ ) is a regenerative peptide that was hypothesized to promote healing of fractured bone. The first experiments of this thesis revealed that  $T\beta_4$  treatment in mice enhanced mechanical properties and increased bone volume density (BV/TV) of the fracture callus, which provided novel evidence of the therapeutic potential of this peptide for treating bone fractures. Subsequent studies found that neither  $T\beta_4$  nor shorter peptide sequences of  $T\beta_4$  had any effect on proliferation, differentiation or mineralization of osteoblast-like cells *in vitro*, which possibly indicated that healing was enhanced via alternate processes.

Traumatic brain injury (TBI) has long been associated with enhanced fracture healing, however, despite these associations the relationship between TBI and bone metabolism as well as fracture healing remains poorly understood. Therefore, the next set of experiments investigated the influence of TBI on bone homeostasis in a rat model. Analysis revealed significant systemic bone loss with reductions in cortical and trabecular bone volume at the distal metaphyseal region of rat femora post-TBI. Additional experiments indicated that these reductions in bone volume were attenuated in rats treated with sodium selenate (a potential TBI treatment), however, femora from selenate-treated groups were shorter. These results suggest a link between TBI and altered bone remodelling. Finally, in order to investigate the effect of TBI on fracture healing, a novel trauma model featuring closed-skull weight-drop TBI and concomitant tibial fracture was developed in mice. Fracture calluses from brain-injured mice had a greater bone and total volume and displayed higher mean polar moment of inertia than controls, which indicated that TBI induced the formation of a more robust callus. The findings from this thesis will improve the understanding of the effect of TBI on bone and

bone regeneration and allow a better understanding of the complex nature of combined traumatic injuries.

## **Statement of authorship**

This thesis includes work by the author that has been published or accepted for publication as described in the text.

Except where reference is made in the text of the thesis, this thesis contains no other material published elsewhere or extracted in whole or in part from a thesis accepted for the award of any other degree or diploma.

No other person's work has been used without due acknowledgment in the main text of the thesis. This thesis has not been submitted for the award of any degree or diploma in any other tertiary institution

All research procedures reported in the thesis were approved by the relevant Ethics Committee, Safety Committee or authorised officer

Rhys Brady 28/09/2016

## **Acknowledgements**

To my friend and principal supervisor, Brian Grills. Thank you for persevering with me, even though I placed your honours project down the bottom of my preference list and for three weeks ignored your phone calls as you tried to invite me to do your project. I am glad that I finally answered the call. I have learnt so much from being under your tutelage, never to bet on anything that can talk and that sometimes there are more important things in life than remembering molecular pathways, like being able to remember the final score of the 1977 drawn grand final. In all seriousness, I have thoroughly enjoyed coming to uni each morning and am forever grateful for all of your time, effort and support.

To my supervisor Stuart McDonald. Thank you for staying back late with me and teaching me stats, for picking me up early and driving me to Melbourne Uni so we could do surgery all day and into the night. You have taught me a great deal about science but even more about life, like the importance of having a PhD student at conferences with you to hang your poster up before the first session because the hops in the beer from the night before has made you feel “unwell”. Your support and encouragement over the years has been greatly appreciated. You have shown incredible faith in me and I am forever grateful.

To my supervisor Jarrod Church. It was a privilege to have someone of your calibre in the lab and to be able to ask questions and get assistance from. The little tips, tricks and shortcuts I learnt from you in the lab are invaluable and are much appreciated

I would also like to thank my friend and mentor, Sandy Shultz, I have learnt so much about how to write, design experiments and what it takes to be a productive researcher from sharing a quiet drink and a stogie with you. You have demonstrated the work ethic required to be successful and taught me a number of valuable lessons.

I would like to extend my thanks to Nicole Walsh for teaching me how to run  $\mu$ CT scans and analysis. It was a pleasure working with you and nice to know you were always there for advice whenever I needed it.

I also thank, Tania Romano for your assistance with the pQCT scans and showing me the best ways to snag a park at Melbourne Uni.

I would like to thank Julian Quinn and Damian Eeles for teaching me the basics of culturing osteoblastic and osteoclastic cells. In my short stay at Prince Henry's I learnt a great deal about molecular biology had had ball learning it from you both.

I would also like to extend my thanks to all the staff from the department of Human Biosciences. In particular Karen Griggs, John Schuijers, Tom Samiric, Alex Ward, Amy Larsen, Chris van der Poel and Aaron McDonald for your assistance with my experiments. Thank you to Paul Moon for your technical support, I thoroughly enjoyed being able to have a laugh with you in the morning.

I would also like to acknowledge the past and present students and demonstrators, particularly Karlene Scheller, Heath McGowan, Belinda Ash, Stuart James, Kristina Anevaska, Maddie Johnstone Yeukai Mangwiro and Jordanna Master it has been a pleasure to at some stage have shared an office with you. Thanks for your friendship and technical assistance.

To my loving family, Mum, Dad and Shelby. Thank you for your encouragement support and belief in me.

*In memory of my great uncle, Alex Fraser (09/01/1930-14/8/2013)*

## Abbreviations

%	Percentage
<	Less than
=	Equals
>	Greater than
±	Plus minus
×	Multiply
°C	Degrees Celsius
α	Alpha
α-MEM	Minimal essential media alpha
ALP	Alkaline phosphatase
ATP	Adenosine triphosphate
β	Beta
BBB	Blood brain barrier
BMD	Bone mineral density
BMP	Bone morphogenetic protein
BMUs	Basic multicellular units
BV	Bone volume
BV/TV	Bone volume fraction
CART	Cocaine and amphetamine regulated transcript
Col	Collagen
CSA	Cross-sectional area
Da	Daltons
DMP-1	Dentin matrix protein 1
EGF	Epidermal growth factor

FBS	Foetal Bovine Serum
FDA	Food and Drug Administration
FGF	Fibroblast growth factor
FPI	Fluid percussion injury
GH	Growth hormone
h	Hour
HIF-1 $\alpha$	Hypoxia inducible factor
HMTV <sub>c</sub>	New highly mineralized tissue volume of callus
HMTV <sub>c</sub> /TV <sub>c</sub>	Fractional volume of new highly mineralized tissue
HUVEC	Human umbilical vein endothelial cells
ICAM-1	Intercellular Adhesion Molecule 1
IGF-1	Insulin growth factor
IL	Interleukin
ILK	Integrin-linked kinase
i.p.	Intraperitoneal
LM-5	Laminin-5
miR	MicroRNA
M-CSF-1	Macrophage colony stimulating factor
g	Grams
l	Litre
m	Milli-
min	Minutes
MMI	Mean polar moment of inertia
MMPs	Matrix metalloproteinases
mRNA	Messenger ribonucleic acid

MTVc	Mineralized tissue volume of callus
MTVc/TVc	Fractional volume of new mineralized tissue
NFκB	Nuclear factor kappa-light-chain-enhancer of activated B cells
NGF	Nerve growth factor
NHO	Neurological heterotopic ossification
OCN	Osteocalcin
OPCs	Osteoprogenitor cells
OPG	Osteoprotegerin
Osx	Osterix
PDGF	Platelet-derived growth factor
pH	$-\log_{10}[\text{H}^+]$
PMNs	Polymorphonuclear leukocytes
PP2A	Protein phosphatase 2A
PR55	PR55 regulatory B-subunit
RANK	Receptor activator of nuclear factor-kappa β
RANKL	Receptor activator of nuclear factor κβ ligand
ROS	Reactive oxygen species
RPPM	Reverse phase protein microarray
Runx2	Runt-related transcription factor 2
s	Second
SIRS	Systemic inflammatory response syndrome
T.Ar	Mean tissue area
TBI	Traumatic brain injury
TGF-β	Transforming growth factor-β
TNF-α	Tumor necrosis factor alpha

Total.Ar	Total area
Trab.Ar	Area of trabecular bone
TRAP	Tartrate-resistant acid phosphatase
TV	Total volume
TVc	Total volume of callus
T $\beta$ <sub>4</sub>	Thymosin beta 4
Tph2	Tryptophan hydroxylase 2
$\mu$	Micro
VEGF $\alpha$	Vascular endothelial growth factor alpha

## Publications

### Articles published or accepted to refereed journals

**Brady R.D.**, Grills B.L., Church J.E., Walsh N.C., McDonald A.C., Agoston D.V., Sun M., O'Brien T.J., Shultz S.R and McDonald S.J. Closed head experimental traumatic brain injury increases size and bone volume of callus in mice with concomitant tibial fracture. *Scientific Reports* (2016) 6 34491.

**Brady R.D.**, Shultz S.R., Sun M., Romano T., van der Poel C., Wright D.K., Wark J.D., O'Brien T.J., Grills B.L and McDonald S.J. Experimental traumatic brain injury induces bone loss in rats. *Journal of Neurotrauma* (2016) 1;33 23 2154-60.

Wright D., Liu, S., van der Poel C., Taylor L., McDonald S.M., **Brady R.D.**, Ordidge R., O'Brien T.J., Johnston L and Shultz S.R. *Traumatic brain injury results in cellular, structural, and functional changes resembling motor neuron disease*. *Cerebral Cortex* (2016).

**Brady R.D.**, Grills B.L., Romano T., Wark J.D., O'Brien T.J., Shultz S.R and McDonald S.J. Sodium selenate treatment mitigates reduction of bone volume following traumatic brain injury in rats. *Journal of Musculoskeletal and Neuronal Interactions* (2016) 16 4 369-76.

Shultz S.R., Sun M., Wright D.K., **Brady R.D.**, Liu S., Beynon S., Schmidt S.F., Kaye A.H., Hamilton J.A., O'Brien T.J., Grills B.L and McDonald S.J. Tibial fracture exacerbates traumatic brain injury outcomes and neuroinflammation in a novel mouse model of multitrauma. *The Journal of Cerebral Blood Flow & Metabolism* (2015) 35 8 1339-1347

**Brady R.D.**, Grills B.L., Schuijers J.A., Ward A.R., Tonkin B.A., Walsh N.C and McDonald S.J. Thymosin beta 4 administration enhances fracture healing in mice. *Journal of Orthopaedic research* (2014) 32 10 1277-82.

### Conference presentations

**Brady R.D.**, Grills B.L., Church J. E., Walsh N.C., Sun M., O'Brien T.J., Shultz S.R and McDonald S.J. Closed-head experimental traumatic brain injury promotes fracture healing in mice. (2016). National Neurotrauma Symposium, Lexington, Kentucky, June 2016. (Poster 105)

McDonald S.J., Sun M., **Brady R.D.**, Liu S., Semple B.D., O'Brien T.J and Shultz S.R. The effects of interleukin-1 receptor antagonist treatment in an animal model of multitrauma. (2016). National Neurotrauma Symposium, Lexington, Kentucky, June 2016. (Poster 133)

**Brady R.D.**, Shultz S.R., Sun M., Romano T., Wright D., Wark J.W., O'Brien T.J., Grills B.L and McDonald S.J. (2015). Sodium selenate treatment ameliorates bone loss in the femoral distal metaphysis following traumatic brain injury in rats. Australian New Zealand Bone & Mineral Society Annual Scientific Meeting, Hobart, November 2015. (Plenary Poster).

Johnstone M., **Brady R.D.**, Schuijers J., McDonald S.J and Grills B.L. (2015). Effects of the specific trkA receptor agonist, gambogic amide, on fracture healing in mice: a pilot study.

Australian New Zealand Bone & Mineral Society Annual Scientific Meeting, Hobart, November 2015.

**Brady R.D.**, Shultz S.R., Grills B.L and McDonald S.J. (2015). The effect of traumatic brain injury on bone and fracture healing in a mouse model. 6th Annual Australian Neurotrauma Forum, Adelaide, October 2015. Oral.

Sun M., Wright, D.K., **Brady R.D.**, Liu S., Beynon S., Schmidt S.F., Kaye A.H., Hamilton J.A., O'Brien T.J., Grills B.L., McDonald S.J and Shultz S.R. (2015). Tibial fracture exacerbates traumatic brain injury outcomes and neuroinflammation in a novel mouse model of multi-trauma. 6th Annual Australian Neurotrauma Forum, Adelaide, October 2015.

**Brady R.D.**, Shultz S.R., Sun, M., Romano T., Wright, D.K., Wark J.D., O'Brien T.J., Grills B.L and McDonald S.J. (2015) Experimental traumatic brain injury: Bad to the bone? Canadian Association of Neuroscience, Vancouver, Canada 2015. May 2015.

**Brady R.D.**, Grills B.L., Romano T., Wark J.D., O'Brien T.J., Shultz S.R and McDonald S.J. (2014). Traumatic brain injury is detrimental to bone microstructure. 5th Annual Australian Neurotrauma Symposium, Adelaide October 2014.

Beynon S., Schmidt S.F., **Brady R.D.**, McDonald S.J and Shultz S.R. (2014). Does multitrauma worsen outcome of traumatic brain injury? 5th Annual Australian Neurotrauma Symposium, Adelaide October 2014.

**Brady R.D.**, Grills B.L., Romano T., McGowan H.W., McDonald A.C., O'Brien T.J., Shultz S.R and McDonald S.J. (2014). Influence of experimental traumatic brain injury on bone. Proc. ANZBMS. Poster 75

**Brady R.D.**, McDonald S.J., Grills B.L., Schuijers J.A., Ward A.R., Tonkin B.A., Walsh N.C and Grills B.L. (2014). Thymosin  $\beta$ 4 enhances mechanical and morphological properties of healing murine fractures. Proc. ANZBMS. Oral 19.

**Brady R.D.**, Grills B.L., van der Poel C., Romano T., O'Brien T.J., Shultz S.R and McDonald S.J. (2013). Influence of experimental traumatic brain injury on bone. 4th Australian Neurotrauma Symposium.

van der Poel C., Dankha A., **Brady R.D.**, McDonald S.J., Wright D.K., O'Brien T.J and Shultz S.R. (2013). Influence of experimental brain injury on skeletal muscle function. 4th Australian Neurotrauma Symposium.

**Brady R.D.**, McDonald S.J., Schuijers J.A., Ward A.R and Grills B.L. (2012). Thymosin  $\beta$ 4 administration enhances the biomechanical properties of healing mouse fractures. Proc. Asia Pacific Bone and Mineral Society Meeting and ANZBMS, Plenary poster 5.

**Brady R.D.**, McDonald S.J., Schuijers J.A., Ward A.R & Grills B.L. (2012). Thymosin  $\beta$ 4 administration enhances fracture healing in mice. 7<sup>th</sup> Clare Valley bone meeting 23-26 March 2012. Oral.

## Contents

Understanding novel aspects of bone metabolism and fracture healing .....	i
Abstract .....	ii
Abbreviations.....	viii
List of Figures.....	xvii
List of Tables .....	xix
1 Literature review .....	1
1.1 Introduction .....	2
1.2 Bone .....	3
1.2.1 Bone structure.....	3
1.2.2 Cortical bone .....	4
1.2.3 Trabecular bone .....	5
1.3 Bone cells .....	5
1.3.1 Osteoprogenitor cells .....	5
1.3.2 Osteoblasts.....	6
1.3.3 Osteocytes .....	7
1.3.4 Osteoclasts.....	8
1.4 Bone remodelling.....	9
1.4.1 Bone remodelling disorders.....	11
1.5 Long bone growth.....	14
1.6 Biology of bone fracture healing .....	14
1.6.1 Inflammatory phase .....	15
1.6.2 Soft callus formation.....	16
1.6.3 Hard callus formation.....	17
1.6.4 Callus remodelling .....	18
1.7 Thymosin $\beta_4$ ( $T\beta_4$ ).....	20
1.7.1 Physical properties of $T\beta_4$ .....	20
1.7.2 Mechanisms of action .....	21
1.7.3 The possible effects of $T\beta_4$ on fracture healing .....	26
1.8 Traumatic brain injury (TBI).....	29

1.8.1	Potential effect of TBI on bone .....	32
1.8.2	Potential effect of TBI on bone fracture healing .....	33
1.8.3	Treatment.....	35
1.9	Summary and aims.....	37
2	The effect of T $\beta$ <sub>4</sub> treatment on fracture healing in a murine model.....	39
2.1	Introduction .....	40
2.2	Methods.....	41
2.2.1	Animal surgery and T $\beta$ <sub>4</sub> treatment.....	41
2.2.2	Biomechanical assessment .....	42
2.2.3	$\mu$ CT .....	43
2.2.4	Histological processing, staining and histomorphometry .....	44
2.3	Results .....	45
2.3.1	Mechanical testing .....	45
2.3.2	$\mu$ CT analyses .....	46
2.3.3	Histology and Histomorphometric Analysis .....	47
2.4	Discussion.....	51
3	The influence of T $\beta$ <sub>4</sub> treatment on proliferation, differentiation and mineralization of osteoblast-like cells .....	54
3.1	Introduction .....	55
3.2	Materials and methods .....	57
3.2.1	Animal surgery and T $\beta$ <sub>4</sub> treatment.....	57
3.2.2	RT-PCR of fracture calluses.....	57
3.2.3	Cells and reagents .....	58
3.2.4	Cell proliferation assay .....	58
3.2.5	RT-PCR of Kusa-O cells.....	59
3.2.6	Alkaline phosphatase (ALP) assay .....	60
3.2.7	Mineralization assay .....	60
3.2.8	Statistical analyses .....	60
3.3	Results .....	61
3.3.1	RT-PCR.....	61
3.3.2	Cell proliferation assay .....	64
3.3.3	Alkaline phosphatase assay .....	64

3.3.4	Mineralization assay .....	64
3.4	Discussion.....	66
4	The effect of experimental traumatic brain injury on bone.....	71
4.1	Introduction .....	72
4.2	Methods.....	74
4.2.1	Subjects .....	74
4.2.2	Experimental Groups .....	74
4.2.3	Injury procedure.....	74
4.2.4	Acute assessment of injury severity.....	75
4.2.5	Open-field testing .....	75
4.2.6	Peripheral quantitative computed tomography (pQCT).....	75
4.2.7	Histological processing, staining, and histomorphometry .....	76
4.2.8	Mechanical testing .....	76
4.2.9	Statistical analyses .....	77
4.3	Results .....	79
4.3.1	Acute Injury Severity Measures .....	79
4.3.2	Locomotor Activity.....	79
4.3.3	pQCT.....	79
4.3.4	Histologic and histomorphometric analysis .....	81
4.3.5	Mechanical testing .....	81
4.4	Discussion.....	84
5	The effect of sodium selenate treatment on traumatic brain injury-induced bone loss in rats	87
5.1	Introduction .....	88
5.2	5.2 Materials and Methods .....	90
5.2.1	Subjects .....	90
5.2.2	Experimental groups .....	90
5.2.3	Surgery and FPI .....	90
5.2.4	Acute injury severity.....	91
5.2.4	Open-field testing .....	91
5.2.5	pQCT.....	91
5.2.6	Histological processing, staining, and histomorphometry .....	91

5.2.7	Mechanical testing .....	91
5.2.8	Statistical analyses .....	91
5.3	Results .....	93
5.3.1	Acute injury severity .....	93
5.3.2	Locomotor Activity .....	93
5.3.3	Histologic and histomorphometric analysis .....	94
5.3.4	pQCT .....	94
5.3.5	Mechanical testing .....	94
5.4	Discussion .....	98
6	The effect of closed-head traumatic brain injury on fracture healing in mice .....	102
6.1	Introduction .....	103
6.2	Materials and methods .....	105
6.2.1	Mice .....	105
6.2.2	Experimental Groups .....	105
6.2.3	Tibial Fracture .....	105
6.2.4	Closed-skull weight-drop model of TBI .....	106
6.2.5	Acute assessment of injury severity .....	107
6.2.6	$\mu$ CT .....	107
6.2.7	Histological processing, staining, and histomorphometry .....	108
6.2.8	Statistical analyses .....	108
6.3	Results .....	109
6.3.1	$\mu$ CT .....	109
6.3.2	Histology and histomorphometric analysis .....	109
6.4	Discussion .....	114
7	Conclusions and future directions .....	119
7.1	T $\beta$ 4 and bone healing .....	120
7.2	Influence of TBI on bone homeostasis and fracture healing .....	123
	References .....	129
8	Appendices .....	163
8.1	Appendix A, Declaration of contribution .....	163

## List of figures

Figure 1.1. Cross-sectional view of long bone structure.....	4
Figure 1.2. Osteoblasts and osteocytes controlling osteoclastic differentiation.....	13
Figure 1.3. The sequence of a simple, healing long bone fracture..	19
Figure 1.4. Proposed T $\beta$ 4 signalling .....	24
Figure 1.5. Possible pathways through which TBI may alter bone metabolism .....	37
Figure 2.1. Longitudinal, mid-point views of representative $\mu$ CT 3D reconstructions .....	49
Figure 2.2. Histomorphometric analysis of bone parameters at 14 and 21 days. ....	50
Figure 3.1. Gene expression in 7, 14, and 21 day-fracture callus. ....	61
Figure 3.2. mRNA levels of early stage markers of osteoblastic differentiation.....	62
Figure 3.3. mRNA levels of osteoblastic differentiation markers .....	63
Figure 3.4. The effect of T $\beta$ 4, 1-4, 1-15 and 17-23 treatment on proliferation, differentiation (ALP activity) and mineralization. ....	65
Figure 4.1. Distance travelled in an open-field.....	79
Figure 4.2. pQCT analysis of bone parameters .....	80
Figure 4.3. Representative longitudinal histological sections of distal metaphyseal region of femora.....	82
Figure 5.1. Distance travelled in an open-field.....	93
Figure 5.2. Longitudinal histological sections of the distal metaphyseal region of femora... 95	
Figure 5.3. pQCT analysis of bone parameters of femora. ....	96
Figure 6.1. Tibial fracture of the mid-diaphysis..	106
Figure 6.2. Longitudinal midpoint views of $\mu$ CT reconstructions of hemi-calluses .....	111
Figure 6.3. Histological sections of undecalcified calluses from FX and MULTI mice .....	112
Figure 6.4. Histological sections of undecalcified calluses stained for TRAP.....	113

## List of Tables

Table 2.1. Mechanical characteristics of control and T $\beta$ <sub>4</sub> -treated samples at 42 days post-fracture.....	46
Table 2.2. $\mu$ CT analysis of control and T $\beta$ <sub>4</sub> -treated calluses at 14 and 21 days post-fracture.	48
Table 3.1. RT-PCR primer sequences.....	59
Table 4.1. Mechanical characteristics of sham and TBI samples at 1 and 12 weeks post-injury. ....	83
Table 5.1. Acute injury severity measures. ....	93
Table 5.2. Biomechanical characteristics of sham-vehicle, sham-selenate, FPI-vehicle and FPI-selenate femoral samples. ....	97
Table 6.1. Acute injury severity measures .....	107

# **1 Literature review**

## 1.1 Introduction

Fractures and their associated complications are a major health issue, with treatment becoming increasingly expensive and complex. By 2022, the total financial cost relating to fracture is predicted to be \$2.59 billion in Australia.<sup>1, 2</sup> Recent reports indicate that up to 25% of patients with femoral and tibial shaft fractures develop delayed union or non-union,<sup>3, 4</sup> and that the total care cost of these patients is almost double that of patients without non-union, which represents a significant economic burden.<sup>2, 5</sup> In addition, delayed healing often requires patients to have multiple surgeries that are frequently associated with a range of symptoms that include ongoing pain, swelling and stiffness; all of which can prevent weight-bearing in the affected limb.<sup>6</sup> Therefore, an increasing number of human and animal studies have been undertaken to further understand the cellular and molecular mechanisms involved in fracture healing. The aim of the present studies is to develop therapeutic strategies that enhance this regenerative process and reduce the time taken to return to pre-injury activity, as well as reduce the risk of complications such as non-union. Currently the only FDA approved molecular therapy for bone healing is localized bone morphogenetic protein 2 (BMP-2) treatment, however both the clinical and cost effectiveness of this therapy remains controversial.<sup>7</sup> While other molecular therapies including BMP-7,<sup>8</sup> bisphosphonates,<sup>9</sup> fibroblast growth factor (FGF-2),<sup>10</sup> platelet-derived growth factor (PDGF),<sup>11</sup> parathyroid hormone 1-34 (PTH 1-34)<sup>12</sup> and PTH 1-84,<sup>13</sup> have been used to promote fracture healing there is a need for safer and more effective therapeutic interventions to enable or enhance fracture healing.<sup>14</sup> Numerous clinical and animal studies have demonstrated that thymosin beta 4 (T $\beta$ <sub>4</sub>), a multifunctional peptide, promotes tissue healing, however, the influence T $\beta$ <sub>4</sub>-treatment has on fracture healing is unknown.<sup>15-18</sup> The first part of this review will focus on the potential of T $\beta$ <sub>4</sub> to promote fracture healing.

In a clinical setting, traumatic brain injury (TBI) has long been associated with enhanced fracture healing, however, despite these associations, the relationship between TBI and intact and fractured bone, as well fracture healing remains poorly understood but is important to consider, given that the incidence of TBI and TBI and concomitant fracture is on the rise.<sup>19</sup> Therefore, the second part of this review will discuss TBI with a focus on how this multifaceted disorder has the potential to alter bone microarchitecture.

There is currently no pharmaceutical intervention that improves long-term outcome for TBI patients.<sup>20</sup> However, recent experiments have demonstrated that sodium selenate treatment significantly reduced brain damage and behavioural impairments in rats given a TBI.<sup>21</sup> Therefore, this review will focus on i). how sodium selenate (a potential TBI treatment) may influence any TBI-induced changes to bone remodelling; and ii). the potential of sodium selenate or sodium selenate metabolites to have deleterious effects on skeletal cells, which should be considered, as the use of sodium selenate as a treatment progresses towards clinical trials in TBI patients. Lastly, this review will discuss the phenomenon of TBI enhancing fracture healing and the incongruities that exist in the current literature relating to the effect of TBI on bone healing.

## **1.2 Bone**

### **1.2.1 Bone structure**

Bone is a dynamic connective tissue that is constantly being resorbed and re-formed in order to maintain its structural integrity. It plays a critical role in the maintenance of blood calcium levels, haematopoiesis, locomotion and organ protection.<sup>22</sup> The mineral phase of bone is comprised of hydroxyapatite crystals, which are attached to a proteinaceous matrix that is composed predominantly of type I collagen.<sup>22, 23</sup> The arrangement of collagen fibrils is irregular in immature (woven) bone, which is formed rapidly during embryonic development as well as following bone fracture.<sup>22, 23</sup> This woven bone is ultimately remodelled to form

dense, mechanically superior, lamellar bone that is composed of hydroxyapatite crystals deposited on tightly organised collagen fibrils.<sup>22, 24</sup>

Long bones, the focus of this thesis, are comprised of a metaphysis below the growth plates and a rounded epiphysis above the growth plates, at either end of a tubular diaphysis (Figure 1.1).<sup>24</sup> The diaphysis is comprised of a thick, dense type of bone known as cortical bone, whereas the metaphysis and epiphyses are surrounded by a thinner layer of cortical bone but are primarily comprised of porous trabecular bone.<sup>24</sup> Cortical and trabecular bone differ in their location and density but also their function.<sup>25</sup>

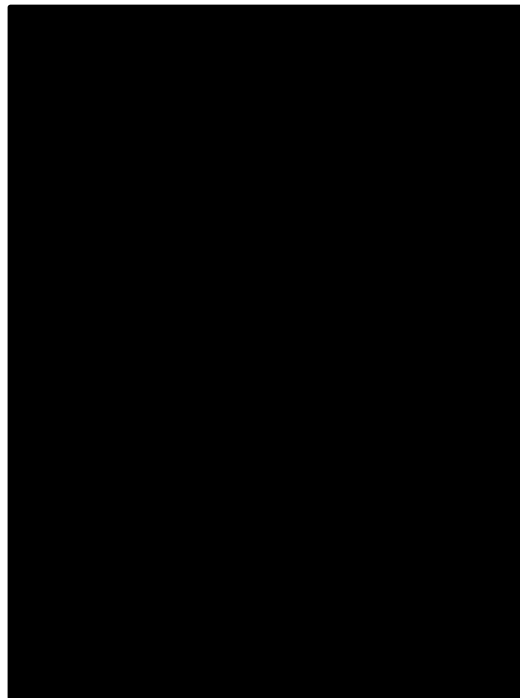


**Figure 1.1.** Cross-sectional view of long bone structure.

### **1.2.2 Cortical bone**

Located at the cortices of all bones, cortical bone is thought to be much more dense than its trabecular counterpart, it therefore has a high resistance to torsion and bending.<sup>24</sup> Cortical bone makes up 80% of the skeleton and is composed of functional units known as osteons that run parallel to each other down the long axis of bone.<sup>25, 26</sup> Osteons are made up of lamellae (mineralized collagen fibrils organised into planar sheets) wrapped in concentric

layers surrounding a canal (Haversian canal) that contains nerves and blood vessels.<sup>25, 26</sup> Encompassing the cortical bone lies an outer membrane referred to as the periosteum.<sup>27</sup>

### **1.2.3 Trabecular bone**

Trabecular bone is also composed of lamellar bone, however, it is thought to be more porous and hence less dense than cortical bone.<sup>22</sup> Representing 20% of skeletal mass but 80% of the skeletal surface,<sup>25</sup> trabecular bone is composed of interconnecting trabeculae and marrow filled cavities, with a rich supply of blood vessels.<sup>22</sup> This porous composition and therefore large surface to volume ratio, together with the high blood supply, allows rapid and constant remodelling of trabecular bone.<sup>24</sup> Accordingly, pathological or physiological enhancement of bone resorption typically has greater effects on trabecular bone than cortical bone.

## **1.3 Bone cells**

Bone formation during developmental and healing processes requires the co-ordinated involvement of a number of cell types that reside in the cortex, periosteum, bone marrow and surrounding muscle.<sup>28</sup> The primary bone cells responsible for bone homeostasis are osteoblasts, osteoclasts and osteocytes. Osteoblasts and osteoclasts are found on bone surfaces and are responsible for bone formation and resorption respectively, whereas osteocytes are the most abundant bone cell and reside within bone. Osteoblasts and osteocytes are derived from mesenchymal stem cells known as osteoprogenitor cells (OPCs), whereas osteoclasts are derived from cells of the monocytic/macrophagic lineage.<sup>28</sup> The actions and interactions of these cells will be detailed below.

### **1.3.1 Osteoprogenitor cells**

OPCs have the ability to differentiate into cells that exhibit either osteoblastic or chondrocytic phenotypes, depending upon the microenvironment and the presence of particular growth and gene transcription factors.<sup>29, 30</sup> OPCs are located in the cambium layer

of the periosteum, within bone marrow, external soft tissue (such as skeletal muscle) and blood vessel walls.<sup>29, 30</sup>

There are two mechanisms through which OPCs can influence bone formation. Firstly, OPCs differentiate into pre-osteoblasts, which then directly differentiate into osteoblasts, which form bone, in a process known as intramembranous ossification.<sup>31</sup> The second mechanism of bone formation is a process known as endochondral ossification, where OPCs differentiate into chondrocytes, which form cartilage that later mineralizes and acts as a template upon which osteoblasts form bone.<sup>32</sup>

### **1.3.2 Osteoblasts**

Osteoblasts are primarily bone forming cells, however, they also perform a array of other functions.<sup>33</sup> These cuboidal cells possess morphological characteristics that allow them to synthesize large amounts of extracellular proteins i.e. sizeable endoplasmic reticulum, pronounced Golgi apparatus, abundant mitochondria and secretory vesicles.<sup>33, 34</sup> Osteoblasts deposit osteoid, which is primarily a collagenous matrix, but also contains non-collagenous proteins such as proteoglycans.<sup>34</sup> Osteoid is subsequently mineralized through the accumulation of calcium phosphate in the form of hydroxyapatite.<sup>34, 35</sup> During mineralization, serum levels of alkaline phosphatase (ALP) and osteocalcin (OCN) rise and are widely used as markers of bone formation.<sup>33</sup> Following mineralization, osteoblasts are thought to have three distinct fates; some differentiate into osteocytes upon being entombed within the bone matrix, some become quiescent bone lining cells and some undergo apoptosis.<sup>33</sup>

Several factors are thought to regulate osteoblastic differentiation. Runt-related transcription factor 2 (Runx2) is a master regulator of gene transcription factors that influence the osteoblastic phenotype, hence Runx2 is critical for osteoblastic development. Mice lacking Runx2 are unable to form bone, which results in a small skeleton composed entirely of

cartilage and these mice subsequently die shortly after birth;<sup>36</sup> while overexpression of Runx2 has been shown to enhance osteogenic activity both *in vivo* and *in vitro*.<sup>37</sup> Specifically, marrow stromal cells transduced with Ad-Runx2 displayed increased levels of ALP and increased mineralization when compared to controls.<sup>37</sup> Further, subcutaneous implantation of collagen hydrogel or gelatin sponge carriers with marrow stromal cells transduced with Ad-Runx2 into mice increased the amount of bone formed when compared to controls.<sup>37</sup> The interaction of Runx2 with signal transducers of the BMP signalling pathway (Smads) is required to transmit BMP signalling to regulate osteoblastic specific downstream targets.<sup>38</sup> One such downstream target is osterix (Osx), which is also required for osteoblastic development. Deletion of Osx in mouse embryonic stem cells prevented osteoblastic differentiation and hence bone formation in mouse embryos despite normal levels of Runx2.<sup>39</sup> In addition, inactivation of Osx in adult mice prevents new bone formation and causes cartilage to accumulate beneath the growth plate.<sup>40</sup>

### **1.3.3 Osteocytes**

Osteocytes are derived from osteoblasts and are increasingly considered to be key regulators of bone homeostasis.<sup>41</sup> The cell body of the osteocyte is located in a small tomb within bone known as a lacuna, and osteocytic processes project out from the cell body and these cell processes are located in small channels called canaliculi that extend out to osteoblasts, lining cells, osteoclasts and other osteocytes.<sup>41</sup> The differentiation of osteoblasts to osteocytes coincides with decreased expression of ALP and up-regulation of OCN, dentin matrix protein 1 (DMP-1), and sclerostin (the protein product of the SOST gene).<sup>42</sup> These changes in expression levels of specific proteins are accompanied by a change in morphology; from a cuboidal cell that is specialised to deposit osteoid, to a dendritic cell with several processes that extend to other osteocytes buried within bone and on the bone surface.<sup>41, 42</sup>

Osteocytes are thought to act as mechanosensors by detecting changes in fluid flow induced by mechanical loading, which alter the balance between bone formation and resorption through their regulation of osteoblasts and osteoclasts.<sup>43</sup> It is still not entirely clear how intracellular signalling pathways are activated by changes in mechanical stimuli and exactly by what means osteocytes activate bone remodelling in response to mechanical forces.<sup>44</sup> However, inflammatory cytokines such as tumor necrosis factor (TNF- $\alpha$ ) and interleukin 1 (IL-1) have been reported to increase osteocytic apoptosis, which results in the release of receptor activator of nuclear factor  $\kappa$ B ligand (RANKL) from apoptotic osteocytes that triggers the recruitment of osteoclasts.<sup>41</sup> Further, osteocytic secretion of sclerostin acts to inhibit bone formation, while osteocytic expression of insulin growth factor (IGF-1) has been shown to stimulate osteoblastic activity.<sup>44</sup>

#### **1.3.4 Osteoclasts**

Osteoclasts are large multinucleated cells formed via the fusion and subsequent differentiation of monocytic/macrophagic precursor cells that are responsible for bone resorption.<sup>45</sup> Upon activation, osteoclasts bind to the surface of bone and become polarized. Osteoclasts then form ruffled borders next to bone and release both hydrogen ions that demineralize bone and proteolytic enzymes that breakdown collagen and other organic components.<sup>46</sup> Osteoclasts undergo apoptosis once the required amount of bone resorption has occurred.<sup>47</sup>

Osteoclastic pre-cursors (pre-osteoclasts) from bone marrow and the blood stream are attracted to the bone resorption site by expression of RANKL by cells of the osteoblastic lineage (osteoblasts, lining cells and osteocytes; see Figure 1.2).<sup>41, 47</sup> A recent *in vivo* study has demonstrated that osteocytes are the main RANKL producing cells of trabecular bone.<sup>48</sup> Upon arrival, these pre-osteoclasts are stimulated by haematopoietic factors such as

macrophage colony stimulating factor (M-CSF-1) and RANKL binding to its cell surface receptor activator of nuclear factor-kappa  $\beta$  (RANK) to fuse and form multinucleated osteoclasts.<sup>49</sup> In mature osteoclasts, RANKL binding to RANK causes internal structural changes that potentiate bone resorption.<sup>50, 51</sup> Osteoprotegerin (OPG), a soluble protein also secreted by osteoblasts, blocks RANKL from binding to RANK and thereby acts as a decoy receptor.<sup>46</sup> Accordingly, osteoblasts contribute to the regulation of bone resorption by controlling the activation state of RANK through varying the expression of RANKL and OPG.<sup>51</sup> Consequently, the RANKL/OPG ratio is commonly used as an indicator of bone resorption. Several factors can promote osteoclastic formation and activation by regulating expression of RANKL, M-CSF-1, OPG, such as inflammatory cytokines interleukin-6 (IL-6), TNF- $\alpha$ , interleukin-17 (IL-17) and interleukin-1-  $\beta$  (IL-1 $\beta$ ).<sup>27, 52</sup>

#### **1.4 Bone remodelling**

Bone remodelling is a complex process that involves the coupling of bone resorption by osteoclasts to bone formation by osteoblasts. This process occurs throughout life and is necessary for repair and maintenance of bone structure and function. An imbalance of bone resorption or formation causes a change in bone mass. Typically 5-10% of the human skeleton is replaced each year, although this turnover decreases with age.<sup>53</sup> Bone remodelling plays an important role in calcium homeostasis and is influenced by mechanical stresses and strains.<sup>54</sup> In addition, remodelling of fracture callus (the new tissue in and around the fractured ends of bone) is critical to the restoration of normal bone structure and function following bone fracture.<sup>55</sup>

Remodelling occurs throughout the skeleton at sites referred to as basic multicellular units (BMUs),<sup>54, 56</sup> which are surrounded by a canopy of bone lining cells and osteoblasts near a blood vessel supplying the BMU.<sup>57</sup> Cells of the monocytic/macrophagic lineage migrate from

marrow and the nearby blood vessels.<sup>57</sup> The remodelling process is initiated when osteoclasts are stimulated to differentiate and facilitate bone resorption. Following resorption of bone, osteoclasts are known to undergo apoptosis, however, the precise signals that result in osteoclastic apoptosis are not fully known. In addition, the signalling mechanisms responsible for initiating cells of the osteoblastic lineage to differentiate and subsequently form bone are also not well understood. Recent reports, however, suggest that within each BMU there is constant signalling and communication between cells of the osteoblastic and osteoclastic lineages and immune cells.<sup>54</sup> Furthermore, locally-generated cytokines, which can be regulated via the endocrine and nervous system, influence communication between cells of the osteoblastic and osteoclastic lineages.<sup>54</sup>

A rapidly expanding body of evidence suggests a significant role of the central nervous system in regulating bone homeostasis. Neuronal control of remodelling was first established upon discovery that leptin can regulate bone formation through the central nervous system.<sup>58</sup> Neurons of the ventromedial hypothalamus play a key role in leptin-induced regulation of bone mass, with chemical destruction of these neurons shown to result in a high bone mass phenotype in mice.<sup>59</sup> Leptin stimulates the sympathetic nervous system, which through the actions of  $\beta_2$  adrenergic receptors, the most highly expressed adrenergic receptor in osteoblasts, causes a reduction in bone mass by decreasing osteoblastic proliferation and inducing RANKL expression.<sup>60</sup> Furthermore leptin is also thought to influence bone metabolism through its actions on serotonin.<sup>61</sup> Serotonin is a neurotransmitter produced by the action of tryptophan hydroxylase 2 (Tph2) in the central nervous system.<sup>61</sup> Tph2<sup>-/-</sup> mice have low bone mass, while brain-stem derived serotonin binding to 5-Hydroxytryptamine Receptor 2C promotes bone formation.<sup>61</sup> Leptin is thought to inhibit the synthesis and firing of serotonergic neurons to reduce bone formation.<sup>61</sup> Conversely, peripherally-acting leptin promotes bone formation.<sup>62, 63</sup> Initial evidence suggests that neuropeptide Y (NPY) also

contributes to the central regulation of bone mass. NPY is expressed by central and peripheral neurons, NPY knockout mice develop a high bone mass phenotype in the absence of any significant differences in body weight.<sup>64</sup> While, overexpression of NPY in hypothalamic neurons results in a reduction in bone mass.<sup>65</sup> Subsequently, other neurotransmitters and neuropeptides including; neuromedin U and CART (cocaine and amphetamine regulated transcript) may also regulate bone remodelling.<sup>59</sup>

The bone remodelling cycle can also be altered by a range of factors such as age, changes in physical activity, drugs, menopause-related hormonal changes and diseases that may cause various disorders of bone remodelling.<sup>66</sup> Osteoporosis is a common bone remodelling disorder that is characterised by compromised bone strength that predisposes individuals to an increased risk of bone fracture.<sup>67</sup>

#### **1.4.1 Bone remodelling disorders**

It is estimated that by 2022, 6.2 million Australians aged 50 and over will have osteopenia (decreased bone density but not to the extent of osteoporosis) or osteoporosis (a disease in which the density and quality of bones is severely reduced) that contributes to over 180,000 fragility fractures each year of which approximately 30,000 are hip fractures.<sup>2</sup> The risk of mortality is approximately 3-4 times greater for hip fracture patients in the first 3 months post-fracture compared to those of a similar age without fracture.<sup>68</sup> Though osteoporosis can cause loss of cortical bone, this disease most dramatically reduces the amount of trabecular bone and therefore the majority of osteoporotic fractures occur in regions where trabecular bone predominates e.g. spine, wrist and hip.<sup>68</sup> Common causes of osteoporosis include; a decline in plasma oestrogen levels associated with menopause, age-related osteoporosis, immobilization-related osteoporosis as well as other diseases.<sup>66</sup>

Other common bone remodelling disorders include osteomalacia (and rickets) as well as Paget's disease. Osteomalacia (adult) and rickets (juvenile) results in poorly mineralized bone that results in bowing of bone as well as bone pain and is commonly caused by alterations in vitamin D metabolism.<sup>66</sup> The abnormal bone remodelling seen in Paget's disease ultimately results in thickened, porous bone that is liable to bow and fracture.<sup>66</sup> The exact aetiology and pathogenesis of Paget's disease is relatively unknown, the disorder occurs in a strong familial pattern that suggests genetics play a role, while this disease has also been associated with chronic viral infections.<sup>66</sup> An uncommon bone disease of abnormal remodelling is the disease osteopetrosis, which results in thickened bone due to a lack of osteoclastic bone resorption due a genetic mutation in osteoclasts.<sup>66</sup> Details of these diseases are beyond the scope of the current review. The reader is therefore referred to a comprehensive review of these bone diseases.<sup>66</sup>

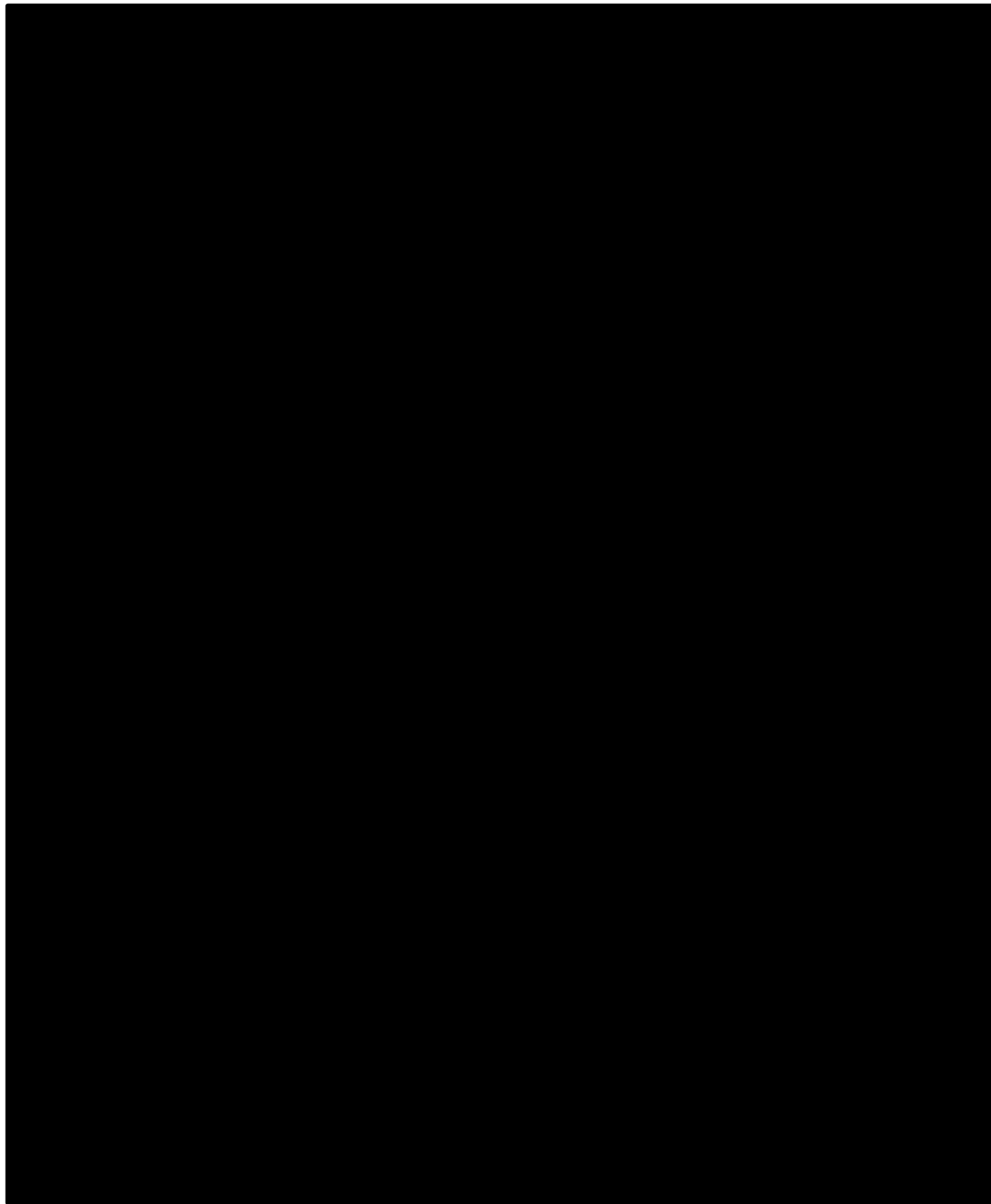


**Figure 1.2.** Osteoblasts and osteocytes controlling osteoclastic differentiation. Osteoblasts express RANKL, which binds to the RANK receptor on the surface of pre-osteoclasts causing them to fuse and form multinucleated osteoclasts. Osteoblasts and osteocytes also express OPG, which acts as a decoy receptor by blocking RANKL from binding to RANK on the surface of osteoclasts and pre-osteoclasts (Adapted from Tilg *et al.*, 2008).<sup>69</sup>

## **1.5 Long bone growth**

Endochondral ossification is the process through which long bones elongate and occurs in epiphyseal cartilage growth plates at the ends of long bones. In growing individuals, the cartilage growth plate of long bones consists of distinct zones of chondrocytes at different stages of maturation.<sup>70</sup> This carefully organised arrangement of chondrocytes facilitates osseous elongation. The chondrocytic region closest to the epiphyseal plate is comprised of resting chondrocytes.<sup>32</sup> Moving towards the ossification front, flattened chondrocytes in multicellular columns undergo an intense phase of proliferation, then subsequently stop proliferating, enlarge (hypertrophy) and begin secreting a cartilaginous matrix rich in type X collagen, the proteoglycan aggrecan as well as various other chemoattractants.<sup>70</sup> Chondrocytic proliferation, coupled with matrix deposition, results in elongation of the growth plate. Following hypertrophy, some chondrocytes die via apoptosis or extended autophagy. Findings of a recent publication suggest that other hypertrophic chondrocytes survive and differentiate into osteoblasts and osteocytes that become part of cortical and trabecular bone.<sup>71</sup>

Various factors released by hypertrophic chondrocytes promote blood vessel invasion to bring in osteoclasts, OPCs and osteoblasts.<sup>32</sup> Osteoclasts then remove the calcified cartilaginous matrix. This removal is a pivotal step in the process of endochondral ossification. Osteoblasts use the remnants of the calcified cartilaginous matrix as a template on which to form bone.

## **1.6 Biology of bone fracture healing**

Fracture healing involves a carefully orchestrated sequence of events that can be altered by pharmacological intervention, environmental factors and genetic perturbations.<sup>55, 72</sup> Unlike damaged soft tissue, fractured bone normally heals without the formation of scar tissue, with

the resultant healed bone tissue identical to the pre-injured tissue. The fracture healing sequence includes four consecutive overlapping phases; beginning with an inflammatory phase, which is characterised by the release of chemokines and cytokines that initiate the healing response. This is then followed by the formation of a fibrocartilaginous soft callus to bridge the fractured bone ends. Then there is subsequent mineralization of the soft callus to form a hard callus, which provides restoration of both stiffness and toughness to the fracture site, and finally a remodelling phase in which the hard callus is reduced to its pre-injured bone structure.

### **1.6.1 Inflammatory phase**

Bone fracture causes disruption of vasculature that supplies bone as well the disturbance of soft tissue and marrow that leads to activation of wound healing pathways. Blood released from severed vessels is contained by muscle surrounding the fracture site, and a haematoma forms between the fractured ends, which soon develops into a fibrinous thrombus.<sup>28, 73</sup> Haematoma associated cytokines TNF- $\alpha$ , IL-1 and IL-6, attract platelets and inflammatory cells.<sup>28, 72, 74</sup> Firstly, neutrophils migrate to the site of injury within the first 24 hours post-fracture. This is then followed by macrophages, which migrate over the next 24-48 hours.<sup>75</sup> Degranulating platelets and monocytes also potentiate the inflammatory response.

Osteoclasts and macrophages remove necrotic bone and phagocytose other cellular debris.<sup>28</sup> Importantly, inflammation and haematoma formation are necessary for healing to progress. Removal of the haematoma delays healing, conversely, sustained inflammation is also detrimental to healing. An acute, tightly-regulated pro-inflammatory response is required for healing to progress.<sup>76</sup>

The previously mentioned inflammatory cells, as well as dead and dying native cells release growth factors that include transforming growth factor- $\beta$  (TGF- $\beta$ ),<sup>76</sup> vascular endothelial

growth factor alpha (VEGF $\alpha$ ),<sup>77</sup> hypoxia inducible factor-1 alpha (HIF-1 $\alpha$ ),<sup>77</sup> IL-1,<sup>74</sup> and IL6,<sup>74</sup> and TNF- $\alpha$ .<sup>72</sup> These endogenous factors are responsible for the promotion of angiogenesis and infiltration of mesenchymal cells and OPCs, which migrate from a number of niches; the periosteum, circulation, marrow and surrounding muscle.<sup>28,72,74,76</sup>

### **1.6.2 Soft callus formation**

The fibrinous thrombus formed in the early stages (24-72 hours) post-fracture is re-organised into granulation tissue, which is subsequently (largely) replaced by cartilage. The initial fibrocartilaginous plug that develops between the fractured ends can tolerate movement, whilst providing structural support.<sup>28</sup> Formation of a fibrocartilaginous soft callus is decreased by fixation and increased by instability; hence the amount of soft callus formed varies depending upon the fracture model.

Soft callus formation is initiated when fibroblasts, myofibroblasts and OPCs migrate from the circulation, surrounding muscle and periosteum to the fracture site, after being attracted by factors released from within the clot (see: Figure 1.3b,c).<sup>55</sup> Cells that migrate to regions where oxygen tension is low and mechanical stress high (typically the central fracture site) differentiate into fibroblast-like cells that form a fibrous callus (see: Figure 1.3d).<sup>28, 72</sup> Chondrocytes that are derived from OPCs subsequently enter an intense phase of cellular division before becoming hypertrophic. These hypertrophic chondrocytes then deposit a cartilaginous matrix until all of the fibrous tissue has been replaced by cartilage (Figure 1.3e).<sup>55, 72, 73</sup> Subsequent remodelling of this cartilage is mediated by matrix metalloproteinases (MMPs) and results in the release of angiogenic factors that further promote vascular invasion.<sup>78,79</sup>

At regions where mechanical stability and vascularity of the callus is sufficient, bone formation gradually occurs via endochondral ossification, in a similar manner to that which occurs at the epiphyseal growth plates as explained previously (see: Figure 1.3e).<sup>28, 55, 73</sup>

### **1.6.3 Hard callus formation**

Hard callus can form directly via intramembranous ossification (formation of bone without use of cartilaginous template) in a microenvironment where both oxygen tension and mechanical stability are high. However, in the majority of fractures, there is usually some degree of mechanical instability and low oxygen tension, hence hard callus formation occurs via a combination of endochondral ossification and intramembranous ossification.<sup>28</sup>

Vascular invasion is essential in order for mineralization to occur as sufficiently high oxygen tension is necessary to promote osteoblastic differentiation.<sup>77, 80</sup> Blood vessels are responsible for providing oxygen and nutrients as well as calcium and phosphate, which are all necessary for mineralization.<sup>28, 77</sup> An adequate blood supply is critical for successful healing of fractured bone. At the fracture site, angiogenesis is stimulated by factors such as HIF-1 $\alpha$ , VEGF $\alpha$ , MMPs, BMPs, FGF-1 and TGF- $\beta$ .<sup>77, 80</sup> Inhibition of VEGF $\alpha$  has been shown to result in delayed healing of experimental models of femoral fracture and cortical bone defects, while local administration of VEGF $\alpha$ , enhanced healing in both of these bone injury models.<sup>77</sup> In addition, other interventions that stimulate blood vessel formation have also been shown to enhance fracture healing.<sup>80-83</sup>

Mineralization occurs first where oxygen tension and mechanical stability is high; typically in the endosteum and periosteum and in the peripheral callus where a cortical shell begins to form to provide structural rigidity via intramembranous ossification (see: Figure. 1.3d).<sup>28, 73</sup> The mineralization front then moves inward toward the fractured ends. The cartilage is then removed as osteoblasts deposit mineralized matrix on the cartilaginous template until the

entire callus is mineralized (see: Figure 1.3d-f). Removal of cartilage is a critical step in the fracture healing process.<sup>55</sup> The callus is then remodelled inward until resolution (see: Figure 1.3f-h). Initially, hard callus is composed of woven/trabecular bone, which over time is remodelled to form dense cortical bone.<sup>84</sup>

#### **1.6.4 Callus remodelling**

In the case of long bone fracture, woven bone is initially formed and is gradually remodelled into organised lamellar bone that resembles pre-injured cortical bone tissue. This remodelling process allows restoration of the bone's original geometry and mechanical properties, but also allows Haversian systems to be re-established. Osteoclasts are the main cells involved in the resorption of this woven bone. As the cortical shell is remodelled, osteoblasts form bone on the endocortical surface toward the fracture zone, while osteoclasts resorb bone on the periosteal surface of the shell.<sup>55</sup> Prolonged, increased bone volume and persistence of the cortical shell indicates a lack of remodelling as is observed in rodent studies that block osteoclastic formation and activity.

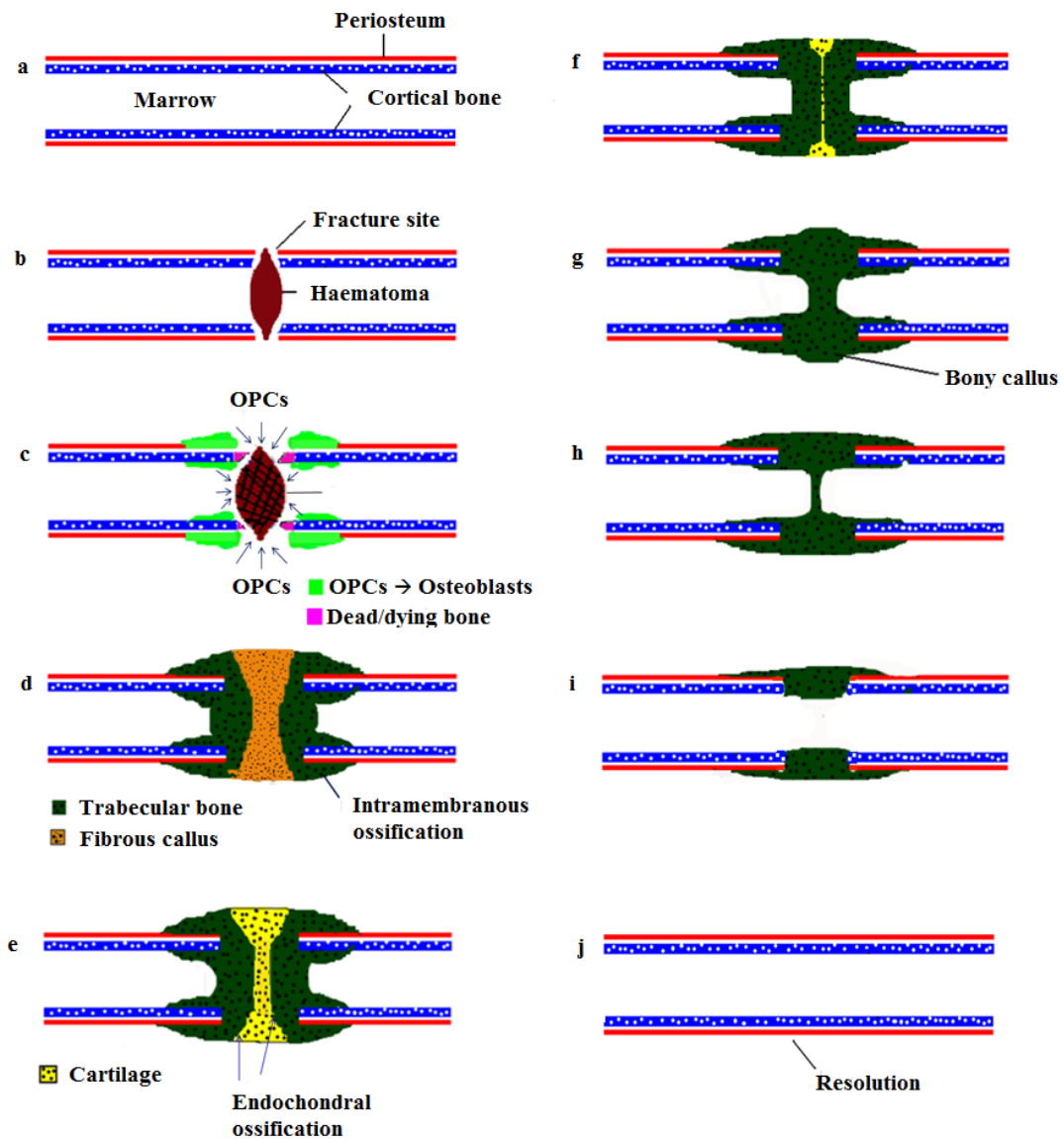


**Figure 1.3.** The sequence of a simple, healing long bone fracture. (a) Uninjured long bone. (b,c) Haematoma releasing endogenous factors that attract OPCs. OPCs migrate from surrounding soft tissue, marrow, endocortical regions of bone and the periosteum. In regions where oxygen tension is high, OPCs differentiate into osteoblasts, which form bone directly via intramembranous ossification (fluorescent green). (d) Where oxygen tension is low, OPCs differentiate into fibroblast-like cells (brown), which form a soft fibrous callus before later differentiating into chondrocytes. Intramembranous ossification proceeds simultaneously (dark green). (e) OPCs differentiate into chondrocytes that form cartilage (soft callus; yellow). (f) Endochondral ossification occurring at the bone/cartilage interface. (g) Bony callus. (h,i) Remodelling of trabecular bone and formation of cortical bone as per Wolff's law. (j) Fully healed long bone.

## 1.7 Thymosin $\beta_4$ (T $\beta_4$ )

One focus of this thesis is to investigate the effect of T $\beta_4$ , a peptide with several attributes that have been shown to promote repair and regeneration of injured tissues, on bone fracture healing.

The  $\beta$ -thymosins are a family of more than 15 proteins that possess structurally similar amino acid sequences.<sup>85</sup> Thymosin peptides belong to a family of biological response modifiers that regulate the immune response and also influence tissue repair and regeneration.<sup>15</sup> Three  $\beta$  thymosins are found in humans; T $\beta_4$ , T $\beta_{10}$  and T $\beta_{15}$ , however this review will focus on T $\beta_4$ .<sup>86</sup>

T $\beta_4$  is found in eukaryotic cells and represents 70-80% of the total  $\beta$  thymosin content of mammalian tissue.<sup>85</sup> T $\beta_4$  was first isolated from bovine thymus in 1981 by Goldstein and Low,<sup>86</sup> and has since been found to be present in body fluid (saliva,<sup>87</sup> wound fluid,<sup>88</sup> tears,<sup>89</sup> and plasma<sup>90</sup>) and all cells with the exception of erythrocytes.<sup>90</sup> T $\beta_4$  is found in particularly high concentrations (13  $\mu\text{g/ml}$ ) in wound fluid,<sup>91</sup> which led to the hypothesis that endogenous T $\beta_4$  has a role in repair and regeneration of injured tissues.<sup>92</sup> Since these initial findings, several studies have demonstrated the therapeutic potential of T $\beta_4$  administration for promoting healing of dermal,<sup>18</sup> corneal,<sup>93</sup> cardiac<sup>94</sup> and brain injuries.<sup>95</sup> T $\beta_4$ -induced promotion of tissue repair and regeneration has been attributed to multiple actions of the peptide, which include; anti-apoptotic properties,<sup>96</sup> modulation of inflammation,<sup>97</sup> enhancement of progenitor cell recruitment and differentiation,<sup>98</sup> promotion of the orderly arrangement of collagen<sup>99</sup> and stimulation of angiogenesis.<sup>100</sup>

### 1.7.1 Physical properties of T $\beta_4$

T $\beta_4$  is a small peptide (4,964 Da) that is highly water soluble due to the presence of a large percentage of charged (~45%) and polar (~17%) amino acid residues.<sup>17</sup> Furthermore, T $\beta_4$  does not bind to heparin or other extracellular matrix molecules, which allows it to diffuse

deeply into tissue and promote healing.<sup>17</sup> T $\beta$ <sub>4</sub> has been localised to both the cytoplasm and nucleus, however, exactly how T $\beta$ <sub>4</sub> enters the nucleus has not yet been established,<sup>91</sup> although internalization of exogenous T $\beta$ <sub>4</sub> seems essential for influencing cellular functions.<sup>101</sup>

## **1.7.2 Mechanisms of action**

As mentioned above, T $\beta$ <sub>4</sub> promotes healing and repair in a number of different cells and tissues, which stems from its ability to augment endogenous restorative processes. The various mechanisms through which T $\beta$ <sub>4</sub> acts are only just beginning to be determined. It is clear from initial experiments that T $\beta$ <sub>4</sub> is a multifaceted regenerative peptide that seems to potentiate healing in a tissue specific manner.

### **1.7.2.1 Modulation of inflammation**

Accumulating evidence suggests one of several mechanisms through which T $\beta$ <sub>4</sub> enhances healing is through the modulation of inflammatory processes.<sup>102</sup> *In vitro* studies have revealed that when human corneal epithelial cells were stimulated with the inflammatory cytokine TNF- $\alpha$ , subsequent treatment with T $\beta$ <sub>4</sub>, reduced activity and protein levels of nuclear factor kappa-light-chain-enhancer of activated B cells (NF $\kappa$ B) and p65 subunit phosphorylation.<sup>97</sup> These results suggest that T $\beta$ <sub>4</sub> treatment suppresses the inflammatory response by inhibiting NF $\kappa$ B inflammatory signalling in the cornea.<sup>102</sup> T $\beta$ <sub>4</sub> treatment *in vivo* following corneal alkali (NaOH) injury in mice decreased infiltration of polymorphonuclear leukocytes (PMNs) by downregulating levels of two specific inflammatory mediators; macrophage inflammatory protein 2 and keratinocyte chemokine.<sup>103</sup> The authors of this paper hypothesised that the reduced levels of MMP-9 observed in T $\beta$ <sub>4</sub>-treated cornea also contributed to the decreased numbers of PMNs, as MMP-9 cleaves inflammatory cytokine interleukin 8 (IL-8), which enhances its chemotactic effects on PMNs.<sup>103</sup> Excess MMP-9 has been associated with corneal and epithelial repair defects.<sup>103</sup>

In addition to the findings of reduced inflammation following corneal injury, T $\beta$ <sub>4</sub> has also been shown to downregulate inflammation of injured cardiac tissue.<sup>104, 105</sup> A recent study suggests that treatment with T $\beta$ <sub>4</sub> via subcutaneously implanted osmotic pumps for 5 weeks in mice reduced the incidence of cardiac rupture and improved cardiac function post-myocardial infarction by modulating inflammatory processes, cardiomyocyte apoptosis and increasing re-vascularisation.<sup>104</sup> Specifically, numbers of infiltrating neutrophils and macrophages in infarcted cardiac tissue were reduced in T $\beta$ <sub>4</sub>-treated mice compared to vehicle-treated mice. Expression levels of Intercellular Adhesion Molecule 1 (ICAM-1; a signalling molecule involved in the recruitment of neutrophils and macrophages) were significantly decreased in T $\beta$ <sub>4</sub>-treated mice.<sup>104</sup> Therefore, it seems that T $\beta$ <sub>4</sub> treatment may, in part, reduce the numbers of neutrophils and macrophages by downregulating expression levels of ICAM-1 post-injury.<sup>104</sup> Other studies have shown via animal models of myocardial infarction and heart failure that T $\beta$ <sub>4</sub> reduced activation of the pro-inflammatory mediator, NF $\kappa$ B, which provides additional evidence that T $\beta$ <sub>4</sub> suppresses the inflammatory response.<sup>105</sup>

#### **1.7.2.2 T $\beta$ <sub>4</sub> promotes cell survival**

Another complementary action of T $\beta$ <sub>4</sub> is the promotion of cell survival following injury to the brain, cornea and heart.<sup>104, 106, 107</sup> A growing number of studies have demonstrated that T $\beta$ <sub>4</sub> treatment enhances neurological recovery in experimental animal models of embolic stroke and TBI.<sup>108-110</sup> Treatment with T $\beta$ <sub>4</sub> at the time of TBI appears to have a neuroprotective effect by reducing lesion size, which is likely to be in part through the promotion of cell survival.<sup>109</sup> In a rat model of stroke, T $\beta$ <sub>4</sub> has been found to inhibit oxygen glucose deprivation-induced apoptosis via the epidermal growth factor receptor signalling pathway in cells isolated from the subventricular zone following middle cerebral artery occlusion.<sup>108</sup> In addition, T $\beta$ <sub>4</sub> also has anti-apoptotic effects on corneal cells, with *in vitro* data indicating that T $\beta$ <sub>4</sub> treatment reduced ethanol-induced apoptosis of corneal epithelial cells by inhibiting caspase-2,-3,-8 and

-9 and decreasing the release of (Bcl-2) B cell lymphoma 2 from mitochondria.<sup>107</sup> In addition, subsequent reports suggest that T $\beta$ <sub>4</sub> may reduce cardiomyocyte apoptosis following experimental myocardial infarction in rats by downregulating protein expression of tumour suppressor protein p53; a mediator of cell apoptosis.<sup>104</sup>

### 1.7.2.3 Promotion of cell migration

Both *in vivo* and *in vitro* studies have demonstrated that T $\beta$ <sub>4</sub> has a chemotactic effect on epithelial cells, keratinocytes and endothelial cells.<sup>18, 111-113</sup> In the cornea, *in vivo* studies using rodent models of debridement (i.e. via heptanol and alkali burns) have demonstrated that T $\beta$ <sub>4</sub> treatment increased re-epithelialisation of wounds.<sup>102, 114, 115</sup> This accelerated re-epithelialisation was attributed to T $\beta$ <sub>4</sub>-induced upregulation of laminin-5 (LM-5), a glycoprotein located on the basement membrane of cells, which is thought to play a crucial role in epithelial cell migration and adhesion.<sup>112</sup> Both *in vivo* and *in vitro* models of scrape wounds treated with T $\beta$ <sub>4</sub> found that treatment caused an increase in LM-5 expression in corneal epithelial cells.<sup>112</sup>

Though several studies have demonstrated that T $\beta$ <sub>4</sub> treatment has a chemotactic effect on endothelial cells,<sup>18, 111, 116, 117</sup> a recent study has suggested a possible mechanism underlying this effect. Freeman and co-workers, reported that the adenosine triphosphate (ATP)-responsive, P2X<sub>4</sub> receptor is required for T $\beta$ <sub>4</sub>-induced endothelial cell migration.<sup>113</sup> Silencing the P2X<sub>4</sub> receptor in endothelial cells resulted in a loss of cell migration in response to T $\beta$ <sub>4</sub> *in vitro*.<sup>113</sup> This observation led the authors to conclude that P2X<sub>4</sub> is likely to be a downstream signalling component of T $\beta$ <sub>4</sub>-induced endothelial cell migration that allows ATP synthesis but blocks ATP hydrolysis.<sup>113</sup> It was proposed that T $\beta$ <sub>4</sub> acts on ecto-ATP synthase to increase cell surface ATP levels and by signalling through purinergic receptor, P2X<sub>4</sub>, promotes cell migration (see figure 1.4).<sup>113</sup> These findings suggest that purinergic signalling

may be a possible mechanism through which  $T\beta_4$  induces migration of endothelial cells, however, additional studies are required in order to determine the mechanisms through which  $T\beta_4$  affects other cell types.

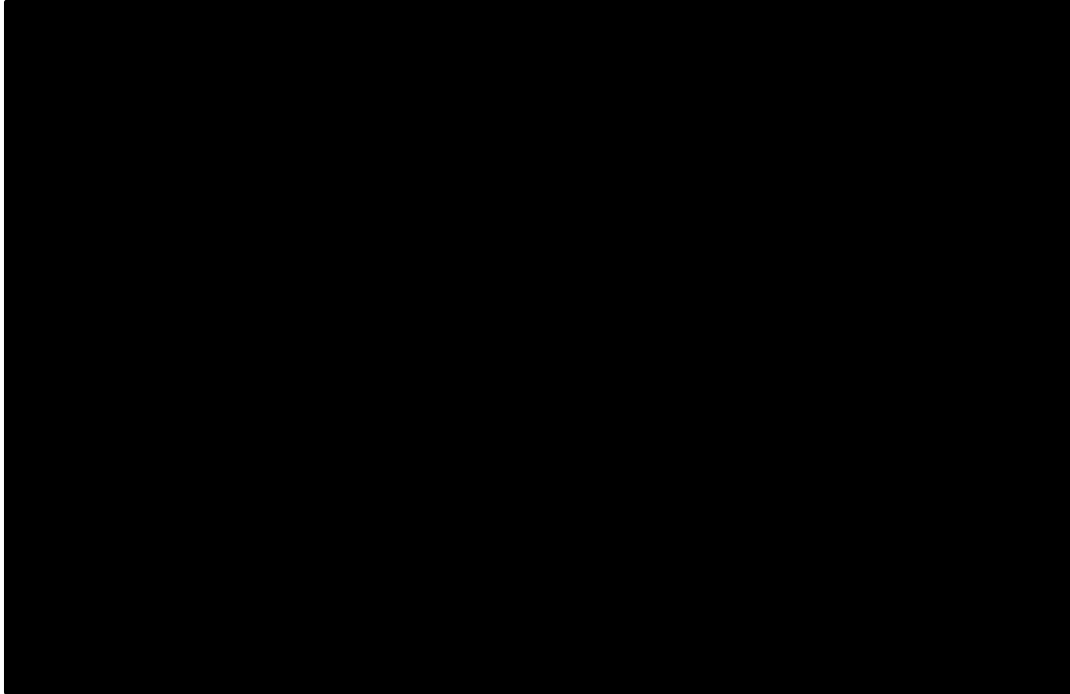


**Figure 1.4.** Proposed  $T\beta_4$  signalling.  $T\beta_4$  increases ATP levels by (1) blocking ATP hydrolysis while, (2) allowing ATP synthesis (2). (3) The elevated ATP levels activate the P2X4 receptor to stimulate cell migration (4). (Adapted from Freeman *et al.*, 2011).<sup>113</sup>

#### 1.7.2.4 $T\beta_4$ promotes angiogenesis

Following on from early work demonstrating that  $T\beta_4$  promotes endothelial cell migration,  $T\beta_4$  was found to increase proliferation, differentiation and tube formation of human umbilical vein endothelial cells (HUVEC) on matrigel.<sup>117</sup> Further, the addition of  $T\beta_4$  to the coronary artery ring angiogenesis assay promoted capillary sprouting.<sup>117</sup> The precise mechanism through which  $T\beta_4$  enhances angiogenesis and whether certain fragments of the peptide elicit this activity is still relatively unknown and remains controversial. Using naturally occurring  $T\beta_4$ , proteolytic fragments and synthetic peptides in human umbilical vein endothelial cells and vessel sprouting assays using chick aortic arches, Philp and co-workers reported that a seven amino acid actin-binding motif of  $T\beta_4$  (LKKTETQ) promoted angiogenesis.<sup>100</sup> They concluded that the central binding domain of  $T\beta_4$  initiates angiogenesis

by interacting with endothelial cells. Smart and colleagues, however, point out that T $\beta$ <sub>10</sub> is known to inhibit angiogenesis, regardless of the fact it contains the actin binding motif (LKKTETQ).<sup>118</sup>

Recent work suggests that T $\beta$ <sub>4</sub>-treatment induces angiogenesis of HUVEC via the Notch signalling pathway, specifically by increasing levels of HIF-1 $\alpha$  and expression of its downstream target VEGF $\alpha$ , a primary pro-angiogenic factor.<sup>119</sup> In addition, it is known that MMPs are essential for vascular remodelling and angiogenesis. MMP-2 is necessary to breakdown the basement membrane,<sup>111</sup> which allows endothelial cells to penetrate the substratum and form new vessels.<sup>111</sup> T $\beta$ <sub>4</sub> has been shown to upregulate certain MMPs *in vitro*; with expression levels of MMP-2 in T $\beta$ <sub>4</sub>-treated HUVECs being up-regulated compared to controls.<sup>111</sup> Furthermore, T $\beta$ <sub>4</sub>-treatment of keratinocytes, endothelial cells, and fibroblasts increased expression of MMP-1,-2 and 9.<sup>120</sup>

#### **1.7.2.5 Promotion of the orderly arrangement of collagen**

T $\beta$ <sub>4</sub> also contributes to healing and regeneration by promoting the orderly arrangement of collagen in dermal and cardiac injury models.<sup>99, 105, 121</sup> Incisional dermal wounds treated with T $\beta$ <sub>4</sub> displayed superior mechanical characteristics compared to controls.<sup>99</sup> Specifically, wounds of T $\beta$ <sub>4</sub>-treated rats had a more mature and highly organised arrangement of collagen fibres with fewer myofibroblasts.<sup>99</sup> In addition to their role in angiogenesis, MMPs contribute to wound debridement and remodelling of collagen.<sup>120</sup> As stated above, it was found that keratinocytes, endothelial cells and fibroblasts increased expression of MMP-1,-2 and 9 in healing wounds treated with T $\beta$ <sub>4</sub>.<sup>120</sup> These results suggest that one such mechanism through which T $\beta$ <sub>4</sub> promotes the organised arrangement of collagen is through up-regulating expression of metalloproteinases in various cell types involved in wound repair.<sup>120</sup>

### **1.7.2.6 Promotion of cell differentiation**

As discussed above, it has been established that exogenous T $\beta$ <sub>4</sub> promotes cell differentiation to facilitate angiogenesis. A number of studies have shown that T $\beta$ <sub>4</sub> induces differentiation of oligodendrocytic progenitor cells.<sup>106, 109, 110, 122, 123</sup> T $\beta$ <sub>4</sub> treatment enhances neurological recovery in experimental animal models of embolic stroke and TBI.<sup>108-110</sup> T $\beta$ <sub>4</sub> is thought to promote neurological recovery by stimulating differentiation of oligodendrocytic progenitor cells into myelin-secreting oligodendrocytes.<sup>106, 109, 110, 122, 123</sup> A recent study has demonstrated that T $\beta$ <sub>4</sub> treatment induced oligodendrocytic progenitor cell differentiation through a microRNA200 (miR-200)-dependent mechanism.<sup>108</sup> Specifically, T $\beta$ <sub>4</sub> upregulated miR-200, which activated growth factor receptor-bound protein 2 to induce oligodendrocytic progenitor cell differentiation by increasing the formation of myelin basic protein.<sup>108</sup> Differentiation was attenuated by anti-miR-200. There is also evidence that T $\beta$ <sub>4</sub> treatment induces oligodendrocytic differentiation by increasing expression of miR-146a and myelin basic protein.<sup>124</sup> These initial findings on the actions of T $\beta$ <sub>4</sub> on miRNAs are novel, however, further work is required in order to establish how T $\beta$ <sub>4</sub>-mediated messages are relayed among cells.<sup>95</sup> T $\beta$ <sub>4</sub>-induced differentiation of bone cells remains controversial and will be discussed in the section below.

### **1.7.3 The possible effects of T $\beta$ <sub>4</sub> on fracture healing**

It is proposed that the aforementioned regenerative properties of T $\beta$ <sub>4</sub> may also promote bone fracture healing. Promotion of cell survival, migration and differentiation coupled with the modulation of inflammatory processes may augment bone healing. T $\beta$ <sub>4</sub> promotes the highly organised deposition of collagen, which could result in enhanced mechanical properties of the fibrous tissue that forms between the two fractured ends. In addition, the chemotactic properties of T $\beta$ <sub>4</sub> may well increase osteoprogenitor cell migration to the fracture site, while T $\beta$ <sub>4</sub> could possibly stimulate osteoblastic and/or chondrocytic differentiation and through this

mechanism, enhance intramembranous ossification, endochondral ossification, or both. The angiogenic properties of T $\beta$ <sub>4</sub> suggest that T $\beta$ <sub>4</sub> may enhance re-vascularisation of the fracture site, to increase oxygen tension and further promote ossification. Additionally, T $\beta$ <sub>4</sub> may stimulate osteoblasts to deposit osteoid in a highly organised fashion via a similar mechanism through which it promotes the highly organised deposition of collagen by fibroblasts, which would enhance mechanical properties of healing calluses. Finally, increased expression of MMPs in healing dermal wounds suggests that T $\beta$ <sub>4</sub> may stimulate matrix remodelling during both soft and hard callus phases of healing fractures.

Though no studies have investigated the effect of T $\beta$ <sub>4</sub> on long bone fracture healing, recent evidence suggests that T $\beta$ <sub>4</sub> also promotes healing of bone defects. *In vivo* studies have demonstrated that T $\beta$ <sub>4</sub> treatment increased fractional bone volume at the healing site following either tooth extraction or a calvarial defect.<sup>125, 126</sup> The first study to report the effect of T $\beta$ <sub>4</sub> on injured bone used a rat tooth extraction model.<sup>125</sup> Treated rats were administered a 20 amino acid partial peptide of T $\beta$ <sub>4</sub>, which corresponded to amino acids 17-36 of the full length 43 amino acid sequence.<sup>125</sup> T $\beta$ <sub>4</sub> promoted wound healing as well as bone formation in extraction sockets while reducing apoptosis and inflammation at the wound site at 1 day post-injury. At 3 days following injury, mRNA expression of inflammatory factors IL-1, IL1- $\beta$ , IL-6 and TNF- $\alpha$  was reduced in the T $\beta$ <sub>4</sub>-treated group. From days 1-4, a greater volume of granulation tissue at the site of injury was observed in T $\beta$ <sub>4</sub>-treated rats, which led the authors to suggest that treatment promoted angiogenesis, cell proliferation and migration.<sup>125</sup> Expression levels of genes associated with angiogenesis, cell proliferation and migration were higher in T $\beta$ <sub>4</sub>-treated rats when compared to controls. Of greatest relevance to bone formation was the increased percentage of newly formed trabecular bone at 4 and 6 days post-injury in T $\beta$ <sub>4</sub>-treated rats. These results indicate that T $\beta$ <sub>4</sub> may promote bone formation.

The increased mRNA expression of osteogenic genes, BMP-4 and TGF- $\beta$  and increased number of Osx-positive cells may indicate that T $\beta_4$  directly affects bone forming cells.

Subsequently, the same group then employed a rat calvarial defect model to further investigate the effect of T $\beta_4$  on injured bone.<sup>126</sup> Following a calvarial defect, rats were administered a 27 amino acid partial T $\beta_4$  fragment that corresponded to amino acids 17-43 of the full T $\beta_4$  sequence. The results from this experiment supported previous findings; with treated rats displaying an increased percentage of newly formed bone and an increased number of Osx-positive cells at the site of injury. mRNA expression of osteogenic genes 10 days following injury was not different between treated and control rats. Therefore it was suggested that the increased bone formation observed in T $\beta_4$ -treated rats was due to modulation of inflammatory processes, increased cell migration and augmented granulation tissue formation as opposed to T $\beta_4$ -induced promotion of ossification.

This review will now focus on the potential effect of T $\beta_4$  on mesenchymal/osteoprogenitor cells. Only recently have *in vitro* studies begun to examine the direct effect of T $\beta_4$  treatment on osteoblast-like cells. Lee and co-workers found that T $\beta_4$  treatment promoted differentiation and mineralization of immortalized odontoblasts (cells with phenotypical and functional similarities to osteoblasts). T $\beta_4$  treatment increased levels of BMP-2,4 and downstream molecules Smad1/5/8 and Smad2/3, which indicated that T $\beta_4$  signals through the BMP pathway.<sup>127</sup> Further, the BMP inhibitor, Noggin, blocked T $\beta_4$ -induced differentiation and mineralization, which suggests that T $\beta_4$  promotes differentiation of odontoblast-like cells via the integrin/integrin linked kinase (ILK)/BMP signalling pathway.<sup>127</sup> The same group also found that T $\beta_4$  treatment enhanced differentiation and mineralization of immortalized human periodontal ligament cells and cementoblasts and osteoblast-like cells (MG63) via similar pathways to that of the odontoblast-like cells.<sup>127, 128</sup>

In contrast, work done prior to these experiments reported that T $\beta$ <sub>4</sub> treatment of human marrow-derived mesenchymal stem cells inhibited osteogenic differentiation and promoted adipogenic differentiation.<sup>129</sup> Transgenic mice that overexpressed T $\beta$ <sub>4</sub>, however, exhibited abnormally shaped teeth and dull incisors, which led the authors to suggest that excess T $\beta$ <sub>4</sub> is detrimental to enamel matrix deposition.<sup>130</sup> The precise effects of T $\beta$ <sub>4</sub> on osteoprogenitor/osteoblasts are only beginning to be elucidated. Preliminary investigations on the effect T $\beta$ <sub>4</sub>-treatment has on osteoclasts *in vitro* suggest that T $\beta$ <sub>4</sub>-treatment inhibits osteoclastogenesis.<sup>131</sup> Specifically, the addition of T $\beta$ <sub>4</sub> to murine bone marrow-derived macrophages reduced osteoclastic number and function.<sup>131</sup> Despite initial evidence that suggested that T $\beta$ <sub>4</sub>-treatment promoted healing of injured bone, no studies have examined the effect of T $\beta$ <sub>4</sub>-treatment on experimental models of long bone fracture healing. If T $\beta$ <sub>4</sub> can amplify the processes discussed above e.g., angiogenesis, osteoprogenitor cell migration and osteoblastic differentiation and mineralization, it is possible that the peptide will also promote healing of fractured bone.

## **1.8 Traumatic brain injury (TBI)**

Another main focus of this thesis was to examine the effect TBI has on bone metabolism and whether sodium selenate (a pharmaceutical intervention that enhances TBI outcomes) altered TBI-induced effects of bone. Further to this, it was important to investigate potential detrimental effects of sodium selenate on skeletal cells. Finally, it was also of importance to examine the effects of TBI on bone fracture healing due to the high incidence of TBI and multitrauma involving TBI and concomitant long bone fracture.<sup>132</sup> Accordingly, the following sections will discuss TBI pathobiology, outline how sodium selenate is thought to reduce neurodegeneration post-TBI, and detail the confounds of current studies that have examined how fracture healing may be altered by TBI.

TBI is a multifaceted disorder induced by an external mechanical force to the brain.<sup>133, 134</sup> TBI commonly occurs following motor vehicle collisions, falls, violence as well as construction- and sport-related injuries.<sup>135</sup> Prevalence of TBI is higher in men compared to women; it is also more prevalent in both children and the elderly compared with the rest of the population.<sup>135</sup> TBI represents a variety of injury patterns, which range from focal injuries that affect specific brain structures, to more generalised diffuse patterns of injury. TBI severity can also vary from sub-concussive forces in which the effects on the brain are transient to severe that can result in death. A single TBI or repetitive cranial insults may result in various pathological conditions, which include neuroendocrine dysregulation, neurodegenerative diseases, seizures, behavioural, cognitive and motor deficits, psychosomatic conditions and damage to peripheral organs.<sup>136, 137</sup> TBI is a leading cause of death and morbidity and is therefore recognised as a serious public health concern.<sup>133</sup> Alarming, the incidence of TBI is increasing in many countries, which may reflect the growing incidence of sport- and military-related TBIs.<sup>136</sup>

Brain damage caused by mechanical forces at the moment of impact is termed the primary injury, and may involve neurovascular damage, axonal injury, oedema and ischaemia, which contribute to neuronal cell death and ongoing damage.<sup>134, 138</sup> These primary injuries activate a complex cascade of secondary injury pathways that may develop over the minutes, days and months that follow the initial impact.<sup>139</sup> Common secondary injury mechanisms involved in TBI include; excitotoxicity, oxidative stress, neuroinflammation, mitochondrial dysfunction, apoptosis and proteopathies, which involve proteins such as tau.<sup>20, 140</sup>

Shearing of axons and cellular damage caused by mechanical forces to the brain results in increased extracellular amounts of glutamate.<sup>134, 141, 142</sup> Elevated levels of glutamate and other excitatory neurotransmitters ultimately triggers the release of calcium and other ions

into the cell, which leads to cytotoxic oedema and the production of free nitrogen radicals, reactive oxygen species (ROS) and inflammatory cytokines.<sup>134, 141, 142</sup> These factors trigger activation of microglia and astrocytes, which subsequently also release a range of inflammatory cytokines that include IL-1 $\beta$ , IL-6, IL-17 and TNF- $\alpha$ .<sup>139, 143</sup> These cytokines can initiate a self-propagating cycle of damaging events that may cause chronic and dysregulated microglial activation.<sup>144</sup> Human and animal studies suggest that following TBI, microglia can be chronically activated for weeks and months,<sup>143-147</sup> while post-mortem analysis has revealed that microglia can be activated in white matter for up to 16 years post-TBI.<sup>148</sup>

In addition, microglial activation, oxidative stress, inflammatory mediators and injury to the cerebral vasculature disrupt the structural integrity of the blood brain barrier (BBB).<sup>149</sup> The BBB refers to the capillaries and post-capillary venules in the brain and spinal cord and are comprised of endothelial cells that are joined by complex tight junctions and adhesion molecules.<sup>150</sup> This unique structure limits the trafficking of solutes and other factors in and out of the brain.<sup>151</sup> Under normal physiological conditions, the tight junctions of the BBB prevent the migration of immune cells and inflammatory chemokines in and out of the brain parenchyma, however, under pathological conditions such as TBI, the permeability of the BBB is increased.<sup>149</sup> In addition, it has been shown that often following head trauma, the endothelium of blood vessels undergoes shear-injury that can lead to a reduction in cerebral blood flow, metabolic disturbances as well as other complications, which include vasospasm and coagulopathy.<sup>152</sup> In more mild-TBI cases, only the integrity of tight junctions is compromised, which facilitates formation of transendothelial cell channels to allow bi-directional movement of inflammatory cells and molecules from the brain and systemic circulation.<sup>150-153</sup> Movement of inflammatory factors from the injured brain through the compromised BBB and into systemic circulation can lead to activation of the systemic

inflammatory response syndrome (SIRS). SIRS results in inflammatory cells from the circulation invading and damaging peripheral organs, including bone.<sup>154</sup> Additionally, increased circulating levels of other factors, which include epidermal growth factor (EGF), nerve growth factor (NGF), have been observed in the serum of patients following TBI.<sup>186</sup>

In addition to its central effects, TBI can cause post-traumatic hypopituitarism, which can lead to several chronic endocrinopathies, which include deficiencies in growth hormone (GH) and IGF-1.<sup>155</sup> GH deficiency can cause several metabolic disturbances, including reduced lean muscle mass, increased visceral and subcutaneous fat and reduced bone mass.<sup>156, 157</sup> Additionally, GH stimulates the synthesis of IGF-1, which is required for bone growth, bone mass acquisition and maintenance.<sup>158</sup> As such, GH and IGF-1 deficiency has been associated with an increased risk of bone fractures.<sup>156</sup>

TBI has also been associated with sympathetic hyperactivity, which is thought to be caused by the sharp increase in intracranial pressure.<sup>159-161</sup> Activation of the sympathetic nervous system following TBI causes large secretions of adrenaline and noradrenaline into the peripheral circulation in a dose-response fashion that is dependent on injury severity.<sup>161</sup> Adrenaline and noradrenaline have the potential to activate  $\beta$ -adrenergic receptors on various cell types including osteoblasts and can regulate expression of inflammatory mediators and other factors.<sup>162, 163</sup> Initial evidence from a human study suggests that there is a relationship between sympathetic hyperactivity and acute systemic inflammation post-TBI.<sup>161</sup>

### **1.8.1 Potential effect of TBI on bone**

A number of the previously discussed factors involved in secondary pathophysiological injury mechanisms of TBI have the potential to alter bone remodelling (see figure 1.5). TBI has been shown to i). compromise the BBB ii). increase the production of both inflammatory cytokines and reactive oxygen species (ROS) and iii). heighten sympathetic outflow. The

increased permeability of the BBB post-TBI facilitates the leakage of ROS and inflammatory factors from the injured brain into the systemic circulation.<sup>164</sup> Increased sympathetic nervous system activation may result in activation of  $\beta$ 2 adrenergic receptors on osteoblasts, which can stimulate bone resorption whilst suppressing bone formation;<sup>162</sup> while ROS can elicit the same effects.<sup>165, 166</sup> A number of inflammatory mediators that become up-regulated in circulation post-TBI (i.e. IL-1 $\beta$ , IL-6, IL-17 and TNF- $\alpha$ ) facilitate osteoclastogenesis and osteoclastic activation to result in increased bone resorption.<sup>52, 167</sup> In addition to these effects, TBI-induced deficiencies in GH and IGF-1 may also induce bone loss (Figure 1.5).<sup>156, 157</sup>

While the abovementioned factors may contribute to bone loss following TBI, numerous lines of evidence suggests that TBI can stimulate the formation of bone in soft tissues via a process referred to as neurological heterotopic ossification (NHO). NHO occurs in approximately 5-20% of patients with TBI and commonly occurs around the hip, elbow, knee and shoulder joints.<sup>168, 169</sup> The exact mechanisms responsible for NHO are unknown, therefore further studies are required to characterise factors that are involved in the pathogenesis of NHO,<sup>168</sup> however, *in vitro* studies have demonstrated that serum from rats that have undergone TBI caused increased proliferation of mesenchymal stem cells<sup>170</sup> and that CSF and serum from TBI patients increased osteoblastic proliferation.<sup>171, 172</sup> Conversely, studies have also reported lower bone mineral density and an elevated risk of fracture in brain-injured patients.<sup>173-176</sup> It is clear that TBI stimulates a number of physiological mechanisms that have the potential to affect bone and therefore experiments in this area require further investigation. Indeed, accumulating evidence suggests that TBI enhances the healing of concomitant long bone extremity fractures in a multitrauma setting.<sup>19, 177-183</sup>

### **1.8.2 Potential effect of TBI on bone fracture healing**

In the late 1980s, reports of TBI rapidly stimulating bone fracture callus formation began to accumulate, however, whether TBI influences fracture healing is yet to be established and

remains controversial.<sup>19, 178</sup> Other studies have shown a possible correlation between TBI severity and increased rate and size of callus formation, which may represent a form of NHO.<sup>184, 185</sup> Preliminary clinical studies have speculated TBI-induced promotion of callus formation was likely attributed to up-regulation of circulating levels of EGF, NGF and prolactin in patients with both TBI and bone fracture compared to those with fracture-only.<sup>186, 187</sup> Though clinical findings provide some evidence of altered healing of bone in TBI patients, there are several limitations and confounds including; variations in the location and mechanism of brain injury and ambiguous definitions of brain injury severity.

Results from rodent studies examining the effect of TBI on concomitant fracture healing vary, however, most suggest that callus volume is increased in multitrauma animals from between 2-8 weeks post-injury when compared to fracture-only animals.<sup>179-183</sup> Rat studies using the open-skull, controlled cortical impact (CCI) injury model of TBI and femoral fracture are most common. Results from these studies suggest the callus volume is increased at 4 weeks post-injury in multitrauma rats,<sup>179, 181, 182</sup> and can remain elevated even at 8 weeks post-injury.<sup>181, 182</sup> These studies by Wei et al.,<sup>182</sup> and Wang et al.,<sup>181</sup> reported an increased percentage of leptin-positive cells in the callus of multitrauma rats at 4 and 8 weeks post-injury, and elevated serum leptin concentration of multitrauma rats 8 weeks post-injury. This may indicate a possible association between serum and callus leptin levels and increased callus formation.<sup>181, 182</sup> Increased callus formation has also been observed in murine studies using the CCI injury model of TBI and femoral fracture.<sup>179, 180</sup> Callus volume was increased from 2 up to 4 weeks post-injury in the multitrauma group compared to fracture-only group. On the other hand, Locher and colleagues observed increased maximum torque of calluses from mice with TBI at 4 weeks post-injury when compared to calluses from fracture only mice, however, no difference in stiffness was found between the two groups.<sup>179</sup>

Despite closed-skull TBI (TBI in absence of skull fracture) being the most common form of TBI in humans, reports are scarce on the effect closed-skull TBI has on fracture healing. In a closed-skull weight-drop TBI model, femoral fracture calluses from multitrauma rats were stiffer and smaller than calluses from fracture-only rats, however, fractures from brain-injured rats displayed no differences in torsional strength when compared to calluses from fracture-only rats.<sup>170</sup> These findings conflict with the aforementioned studies that used an open-skull CCI TBI.<sup>179-183</sup> Given there have been reports suggesting that osteogenesis is enhanced in distant skeletal sites following burr hole defect in rat tibiae, the craniotomy performed to administer the CCI may, however, be a confounding variable.<sup>188</sup> Other factors may also contribute to the differences observed between callus volumes of open- and closed-head multitrauma models, however, without a craniotomy + fracture group, the potential osteogenic effects of the craniotomy cannot be ruled out. Furthermore, the lack of histomorphometric and  $\mu$ CT data in closed-skull rodent models and conflicting results between open- and closed-skull models, warrants further characterisation of closed-skull multitrauma models.

### **1.8.3 Treatment**

TBI is recognised as a serious global health concern; however, currently there are no therapeutic agents that enhance long-term outcomes for patients with TBI. The delayed and progressive nature in which neurodegeneration occurs, however, may provide a window for a therapeutic agent to enhance recovery.<sup>139</sup> Several phase III prospective clinical trials have failed, which may in part be due to the heterogeneity of clinical TBI, but it may also due to the complex, interactive nature of secondary injury mechanisms initiated following TBI.<sup>20, 189</sup>

A recent proteopathy identified to likely contribute to secondary brain damage is the hyperphosphorylation of the protein “tau”.<sup>20</sup> Intra-axonal accumulations of tau and hyperphosphorylated tau have been identified in brains of patients following TBI, as well as

several other neurodegenerative conditions such as Alzheimer's disease.<sup>21</sup> Tau is a microtubule associated protein that in a normal state constantly binds and un-binds from microtubules, however, when tau is excessively hyperphosphorylated it dissociates from microtubules to cause destabilization and disruption of cellular function.<sup>190</sup> Tau phosphorylation is regulated by protein kinases and tau phosphatases.<sup>190</sup> Protein phosphatase 2A (PP2A) heterotrimers that consist of the PR55 regulatory B-subunit (PP2A/PR55) are the major tau phosphatases in the human brain.<sup>191-193</sup> Downregulation of PP2A/PR55 has been demonstrated to promote hyperphosphorylation of tau,<sup>194</sup> which is attenuated by activation of PP2A/PR55 via treatment with sodium selenate.<sup>21, 195-197</sup> Recently, a 12 week sodium selenate treatment regimen in rats given a TBI significantly increased brain tissue levels of PP2A/PR55 and reduced tau phosphorylation, brain damage and behavioural impairments in rats following TBI compared to controls.<sup>21</sup> Therefore, pharmacologically targeting PP2A/PR55 and hyperphosphorylated tau with sodium selenate may be a novel therapeutic approach to improve clinical outcome following TBI. In doing so, sodium selenate treatment has the potential to effect bone either through attenuation of the brain injury or by directly influencing skeletal cells. A previous study has reported morphological changes in epiphyseal plates of rats treated with sodium selenate, however, the dose was greater (4.88 mg/kg/day)<sup>198</sup> than that found to reduce neurodegeneration post-TBI (1 mg/kg/day).<sup>21</sup> Furthermore, a major metabolite of sodium selenate is sodium selenite, which has been shown to induce growth retardation in rats.<sup>199, 200</sup>

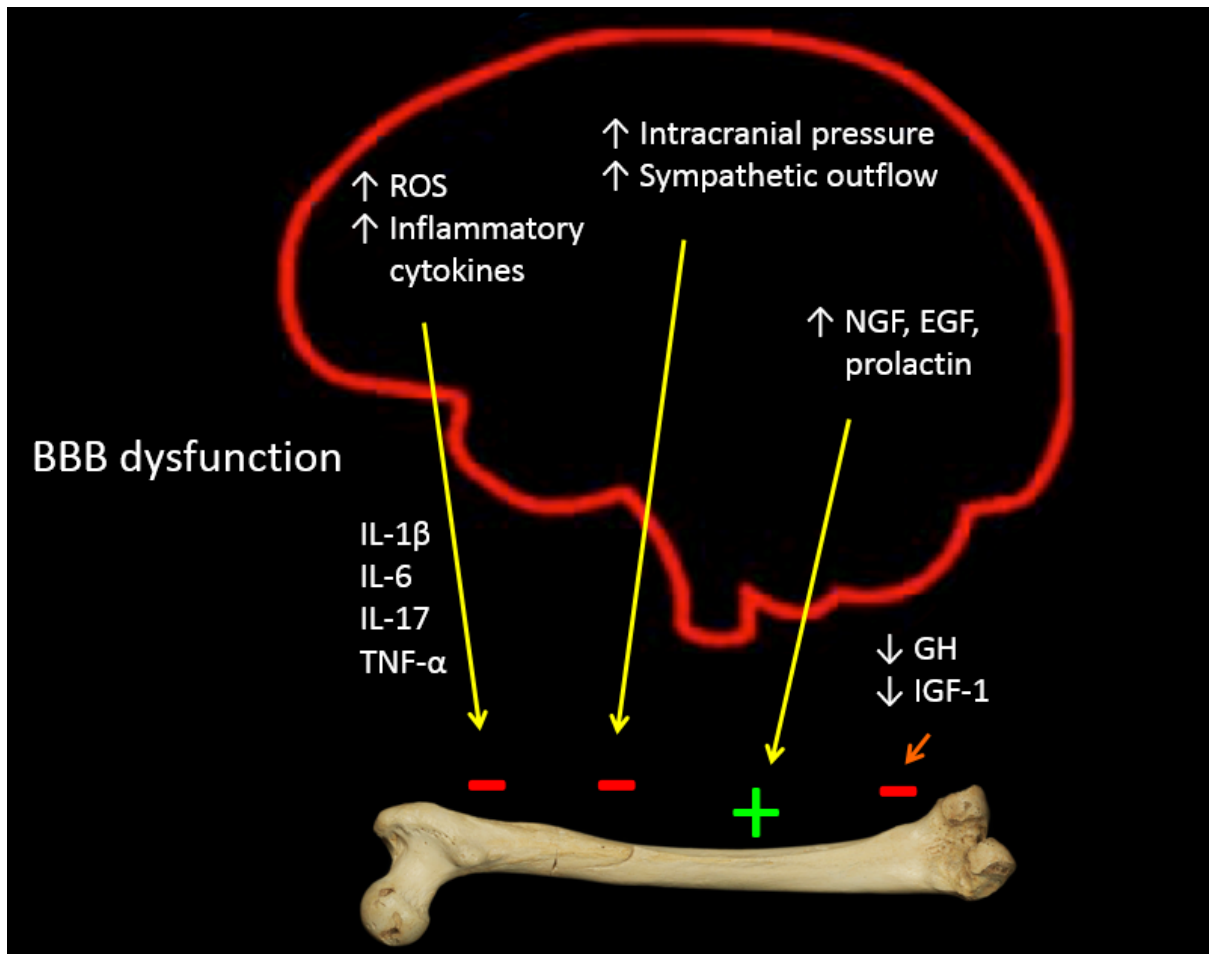


**Figure 1.5.** Possible pathways through which TBI may alter bone metabolism. Secondary injury processes of TBI include elevated levels of pro-inflammatory cytokines as well as heightened sympathetic outflow and reduced levels of GH and IGF that can cause a reduction in bone mineral density (red -). Conversely heightened levels of NGF and EGF have been associated with increased bone formation (green +).

### 1.9 Summary and aims

T $\beta$ <sub>4</sub> promotes healing in a number of tissues. However, the influence of T $\beta$ <sub>4</sub>-treatment on fracture healing is unknown. Hence, the aim of Chapter 1 was to determine whether T $\beta$ <sub>4</sub>-treatment could accelerate fracture healing in mice. The aim of Chapter 2 was to extend upon the findings of Chapter 1 and to examine the effect of treatment with T $\beta$ <sub>4</sub> on OPC proliferation, differentiation and mineralization and to identify the underlying signal transduction pathways involved. The second aim of this chapter was to establish the effect that T $\beta$ <sub>4</sub>-derived fragments 1-4 (Ac-SDKP), 1-15 (Ac-SDKPDMAEIEKFDKS) and 17-23 (LKKKTETQ) had on OPC proliferation, differentiation and mineralization.

TBI has long been associated with bone formation and enhanced fracture healing, however in a clinical setting, brain-injured patients display reduced bone mineral density (BMD). Therefore, the aim of Chapter 3 was to investigate the affect experimental TBI had on bone quantity. Chapter 4 aimed to determine whether sodium selenate treatment altered TBI-induced changes in bone and to see whether sodium selenate had a toxic effect of skeletal cells. Upon determining the role TBI had on homeostasis of un-injured bone, the aim of chapter 5 was to investigate whether closed-skull TBI enhanced fracture healing.

## **2 The effect of T $\beta$ <sub>4</sub> treatment on fracture healing in a murine model**

The information presented in this chapter has been published prior to the completion of this thesis. Journal article: **Brady R.D.,** Grills B.L., Schuijers J.A., Ward A.R., Tonkin B.A, Walsh N.C and McDonald S.J. (2014). Thymosin beta 4 administration enhances fracture healing in mice. *J Orthop Res.* 32(10): 1277-1282.

## 2.1 Introduction

T $\beta$ <sub>4</sub> is a small, naturally occurring peptide that is expressed by most cells. T $\beta$ <sub>4</sub> is found in particularly high concentrations at the site of tissue injury, which suggests that endogenous T $\beta$ <sub>4</sub> plays a role in tissue repair and regeneration.<sup>91</sup> Recently, several studies have demonstrated the therapeutic potential of T $\beta$ <sub>4</sub> administration for stimulating healing of dermal, corneal, and cardiac injuries.<sup>18, 93, 94</sup> Such T $\beta$ <sub>4</sub>-induced promotion of tissue repair has been attributed to several regenerative properties of the peptide that includes: enhancement of stem cell recruitment and differentiation,<sup>98, 201</sup> stimulation of cell survival,<sup>96</sup> modulation of wound site inflammation,<sup>96, 97</sup> prevention of bacterial infection,<sup>202</sup> and promotion of angiogenesis.<sup>100, 203</sup> Further adding to the therapeutic potential of T $\beta$ <sub>4</sub> is that the peptide is quite small (4,964 Da) and does not bind to heparin, which permits T $\beta$ <sub>4</sub> to freely diffuse into tissues and exert its regenerative effects.<sup>17</sup> Furthermore, T $\beta$ <sub>4</sub> is widely considered a safe molecule for therapeutic use, with several animal studies and human clinical trials reporting no adverse effects due to T $\beta$ <sub>4</sub> treatment.<sup>17</sup> Despite the therapeutic potential of T $\beta$ <sub>4</sub> stimulating tissue regeneration, no studies have analysed whether T $\beta$ <sub>4</sub> can also promote healing of long bone fractures.

We hypothesized that T $\beta$ <sub>4</sub> treatment is likely to be beneficial to bone fracture healing, largely due to the well-documented cellular and molecular similarities in the healing processes of bone fractures and the aforementioned soft tissue injuries shown to benefit from T $\beta$ <sub>4</sub> treatment. Firstly, the mitogenic and chemotactic properties of T $\beta$ <sub>4</sub> may enhance osteoprogenitor cell differentiation and recruitment, thereby enhancing the initiation of the repair process. T $\beta$ <sub>4</sub> could also stimulate osteoblastic or chondrocytic differentiation and by

this means increase intramembranous or endochondral ossification. Furthermore, the well-documented pro-angiogenic properties of T $\beta$ <sub>4</sub> may importantly enhance re-vascularization of the fracture site. Finally, T $\beta$ <sub>4</sub> has also been shown to promote wound MMP expression,<sup>120</sup> suggesting T $\beta$ <sub>4</sub> may stimulate matrix remodelling in healing fractures. We hypothesized that if T $\beta$ <sub>4</sub> is able to stimulate any of the aforementioned processes it will likely accelerate bone fracture healing.

Though no studies have reported the effects of T $\beta$ <sub>4</sub> on bone fracture healing, recent preliminary studies suggest T $\beta$ <sub>4</sub> may have potential to enhance bone formation following injury.<sup>125, 126</sup> Intraperitoneal injections of T $\beta$ <sub>4</sub> (partial sequence) in rats with either a calvarial defect or an extracted tooth increased both the percentage cells possessing the osteoblastic transcription factor, Osx, and the fractional bone volume of the healing sites.<sup>125, 126</sup> Additionally, recent studies on the influence of T $\beta$ <sub>4</sub> on cultured odontoblasts provide preliminary evidence of the peptide's ability to promote odontogenic differentiation and formation of mineralized nodules.<sup>127</sup>

In the present study, we aimed to determine whether a series of T $\beta$ <sub>4</sub> injections could accelerate the healing of mid-shaft fibular fractures in mice. We hypothesized that the well-documented regenerative properties of T $\beta$ <sub>4</sub> would enhance both fracture callus formation and remodelling, thereby enhancing the restoration of mechanical integrity of healing fractures.

## **2.2 Methods**

### *2.2.1 Animal surgery and T $\beta$ <sub>4</sub> treatment*

This project was approved by the La Trobe University Animal Ethics Committee (AEC 11-18). Mice were housed individually under a 12-hour light/dark cycle and were given access to food and water *ad libitum* for the duration of the experiment. At the time of surgery, 16 week-old C57Bl/6 male mice (n = 40) weighing 25-30 g received a bilateral fibular

osteotomy whilst under isoflurane-induced anaesthesia. Transverse fractures were created at the midpoint of the tibia approximately 12 mm proximal to the calcaneal tuberosity with microtenotomy scissors as previously described.<sup>204</sup> Half the mice received a 6 mg/kg intraperitoneal (i.p.) injection of T $\beta$ <sub>4</sub> diluted in 100  $\mu$ l of sterile saline at the time of fracture and at 3, 6, 9 and 12 days post-fracture. This injection regimen has been previously shown to increase recovery of neurological function in mice.<sup>205</sup> The remaining mice received an i.p. injection of 100  $\mu$ l of sterile saline only (control) at the same time points as the T $\beta$ <sub>4</sub>-injected animals. Animals were randomly assigned to control and T $\beta$ <sub>4</sub>-treated groups. Fractures from controls and treated mice were harvested at 14 and 21 days post-fracture (6 mice per group) for analysis by  $\mu$ CT and histology, with the remaining 16 animals used to generate fractures that were analysed at 42 days post-injury by three-point bending (left fibula, 7-8 fractures per group) and  $\mu$ CT and histological analyses (right fibula, 4-5 fractures per group).

### 2.2.2 *Biomechanical assessment*

The effect of T $\beta$ <sub>4</sub> treatment on the mechanical properties of healing fibular fractures was assessed using a three-point bending test on calluses at 42 days post-fracture. Fibular fractures were dissected from tibia at autopsy, immersed in silicone oil and stored at -20°C until testing. Samples were allowed to equilibrate for 1 h at room temperature then mounted in the testing apparatus with the fulcrum directly overlying the previous fracture site. Samples were tested using the Mecmesin BFG 10N testing system (Mecmesin limited, UK; accuracy  $\pm$  0.25%, 1000 samples/s) and VectorPro Lite acquisition software (Mecmesin limited, UK). Each fibula was loaded at a constant rate of 1.67 mm/min, with load and deflection data recorded continuously using transducers connected to an x-y plotter digital by preamplifiers. After testing, the ends of each mechanically fractured callus were imprinted into dental wax. Using images of each imprint, cross-sectional (CS) areas (mm<sup>2</sup>) were measured using a Leica DMRBE microscope linked to a PC with Leica Qwin software (Leica

Microsystems, Wetzlar, Germany). The overall cross-sectional area of each callus at its breaking point was then calculated by averaging the measured areas of each mechanically-fractured end. Biomechanical properties of peak force to failure, stiffness, ultimate tensile stress and Young's modulus were calculated from the load deflection data. Mann-Whitney tests were used to compare biomechanical properties between samples of control and T $\beta$ <sub>4</sub>-treated mice.

### 2.2.3 $\mu$ CT

Fractured fibulae were fixed overnight in 4% paraformaldehyde in 0.1M sodium cacodylate buffer (pH 7.4) and stored at 4° C in 0.1M cacodylate buffer containing 10% sucrose (pH 7.4). Images were acquired using a Skyscan 1076 scanner (Bruker MicroCT) in 70% ethanol at 9  $\mu$ m voxel resolution, 0.5 mm aluminium filter, 48 kV voltage, 100  $\mu$ A current, 2400 ms exposure, rotation 0.5° across 180°, frame averaging of 1. Images were reconstructed using NRecon (version 1.6.3.1) and the following parameters: CS to image conversion, 0.0-0.11; ring artefact, 6; pixel defect mask, 5%; and beam hardening correction, 35%. Following reconstruction, the region of interest (ROI) for each bone was determined using CTAN (version 1.11.8.0, Bruker MicroCT) as being a 3 mm region longitudinally centred on the callus (i.e. 1.5 mm either side of the fracture line of the callus); the border of the callus was manually traced. Old cortical bone was excluded using threshold delineation (global threshold > 100) to allow quantification of new bone formation. Quantification of structural parameters was performed using 2 greyscale thresholds in order to distinguish between new mineralized tissue and new highly mineralized tissue. Thresholds were determined using the automatic "otsu" algorithm within CTAn, visual inspection of images and qualitative comparison with histological sections. The algorithms used for structural analysis were as follows: new mineralized tissue (MT) - global threshold of 53-100 and new highly mineralized tissue (HMT) - global threshold of 77-100. 2D and 3D data were generated for

all analyses and 3D models were generated using the “marching cubes” algorithm from thresholded data (in CTAn) and coloured according to threshold (in ParaView version 4.1.0, Kitware Inc. Clifton Park, NY). MicroCT image reconstructions of longitudinal, mid-point hemi-calluses were colour-coded according to the degree of mineralization; red - new mineralized tissue, green - new highly mineralized tissue and blue - original cortical bone. For publication, colour-coded  $\mu$ CT images were imported into Adobe Photoshop Elements 5.0 (Adobe Systems Inc) and the original grey background of the  $\mu$ CT images was converted to a white background to highlight these above three colours i.e. red, green and blue. Following imaging, calluses were prepared for histology.

Mann-Whitney tests were used to compare differences in total volume of the callus (TVc), new mineralized tissue volume of callus (MTVc), new highly mineralized tissue volume of callus (HMTVc), MTVc/TVc (fractional volume of new mineralized tissue) and HMTVc/TVc (fractional volume of new highly mineralized tissue) between samples of control and T $\beta$ <sub>4</sub>-treated mice.

#### *2.2.4 Histological processing, staining and histomorphometry*

Scanned specimens were dehydrated using a graded series of ethanols (70%, 90%, and 100% for 1 h in each solution) and then stored overnight in 100% ethanol at room temperature. Samples were then immersed in chloroform for 2 h changed every hour, to defat the marrow and this was followed by immersion in 100% ethanol for 2 h (changed every hour) before plastic embedding.

Samples were placed in a solution of equal parts 100% ethanol and LR White resin (London Resin Company limited, Reading, England) for 3 h prior to being placed under vacuum for 24 h in LR White resin. Following this, samples were polymerized in LR White resin at 60°C for 24 h in glass moulds. Moulds were broken to release blocks.

Three micron thick longitudinal sections were cut at the midpoint of undecalcified callus on a Leica RM 2155 Rotary Microtome (Leica, Wetzlar, Germany) with a tungsten carbide blade. Sections were stained using Goldner's modification of Masson's trichrome stain. Four sections per group were examined and photographed on a Leica DMBRE microscope. Sections of calluses were assessed both qualitatively and quantitatively. To identify whether  $T\beta_4$  treatment influenced the amount of bone in callus, the area of each callus that contained old cortical bone (identified via its compact/lamellar appearance), new trabecular bone (new non-lamellar bony spicules forming on old cortical bone as well as within callus) and marrow was measured using Leica Qwin software. Composition of calluses from control and  $T\beta_4$ -treated mice were compared using Mann-Whitney tests.

## **2.3 Results**

### *2.3.1 Mechanical testing*

Biomechanical data for 42 day fractures in control and treated mice are shown in Table 2.1. Peak force to failure of fracture samples increased around 41% in  $T\beta_4$ -treated mice compared with control equivalents ( $p < 0.01$ ). Treatment with  $T\beta_4$  also increased stiffness by approximately 26% when compared with control samples ( $p < 0.05$ ). There were no significant differences in cross sectional area, ultimate tensile stress or Young's modulus.

**Table 2.1.** Mechanical characteristics of control and T $\beta$ 4-treated samples at 42 days post-fracture.

Treatment		Peak force (N)	Stiffness (x 10 <sup>4</sup> Nm <sup>2</sup> )	CSA (x 10 <sup>-7</sup> m <sup>2</sup> )	UTS (x 10 <sup>7</sup> Nm <sup>-2</sup> )	YM (x 10 <sup>9</sup> Nm <sup>-2</sup> )
Saline (n = 7)	Mean	2.95	3.77	3.65	1.80	5.33
	± SEM	(0.31)	(0.20)	(0.31)	(0.26)	(0.82)
T $\beta$ <sub>4</sub> (n = 8)	Mean	4.17	4.76	4.05	2.13	4.98
	± SEM	(0.33)	(0.40)	(0.19)	(0.23)	(0.48)
P value		< 0.01	< 0.05	0.25	0.22	0.87

CSA = cross-sectional area, UTS = ultimate tensile stress, YM = Young's modulus. Values are means ± SEM.

### 2.3.2 $\mu$ CT analyses

Analysis of calluses from 14 and 21 day treated and control mice is shown in Table 2.2. Analysis of 14 day calluses showed no differences in any of the measured parameters between the two groups. At 21 days post-fracture, the fractional volume of new mineralized tissue (MTV<sub>c</sub>/TV<sub>c</sub>) was approximately 18% greater in calluses from T $\beta$ <sub>4</sub>-treated mice compared to controls ( $p < 0.01$ ). At this time-point, the fractional volume of new highly mineralized tissue (HMTV<sub>c</sub>/TV<sub>c</sub>) was approximately 26% larger in T $\beta$ <sub>4</sub>-treated mice compared to controls ( $p < 0.05$ ). These changes are depicted in longitudinal, midpoint 3D reconstructions of representative hemi-calluses in Figure 2.1a,b. There were no significant differences in TV<sub>c</sub>, MTV<sub>c</sub> or HMTV<sub>c</sub> at 21 days post-fracture between the two groups.

MicroCT analysis of 42 day calluses was not possible using the threshold settings appropriate to analyse 14 and 21 day samples. Specifically, though our threshold settings allowed for accurate differentiation between old cortical bone (global threshold > 100) and newly formed mineralized tissue (global threshold of 53-100) in calluses at 14 and 21 days post-fracture;

such differentiation was not possible in 42 day calluses as the degree of mineralization of new bone was approaching that of existing cortical bone, thus precluding discreet delineation for these two tissues. There were no differences in the volume of mineralized tissue within calluses between control and treated groups at 42 days post-fracture (results not shown).

### *2.3.3 Histology and Histomorphometric Analysis*

Qualitative histological assessment of calluses at 14 day post-fracture showed no discernable difference between control and treated groups (results not shown). At 21 days post-fracture however, there was an obvious increase in the proportion of new trabecular bone in  $T\beta_4$ -treated calluses compared to controls (Figure 2.1c,d). By 42 days there was no obvious qualitative difference in the histological appearance of calluses between control and treated mice (results not shown). It was noted that cartilage was minimally present or absent in all control and  $T\beta_4$ -treated calluses at all three time points. Data obtained from histomorphometric analysis are shown in Figure 2.2. The histomorphometric data reflected the qualitative histological assessment of calluses. At 14 days post-fracture, there were no differences in callus area, total bone area, old cortical bone area, new trabecular bone area, percentage of new trabecular bone or percentage of total bone between the treated and control groups. At 21 days post-fracture, however, calluses from  $T\beta_4$ -treated mice were almost 23% smaller (Figure 2.2a,  $p < 0.05$ ), had nearly 47% less old cortical bone (Figure 2.2c,  $p < 0.05$ ) and had approximately a 31% increase in new trabecular bone area/total callus area fraction compared with controls (Figure 2.2f,  $p < 0.05$ ). There were no differences in area of total bone, area of new trabecular bone or percentage of total bone between treated and control calluses at 21 days. There were no histomorphometric differences in 42 day calluses between the two groups and all bone in calluses of both groups at this time was cortical (lamellar) in appearance (results not shown).

**Table 2.2.**  $\mu$ CT analysis of control and T $\beta_4$ -treated calluses at 14 and 21 days post-fracture.

	TV <sub>C</sub>	MTV <sub>C</sub>	HMTV <sub>C</sub>	MTV <sub>C</sub> /TV <sub>C</sub>	HMTV <sub>C</sub> /TV <sub>C</sub>
	(mm <sup>3</sup> )	(mm <sup>3</sup> )	(mm <sup>3</sup> )	(%)	(%)
<u>14d callus</u>					
Saline (n = 6)	1.70 (0.36)	0.49 (0.08)	0.16 (0.01)	30.73 (2.96)	11.46 (2.38)
T $\beta_4$ (n = 5)	1.51 (0.24)	0.50 (0.07)	0.18 (0.03)	33.65 (3.37)	11.71 (0.95)
P value	0.56	1.00	0.79	0.66	0.43
<u>21d callus</u>					
Saline (n = 5)	1.74 (0.10)	0.69 (0.06)	0.28 (0.02)	39.57 (2.00)	16.18 (1.07)
T $\beta_4$ (n = 6)	1.38 (0.20)	0.65 (0.10)	0.29 (0.05)	46.79 (1.40)	20.39 (1.10)
P value	0.13	0.54	1	< 0.01	< 0.05

TV<sub>C</sub> = tissue volume of callus, MTV<sub>C</sub> = new mineralized tissue volume of callus, HMTV<sub>C</sub> = new highly mineralized tissue volume of callus, MTV<sub>C</sub>/TV<sub>C</sub> = new mineralized tissue fraction of callus, HMTV<sub>C</sub>/TV<sub>C</sub> = new highly mineralized tissue fraction of callus. Values are means  $\pm$  SEM.

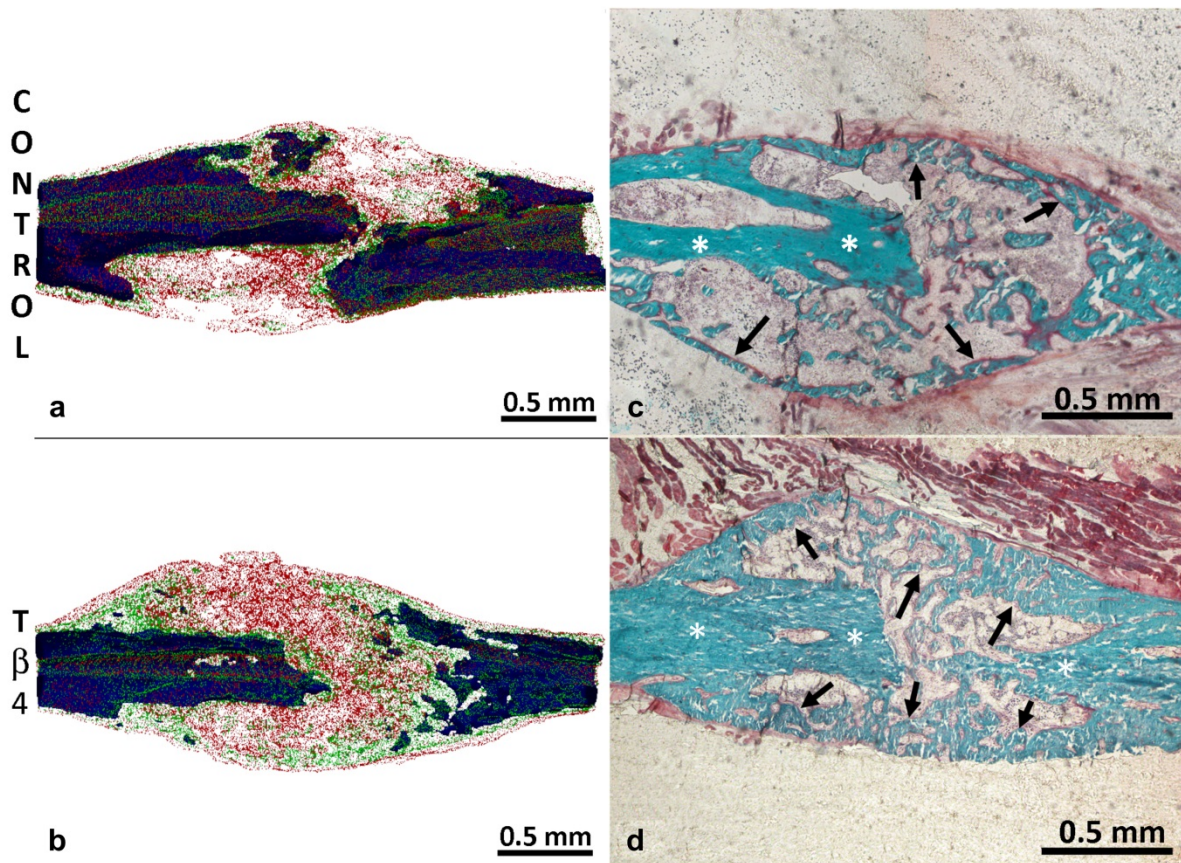


**Figure 2.1.** Longitudinal, mid-point views of representative  $\mu$ CT 3D reconstructions of 21 day fracture hemi-calluses from both control (a) and  $T\beta_4$ -treated mice (b) and corresponding representative histological sections of the same calluses for controls (c) and  $T\beta_4$ -treated animals (d). For  $\mu$ CT images, reconstructions are colour-coded according to the degree of mineralization; red - new mineralized tissue (global threshold 53-100), green - new highly mineralized tissue (global threshold 77-100), blue - original cortical bone (global threshold > 100). Note the increased proportion of both new mineralized tissue (red) and new highly mineralized tissue (green) in  $T\beta_4$ -treated callus (b) compared with control callus (a). Histological assessment shows that  $T\beta_4$ -treated callus (d) had a larger fraction of new trabecular bone (arrows) compared to control callus (c). (\* = old cortical bone, Goldner's trichrome stain; Histology original magnifications x50).

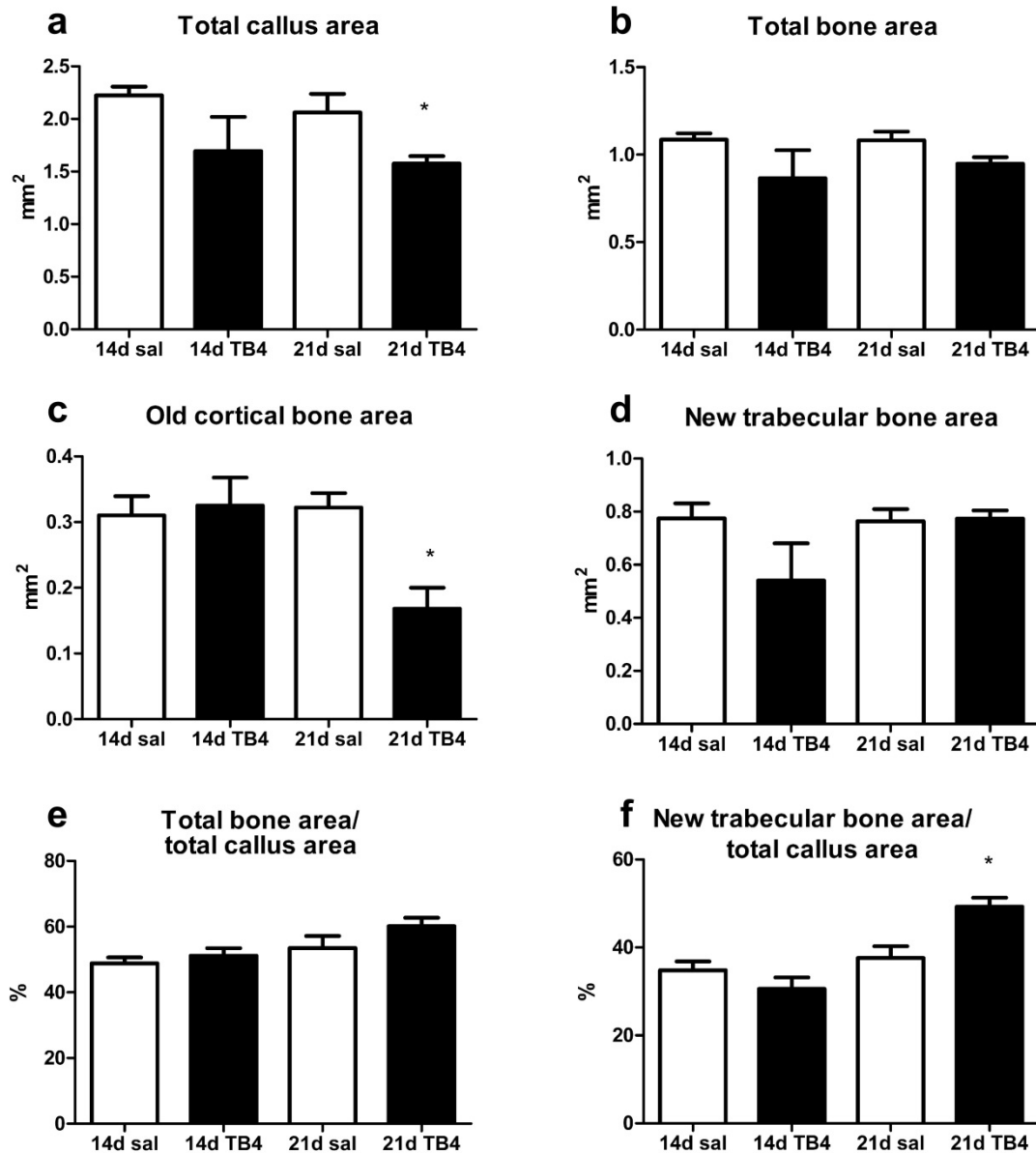


**Figure 2.2.** Histomorphometric analysis of bone parameters at 14 and 21 days post-fracture. Total callus area and old cortical bone area was less at 21 days in T $\beta$ <sub>4</sub>-treated mice compared to controls (a, c, \*p < 0.05). Percentage of new trabecular bone area/total callus area was greater in T $\beta$ <sub>4</sub>-treated mice 21 days post-fracture (f, \*p < 0.05; n = 5 per group). No difference between treated and control groups was observed in any parameter at 14 days post-fracture (a-f; n = 4 per group).

## 2.4 Discussion

This study demonstrates for the first time the therapeutic potential of the regenerative peptide T $\beta$ <sub>4</sub> in treating bone fractures. When compared with healing fibular fractures from saline-treated mice, fractures from animals treated with T $\beta$ <sub>4</sub> had higher fractional bone volume at 21 days post-fracture and increased mechanical integrity at 42 days post-fracture.

Overall, results from our study support the recent findings demonstrating the potential of T $\beta$ <sub>4</sub> to induce bone formation.<sup>125, 126</sup> Three-point bending analysis revealed that calluses from T $\beta$ <sub>4</sub>-treated mice had increased peak force to failure when compared with calluses from control mice, which demonstrates that T $\beta$ <sub>4</sub> treatment may have the potential to reduce re-fracture risk, particularly given that long bones such as the fibula often experience significant bending moments in vivo.<sup>206</sup> Furthermore, fractures from T $\beta$ <sub>4</sub>-treated mice also displayed greater stiffness, which indicates that T $\beta$ <sub>4</sub> treatment is likely to reduce the risk of callus deformation upon loading. Degree of bone stiffness is recognized to strongly correlate to the extent of mineralization,<sup>207, 208</sup> therefore our finding of superior callus stiffness in T $\beta$ <sub>4</sub>-treated mice may indicate that treatment enhanced callus formation and mineralization. This rationale was supported by the  $\mu$ CT results, with T $\beta$ <sub>4</sub>-treated calluses featuring increased fractional volume of new mineralized tissue and new highly mineralized tissue. Increased bone stiffness has been associated with micro-fracture, therefore, future studies would benefit from examining the prevalence of micro-fracture in T $\beta$ <sub>4</sub>-treated mice at chronic time-points (e.g. 6-12 months post fracture). Comparison of  $\mu$ CT and histological images revealed that calluses did not contain any cartilage or calcified cartilage and that it can therefore be assumed that all mineralized and highly mineralized tissue present was new bone formed by intramembranous ossification. Histological results confirmed the notion that T $\beta$ <sub>4</sub>-treatment enhanced formation of bone during fracture healing; there were no differences in bone fractions in 14 day callus, however, by 21 days post-fracture, calluses from T $\beta$ <sub>4</sub>-treated

animals contained significantly higher new trabecular bone fractions than those from controls.

Though these findings provide evidence that T $\beta$ <sub>4</sub> promotes bone fracture healing, the precise cellular and molecular mechanisms through which they occur remains to be determined. mRNA analysis of granulation tissue found in sockets 3 days post-tooth extraction, found T $\beta$ <sub>4</sub> treatment had increased expression of genes associated with angiogenesis and cell proliferation whilst also reducing expression of inflammatory cytokines.<sup>125</sup> These initial findings indicate that T $\beta$ <sub>4</sub> may also promote healing of bone fractures via mechanisms similar to that reported in healing of other tissues.<sup>17</sup> In addition to promoting these nonspecific regenerative processes, recent *in vitro* studies on the influence of T $\beta$ <sub>4</sub> on odontoblasts suggest that T $\beta$ <sub>4</sub> has the potential to increase expression of bone-specific growth factors, BMP-2 and BMP-4, as well as osteoblastic transcription factors, Runx2 and Osx.<sup>127</sup>

Results from this study also provide preliminary evidence that T $\beta$ <sub>4</sub> may accelerate bone remodelling during fracture healing, with calluses from treated animals tending to be smaller in area and containing reduced old cortical volumes at 21 days post-fracture. T $\beta$ <sub>4</sub> has been shown to increase expression of several MMPs during soft tissue wound healing, with researchers concluding that the peptide may promote remodelling of extracellular matrix following injury. Several studies have demonstrated the important role of MMPs in regulating the remodelling of callus at various stages post-fracture.<sup>73</sup> Therefore it is possible T $\beta$ <sub>4</sub> may have increased callus MMP expression and thereby promoted remodelling during healing. Future studies will look at the expression of MMPs in callus post-T $\beta$ <sub>4</sub> treatment and analyse the potential for T $\beta$ <sub>4</sub>-induced promotion of remodelling during fracture healing.

Studies are underway to assess the possible mechanism by which T $\beta$ <sub>4</sub> enhances fracture healing. We hypothesize the multiple tissue regenerating properties of T $\beta$ <sub>4</sub> may also promote

healing of bone fractures in humans and this peptide may prove to be an effective therapeutic treatment to accelerate fracture healing.

### **3 The influence of T $\beta$ <sub>4</sub> treatment on proliferation, differentiation and mineralization of osteoblast-like cells**

### 3.1 Introduction

The previous chapter provided evidence for the first time that the regenerative properties of T $\beta$ <sub>4</sub> may also extend to the healing of fractured bone.<sup>125, 126</sup> Fibular fracture calluses from T $\beta$ <sub>4</sub>-treated mice at 21 days post-fracture had increased fractional bone volume compared to calluses of control-treated mice and at 42 day post-fracture, T $\beta$ <sub>4</sub>-treated calluses displayed superior mechanical properties. The mechanisms through which T $\beta$ <sub>4</sub> enhanced healing, however, were not elucidated. As found in other tissue injury models, T $\beta$ <sub>4</sub> may have promoted healing of bone by modulating inflammatory processes,<sup>102</sup> increasing cell migration,<sup>18, 111-113</sup> cell survival,<sup>104, 106, 107</sup> enhancing vascularisation,<sup>117</sup> and promoting the orderly deposition of collagen.<sup>99, 105, 121</sup> Another possible explanation for T $\beta$ <sub>4</sub> enhancing fracture healing may be that T $\beta$ <sub>4</sub> acts directly on cells of osteoprogenitor/osteoblastic lineage to stimulate bone formation.

Recent findings support a possible direct effect of T $\beta$ <sub>4</sub> on bone cells. An *in vitro* study on immortalized odontoblasts (cells with phenotypical and functional similarities to osteoblasts) found that T $\beta$ <sub>4</sub> treatment promoted differentiation and mineralization via the integrin/ILK/BMP signalling pathway.<sup>127</sup> In addition, the authors reported that inhibition of T $\beta$ <sub>4</sub> by siRNA attenuated odontoblast differentiation, which indicated that differentiation was mediated by a T $\beta$ <sub>4</sub>-dependent mechanism.<sup>127</sup> Subsequent investigations have also reported that T $\beta$ <sub>4</sub> treatment promoted differentiation and mineralization of immortalized human periodontal ligament cells, osteoblast-like cells (MG63) and cementoblasts via a similar mechanism.<sup>128</sup> Conversely, treatment of marrow-derived mesenchymal stem cells with T $\beta$ <sub>4</sub> reportedly inhibited osteogenic differentiation.<sup>129</sup> Taken together, these findings suggest that the direct effects of T $\beta$ <sub>4</sub> on osteoblast-like cells remain inconclusive.

Recent investigations on T $\beta$ <sub>4</sub> have focused on identifying the active sites/domains of the full peptide sequence that may be responsible for specific biological activities. Preliminary evidence suggests that i). the amino-terminal fragment that consists of amino acids 1-4 (Ac-SDKP) may modulate inflammation, ii). fragment 1-15 (Ac-SDKPDMAEIEKFDKS) could increase cell survival, and iii). fragment 17-23 (LKKTETQ) potentially promotes cell migration.<sup>92</sup> Actions of the fragments are in some cases more potent than intact T $\beta$ <sub>4</sub>,<sup>92</sup> while some active sites promote biological activities that full length T $\beta$ <sub>4</sub> does not.<sup>92</sup> In addition, small bioactive fragments also have other advantages over larger peptides, which include increased stability and higher specificity.<sup>92</sup> Despite initial evidence that suggested T $\beta$ <sub>4</sub> has the potential to increase bone formation,<sup>127, 128</sup> no studies have characterized the effect of T $\beta$ <sub>4</sub>-derived fragments on osteoblastic/osteoblast-like cells *in vitro*.

Accordingly, the first aim of this study was to provide insight as to how T $\beta$ <sub>4</sub>-treatment enhanced fracture healing by examining the mRNA levels of genes associated with angiogenesis, cell differentiation and mineralization within fibular fracture calluses. The second aim was to examine the effect of T $\beta$ <sub>4</sub> and T $\beta$ <sub>4</sub>-derived fragments, 1-4, 1-15 and 17-23 on proliferation, differentiation and mineralization of osteoblast-like cells

## 3.2 Materials and methods

### 3.2.1 *Animal surgery and T $\beta$ <sub>4</sub> treatment*

This project was approved by the La Trobe University Animal Ethics Committee (AEC 11-18). The contralateral fracture callus was harvested from mice used in Chapter 2. Briefly, thirty-six C57Bl/6 male mice were given bi-lateral fibular fractures and half the mice were treated with T $\beta$ <sub>4</sub> as previously described in chapter 2. Groups of mice were killed at 7, 14 and 21 days post-fracture (n = 6 per group, at each time-point). Each fibula was trimmed to 2 mm either side of the callus and one callus from each mouse was analysed using RT-PCR.

### 3.2.2 *RT-PCR of fracture calluses*

Total RNA was extracted from each callus using the Aurum<sup>TM</sup> Total RNA Fatty and Fibrous Tissue Kit (Bio-Rad, Hercules, CA, USA) and RNA purity and concentration were determined by spectrophotometer (NanoDrop 2000, Thermo Scientific MA, USA). Reverse transcription was performed from 100 ng of total RNA using the iScript<sup>TM</sup> cDNA Synthesis Kit (Bio-Rad, USA), and RT-PCR was performed using SsoFast<sup>TM</sup> EvaGreen<sup>®</sup> Supermix (Bio-Rad, USA) on an iQ<sup>TM</sup> 96-well PCR system (Bio-Rad, USA). Primers were made commercially by GeneWorks Pty Ltd (Adelaide, SA, Australia). Table 1 lists the details of forward and reverse sequences of primers used in this analysis. Each amplification reaction well contained 1  $\mu$ l of cDNA (50 ng input RNA) and 300nM of primer and was performed in triplicate. Thermal cycling conditions included initial denaturation at 95°C for 30 s, followed by 40 cycles of 95°C for 5 s and 55°C for 5 s. Melt curve analysis was performed post-cycling to confirm specificity of the amplified products. Relative quantification of mRNA expression was normalized to  $\beta$ -actin and expressed relative to calluses from control mice 7 days post-fracture using the  $2^{-\Delta\Delta C_t}$  method.

### 3.2.3 *Cells and reagents*

Kusa cells are a murine osteogenic progenitor cell line first isolated from bone marrow stromal cells.<sup>209</sup> Kusa-O cells are a subline of the original Kusa cell line, which, when incubated with ascorbate and  $\beta$ -glycerophosphate, develop an osteoblastic phenotype and form mineralized nodules.<sup>209</sup> The Kusa-O cells used in this study were kindly provided by Dr. Julian Quinn (Garvan Institute of Medical Research, Australia). Cells were cultured in growth media that consisted of  $\alpha$ -MEM supplemented with foetal bovine serum (FBS; 10% v/v), penicillin (50 U/ml); streptomycin (50  $\mu$ g/ml), L-glutamine (2mM) and Fungizone (0.75  $\mu$ g/ml) (Life Technologies Carlsbad, CA, USA) in a humidified atmosphere of 95% O<sub>2</sub> & 5% CO<sub>2</sub> at 37°C. Cells were used between passages 5 and 20 as Kusa-O cells have been reported to lose their capacity to mineralize after 25 passages.<sup>209</sup> Full length T $\beta$ <sub>4</sub> peptide was purchased from GenWay Biotech, Inc (San Diego, CA) and small T $\beta$ <sub>4</sub> derived peptide fragments 1-4 (ac-SDKP), 1-15 (ac-SDKPDMAEIEKFDKS) and 17-23 (LKKTETQ) were purchased from GL Biochem Ltd (Shanghai, China).

### 3.2.4 *Cell proliferation assay*

Cells were seeded at a density of  $3 \times 10^3$  cells/well in a 96 well plate. After cells had adhered to the plate (approximately 4 h), growth media was replaced with treatment media (growth media supplemented with 2% FBS rather than 10% FBS) either alone (control), supplemented with full-length T $\beta$ <sub>4</sub>, 1-4 fragment, 1-15 fragment or 17-23 fragment (all at 1  $\mu$ g/ml), or supplemented with IGF-1 (100 ng/ml) for 48 h. Additional treatments of growth media with 10% FBS (positive control) and serum-free growth media (negative control) were also used. Following the treatment period, cell proliferation was measured using CellTiter96 AQueous One Solution Reagent according to manufacturer's instructions (Promega, Madison WI, USA) and the absorbance read at OD490nm.

### 3.2.5 RT-PCR of *Kusa-O* cells

Cells were seeded in 6-well plates and differentiation was stimulated by incubation for 7 or 14 days in osteogenic media (OM; growth media supplemented with 50 µg/ml ascorbate and 10mM β-glycerophosphate), with medium replaced every second day. Treatments (1 µg/ml of Tβ<sub>4</sub>, 1-4, 1-15 or 17-23, respectively) were added for the entire differentiation treatment and replenished with each media change. This dose of Tβ<sub>4</sub> has been previously been shown to maximally stimulate differentiation and mineralization of osteogenic cells.<sup>127, 128</sup> RNA was isolated from samples by lysing cells in PureZOL (Bio-Rad, Hercules, CA, USA) according to manufacturer's instructions. RNA concentration, reverse transcription, primer details and thermal cycling conditions were as described above for calluses.

**Table 3.1.** RT-PCR primer sequences.

Gene		Sequence 5'-3'
β-actin	F	GCTGTGCTATGTTGCTCTAG
	R	CGCTGCTTGCCAATAGTG
VEGFα	F	GGCTGCTGTAACGATGAAG
	R	TCTGCTGTGCTGTAGGAAG
Runx2	F	ACTTCGTCAGCATCCTATCAG
	R	CAGCGTCAACACCATCATTC
Collα1	F	CACCAAACCTCAGAAGATGTAGG
	R	ACCAGGAGGACCAGGAAG
BMP-2	F	GTGTTGCTGCTTCCCCAGGTC
	R	TCCCTGTGTGGTCCACCGCAT
DMP-1	F	CGCCGATAAGGAGGATGATG
	R	GTGTGGTGTCTGTGGAGTC
Osteocalcin	F	TCTCTCTGACCTCACAGATCCC
	R	TACCTTATTGCCCTCCTGCTTG
ALP	F	AAACCCAGACACAAGCATTCC
	R	TCCACCAGCAAGAAGAAGCC

### 3.2.6 *Alkaline phosphatase (ALP) assay*

Cells were seeded in 6-well plates and differentiated for 14 days in OM in the presence of full length TB<sub>4</sub> or individual fragments as above. An ALP assay kit (Abcam) was used to detect ALP activity according to manufacturer's instructions and the absorbance read at OD405nm.

### 3.2.7 *Mineralization assay*

Cells were seeded in a 24-well plate and differentiated for 21 days in OM in the presence of full-length TB<sub>4</sub> or individual fragments as above. At 21 days, cells were fixed in 4% paraformaldehyde in 0.1M sodium cacodylate buffer (pH 7.4) for 30 min and rinsed with distilled water. Cells were then stained in 0.5% Alizarin Red S (Sigma-Aldrich, MO, USA) in distilled water pH 4.2 for 30 min.<sup>210</sup> Cells were washed and mineralization was imaged using a flatbed colour scanner. To elute the Alizarin Red S staining for quantification, 10% cetylpyridinium chloride (CPC) in 10mM sodium phosphate, pH 7.0 was added to each well, and the plate was incubated on a rotating platform overnight at room temperature.<sup>211</sup> CPC was eluted and the absorbance read at OD570nm.<sup>211</sup>

### 3.2.8 *Statistical analyses*

Unpaired t-tests were used to analyze callus mRNA expression for each time-point. A one-way ANOVA was used to analyze all other measures. Dunnett's post-hoc comparisons were carried out when appropriate. All data were analyzed using GraphPad Prism 6 (Graphpad Software, La Jolla, CA, USA) with significance defined as  $p < 0.05$ .

### 3.3 Results

#### 3.3.1 RT-PCR

Expression of VEGF $\alpha$  mRNA was significantly elevated in calluses from T $\beta$ <sub>4</sub>-treated mice at 21 days post-fracture when compared to control ( $p < 0.05$ ; Figure 3.1a), however these differences were not observed at day 7 or day 14 post-fracture. No differences were observed in callus mRNA expression of either Runx2 or Coll1 $\alpha$ 1 between T $\beta$ <sub>4</sub>-treated and control mice (Figure 3.1a-c).

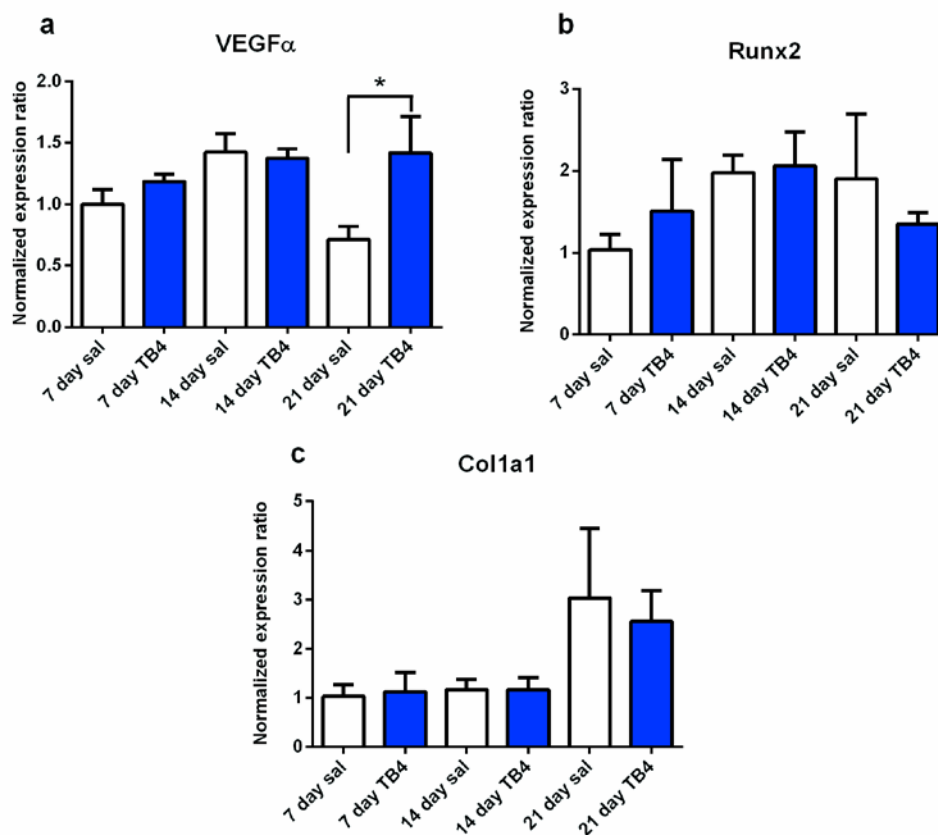


**Figure 3.1.** Gene expression in 7, 14, and 21 day-fracture callus. mRNA levels were normalized to  $\beta$ -actin and expressed relative to 7 day calluses from saline-treated control mice. VEGF $\alpha$  expression was increased 21 days post-fracture in the T $\beta$ <sub>4</sub>-treated group (a; \* $p < 0.05$ ), however no differences between treated and control groups were observed at 7 or 14 days post-fracture. No significant differences in mRNA expression of Runx2 or Coll1 $\alpha$ 1 were observed between treated and control group at any time point. Bars represent mean-fold expression  $\pm$  SEM ( $n = 6$  per group).

*In vitro* differentiation experiments revealed that mRNA expression of differentiation markers BMP-2 and DMP-1, were not significantly different at either 7 days (Figure 3.2a,b) or 14 days (Figure 3.3a,b) in T $\beta$ <sub>4</sub>, 1-4-, 1-15- or 17-23-treated cells, when compared to control. mRNA expression of the early stage differentiation marker Runx2 was not significantly different at 7 days in T $\beta$ <sub>4</sub>, 1-4-, 1-15- or 17-23-treated cells when compared to control (Figure 3.2c), while expression of late-stage differentiation markers OCN, ALP and Colla1, were not significantly different at 14 days in T $\beta$ <sub>4</sub>, 1-4-, 1-15- or 17-23-treated cells, when compared to control (Figure 3.3a-e).

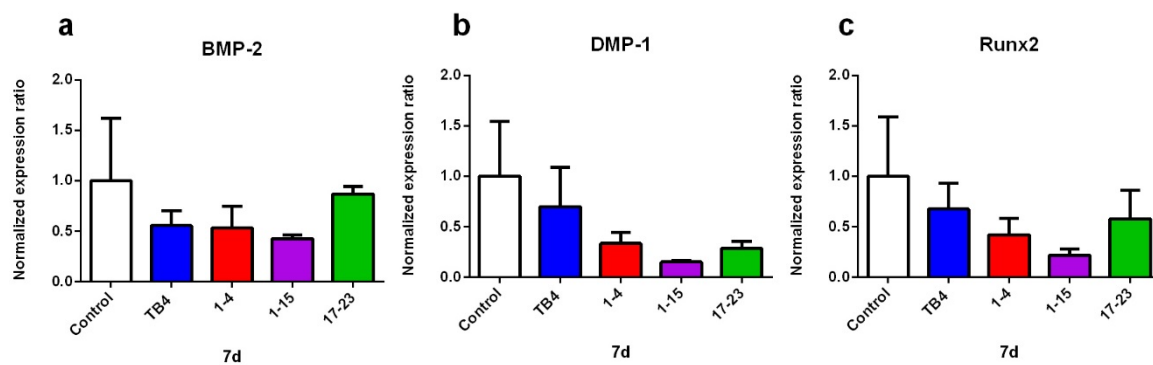


**Figure 3.2.** mRNA levels of early stage markers of osteoblastic differentiation following 7 days *in vitro*. Kusa-O cells were treated with T $\beta$ <sub>4</sub>, 1-4, 1-15 or 17-23 alone for 7 days. mRNA levels were normalized to  $\beta$ -actin and expressed relative to control. No differences in mRNA expression of any genes analysed were observed at 7 days between T $\beta$ <sub>4</sub>, 1-4, 1-15 17-23 groups when compared to controls (a-c). Bars represent mean-fold expression  $\pm$  SEM (n = 5-6 per group).

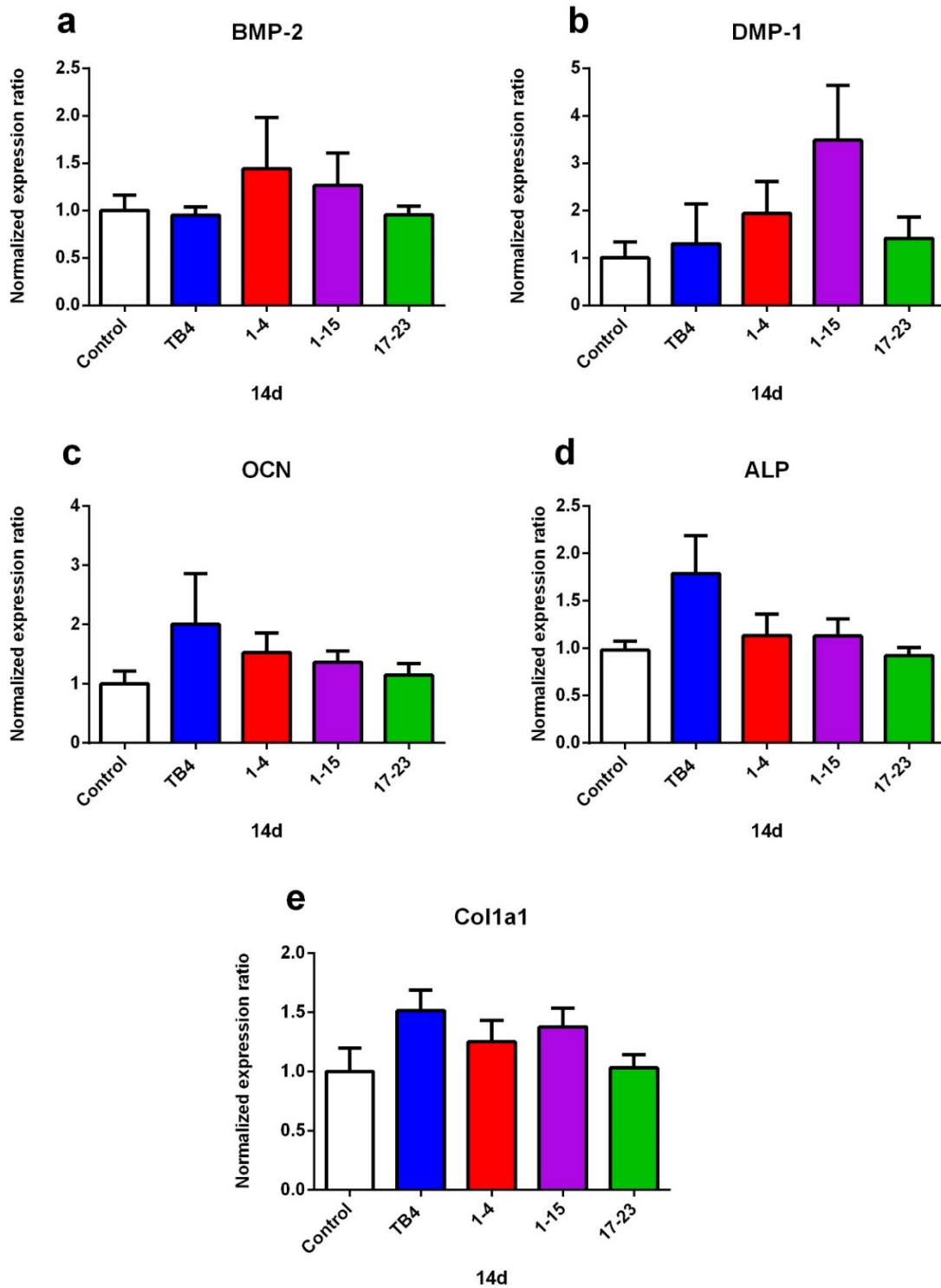


**Figure 3.3.** mRNA levels of osteoblastic differentiation markers following 14 days *in vitro*. Kusa-O cells were treated with Tβ<sub>4</sub>, 1-4, 1-15 or 17-23 alone for 14 days. mRNA levels were normalized to β-actin and expressed relative control. No differences in mRNA expression of any genes analysed were observed at 14 days between Tβ<sub>4</sub>, 1-4, 1-15 17-23 groups when compared to controls (a-c). Bars represent mean-fold expression ± SEM (n = 5-6 per group).

### 3.3.2 *Cell proliferation assay*

Proliferation of Kusa-O cells was significantly increased with IGF-1 and 10% serum, when compared to controls ( $p < 0.05$ ; Figure 3.4a), while proliferation was significantly reduced when cells were cultured in serum-free media ( $p < 0.0001$ ). There were no differences in proliferation of cells treated with  $T\beta_4$ , 1-4, 1-15 or 17-23 when compared to control.

### 3.3.3 *Alkaline phosphatase assay*

ALP activity of Kusa-O cells was not significantly different in  $T\beta_4$ , 1-4-, 1-15- or 17-23-treated cells when compared to controls (Figure 3.4b).

### 3.3.4 *Mineralization assay*

Mineralized nodule formation of Kusa-O cells was significantly reduced compared to control when cells were maintained in the absence of OM, however there were no differences in mineralized nodule formation of cells treated with  $T\beta_4$ , 1-4, 1-15 or 17-23 when compared to controls (Figure 3.4c).

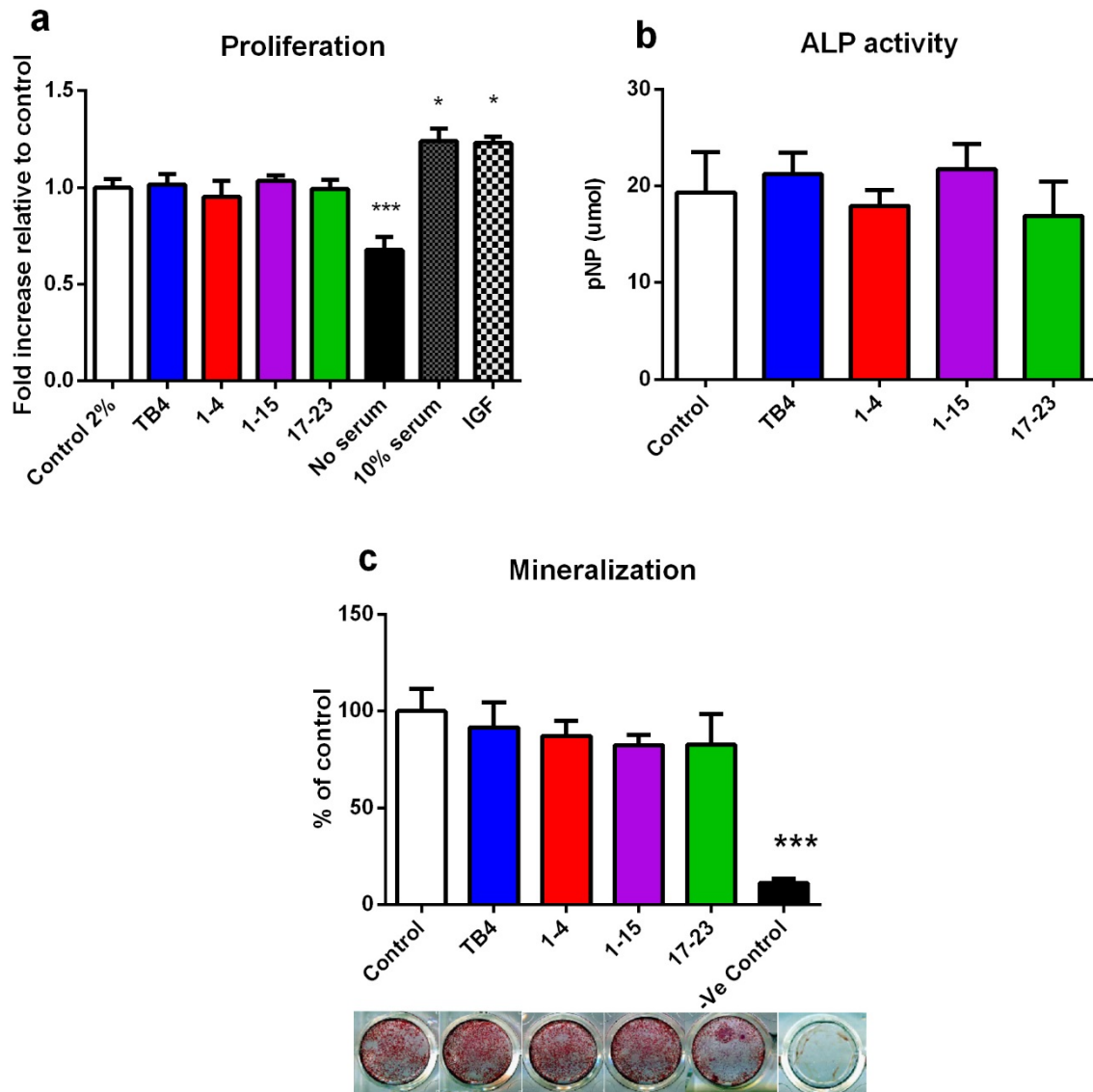


**Figure 3.4.** The effect of Tβ<sub>4</sub>, 1-4, 1-15 and 17-23 treatment on proliferation, differentiation (ALP activity) and mineralization. No differences in Kusa-O cell proliferation (a), ALP activity (b) or mineralization (c) were observed between Tβ<sub>4</sub>, 1-4, 1-15 17-23 groups when compared to controls. Bars represent mean ± SE. \*\*\*p < 0.001, \*p < 0.05 compared to control (n = 5-6 per group).

### 3.4 Discussion

The findings of Chapter 2 showed that T $\beta$ <sub>4</sub>-treatment enhanced healing of fibular fractures in a mouse model, however, the mechanisms through which T $\beta$ <sub>4</sub> enhanced healing were not determined. Accordingly here, the aims of these experiments were to i). examine mRNA expression of genes associated with angiogenesis, cell differentiation and mineralization in a fracture callus and ii). to investigate the effect of T $\beta$ <sub>4</sub>-treatment on osteoprogenitor-like cell proliferation, differentiation and mineralization. Furthermore, as smaller bioactive fragments of T $\beta$ <sub>4</sub> can stimulate biological activities that full length T $\beta$ <sub>4</sub> does not, in addition to having higher specificity and greater stability,<sup>92</sup> an additional aim was to investigate the effect of these bioactive T $\beta$ <sub>4</sub> fragments (1-4, 1-15 and 17-23) on osteoprogenitor-like cells. RT-PCR analysis revealed that mRNA expression of VEGF $\alpha$  was increased in 21-day fracture calluses from T $\beta$ <sub>4</sub>-treated mice when compared to control calluses, however no differences in mRNA expression of genes associated with osteoblastic differentiation or mineralization were observed between T $\beta$ <sub>4</sub>-treated and control calluses. In addition, cell culture investigations indicated that treatment of Kusa-O cells with either T $\beta$ <sub>4</sub>, 1-4, 1-15 or 17-23 did not significantly affect cell proliferation, expression of markers of osteoblastic differentiation, nor mineralized nodule formation *in vitro*.

The increased mRNA expression of VEGF- $\alpha$  at 21 days post-fracture in calluses from T $\beta$ <sub>4</sub>-treated mice may indicate that vascularisation of the fracture site was enhanced. Re-vascularisation is essential for successful healing of fractured bone. Inhibition of VEGF- $\alpha$  has been shown to result in delayed healing of experimental fracture models, while local administration of VEGF- $\alpha$  enhances healing.<sup>77</sup> Therefore, one possible mechanism through which T $\beta$ <sub>4</sub>-treatment enhances fracture healing may involve the stimulation of angiogenesis. Future investigations examining protein expression of VEGF- $\alpha$  and other associated angiogenic factors such as HIF-1 $\alpha$ , as well  $\mu$ CT imaging of callus to determine if T $\beta$ <sub>4</sub>-

treatment enhanced vascularisation, are required to confirm this hypothesis. It is however important to acknowledge that no differences in VEGF- $\alpha$  expression were found at 7 or 14 days post-fracture; therefore given that angiogenesis is thought to be particularly important in the early stages post-fracture, the contribution of elevated VEGF- $\alpha$  expression at 21 days post-fracture to the healing process may be negligible.

No differences in mRNA expression of genes associated with osteoblast differentiation or mineralization were observed between T $\beta_4$ -treated and control groups in either the *in vitro* or *in vivo* experiments. Though these findings provide evidence that osteoblastic formation and function may not be altered by T $\beta_4$  treatment, there are a number of other experiments that should be conducted in order to further establish the influence of T $\beta_4$  on osteoblasts. While *in vivo* experiments revealed no differences in callus mRNA expression of Runx2 and Coll1 $\alpha$ 1, it is possible that T $\beta_4$ -treatment increased expression of other genes associated with osteoblastic differentiation and mineralization and therefore these genes should be examined in future studies. In addition, it may be possible that *in vitro* T $\beta_4$  treatment stimulated ALP activity and mineralization at earlier time points than those featured in this study i.e. ALP activity before day 14 and mineralization prior to day 21, although the lack of stimulation of differentiation markers BMP-2, OCN, DMP-1 and Runx2 at 7 days suggests that this is unlikely.

Other studies using partial peptide sequences of T $\beta_4$  have similarly reported that T $\beta_4$ -treatment did not significantly increase mRNA expression of genes associated with osteoblastic differentiation and mineralization, which suggests that T $\beta_4$  enhances bone healing via mechanisms not directly associated with osteoblasts.<sup>125, 126</sup> A recent study used a rat tooth extraction model to evaluate the effects on bone formation of a 20 amino acid partial T $\beta_4$  peptide that corresponded to amino acids 17-37 of the full length fragment.<sup>125</sup> 17-37-treatment increased wound healing and bone formation in tooth extraction sockets.<sup>125</sup>

Specifically, 17-37 reduced apoptosis and inflammation at the site of injury and mRNA levels of inflammatory factors IL-1 $\alpha$ , IL1- $\beta$ , IL-6 and TNF- $\alpha$  were reduced in extraction sockets of 17-37 rats when compared to control.<sup>125</sup> In addition, the volume of granulation tissue at the site of injury and the mRNA expression of genes associated with angiogenesis, cell proliferation and migration were higher in T $\beta$ <sub>4</sub>-treated rats.<sup>125</sup> Of greatest relevance to bone formation in these tooth extraction sockets was the increased percentage of newly formed trabecular bone at 4 and 6 days post-injury in the T $\beta$ <sub>4</sub>-treated rats. Despite this, no differences in mRNA levels of osteogenic genes BMP-2,-7, ALP or OCN were observed between treated and control groups, which led the authors to suggest that 17-37 increased bone formation by stimulating cell proliferation and migration and angiogenesis at the injury site. A subsequent study by the same group featured a calvarial defect model to examine the osteogenic effects of a 27 amino acid sequence corresponding to amino acids 17-43 of the T $\beta$ <sub>4</sub> molecule.<sup>126</sup> 17-43 treated rats displayed an increased percentage of newly formed bone and an increased number of Osx-positive cells at the injury site. Expression of osteogenic genes 10-days post-injury did not differ between treated and control rats. The results of these studies may suggest that amino acids 1-16 of the T $\beta$ <sub>4</sub> molecule are required to directly stimulate osteoblastic differentiation and activity, or, as the results of the current study indicate, T $\beta$ <sub>4</sub> may stimulate bone formation indirectly, possibly through enhancing angiogenesis of the injury site.

The findings of this study and those mentioned above conflict with those of Lee et al.<sup>127, 128</sup> who reported T $\beta$ <sub>4</sub> treatment increased differentiation and mineralization of human dental pulp cells, human periodontal ligament cells and human cementoblasts (all cell types immortalized via transfection with human telomerase catalytic component) and osteoblast-like cells (MG63). Specifically, treatment with T $\beta$ <sub>4</sub> increased mRNA expression of differentiation markers (ALP, osteopontin, osteocalcin and others specific to each cell type) and also increased ALP activity at 14 days, which indicates that treatment enhanced differentiation of

all cell types examined.<sup>127, 128</sup> Further, T $\beta$ <sub>4</sub>-treatment increased mineralized nodule formation at 7 and 14 days. The incongruence between the results of the current study and those of Lee et al., may be due to differences in cells used. Specifically, the cells used by Lee et al., were all derived from humans, whereas Kusa-O cells used in the current study are a murine cell line,<sup>127, 128</sup> which may suggest that T $\beta$ <sub>4</sub> and fragments may only augment differentiation and mineralization of human-derived cells with the capacity to mineralize. Future studies are required to determine if this is the case in osteoblastic cells derived from either humans or mice. Additionally, although the Kusa-O cells used in these experiments formed mineralized nodules, it may have been more appropriate to use a cell line with a greater osteogenic capacity such as the Kusa 4b10 sub-clone of Kusa cells.<sup>209</sup> A further limitation of this study is that cells were treated with only one dose of T $\beta$ <sub>4</sub> and fragments (1  $\mu$ g/ml). Although other studies reported that this dose of T $\beta$ <sub>4</sub> maximally stimulated differentiation and mineralization of osteogenic cells,<sup>127, 128</sup> future investigations should examine the effect of T $\beta$ <sub>4</sub> and fragments using a range of different doses.

In contrast to the findings of Lee et al.<sup>127, 128</sup> and those of the current study, Ho et al. suggest that T $\beta$ <sub>4</sub> treatment of human bone marrow-derived mesenchymal stem cells inhibited osteogenic differentiation.<sup>129</sup> T $\beta$ <sub>4</sub> treatment reduced mRNA expression of BMP-2 at 1 week, ALP at 1 and 2 weeks and Coll $\alpha$ 1, OCN, osteopontin and osteonectin at 3 weeks post-osteogenic induction.<sup>129</sup> The conflicting findings on the effect of T $\beta$ <sub>4</sub> on differentiation and mineralization may be due to differences in cell types examined. Ho et al. studied the effects of T $\beta$ <sub>4</sub> on mesenchymal stem cells, while Lee et al.<sup>127, 128</sup> and this thesis examined the effects of T $\beta$ <sub>4</sub> on more mature cells (MG63 and Kusa-O cells). Additional studies, however are required to examine the effect that T $\beta$ <sub>4</sub>-treatment has on osteoblast-like cells with the capacity to mineralize at various levels of maturity.

In conclusion, the results of this study suggest that the T $\beta$ <sub>4</sub>-induced enhancement of fracture healing observed in Chapter 2 was not via mechanisms directly involving osteoblastic differentiation and function, however, possibly by increasing vascularisation of the healing site. While T $\beta$ <sub>4</sub> treatment of Kusa-O cells with T $\beta$ <sub>4</sub> and associated fragments 1-4, 1-15 and 17-23 did not significantly affect cell proliferation, differentiation or mineralization. Future studies are required to determine the mechanisms through which T $\beta$ <sub>4</sub> enhanced fracture healing and to assess the potential of this peptide to be a clinically translatable treatment for conditions such as delayed and failed bone healing.

## **4 The effect of experimental traumatic brain injury on bone**

The information presented in this chapter has been published prior to the completion of this thesis. Journal article: **Brady R.D.**, Shultz S.R., Sun M., Romano T., van der Poel C., Wright D.K., Wark J.D., O'Brien T.J., Grills B.L and McDonald S.J. (2015). Experimental traumatic brain injury induces bone loss in rats. *J Neurotrauma* 2015 Feb 16. [Epub ahead of print]

#### **4.1 Introduction**

TBI is a neurodegenerative condition induced by an external mechanical force to the brain and is a leading cause of mortality and disability worldwide.<sup>134, 212</sup> Brain damage caused by mechanical forces at the moment of impact is often categorized as the primary injury, and may involve necrotic cell death, neurovascular damage, axonal injury, oedema and ischaemia.<sup>134</sup> These primary injuries also initiate a complex cascade of secondary injury pathways that may develop over the minutes, days and months that follow.<sup>139</sup> Common secondary injury mechanisms involved in TBI include inflammatory and immune responses, excitotoxicity, oxidative stress, calcium-mediated damage, mitochondrial dysfunction, apoptosis, and proteinopathies.<sup>20, 134</sup> In addition to these central effects, TBI can also result in systemic changes in the immune, endocrine and sympathetic systems.<sup>139, 160, 213</sup> TBI is recognised as a disease process with both central and systemic effects,<sup>133</sup> a number of which have potential to be relevant to bone homeostasis. Indeed, clinical studies have also reported lower bone mineral density and an elevated risk of fracture in TBI patients.<sup>175</sup> There is also evidence of enhanced bone loss and increased risk of fracture in patients following stroke, a brain insult that bears resemblance to TBI.<sup>214</sup> Bone loss in stroke patients has been suggested to be the result of immobilization following injury;<sup>215</sup> however, it is possible that changes in bone homeostasis may result from the other physiological alterations induced by injury.

Amongst the physiological alterations that occur after TBI, a number may affect bone. TBI induces an inflammatory cascade that is characterised by up-regulation of pro-inflammatory cytokines and chemokines, and the activation and migration of immune cells.<sup>139</sup> The disruption of the BBB that occurs after TBI, allows these inflammatory mediators from the

brain to enter the peripheral circulation.<sup>149</sup> In some cases, TBI triggers a systemic SIRS, in which inflammatory cells from the circulation invade and damage peripheral organs.<sup>216-220</sup> Of relevance to bone, it is well established that inflammatory mediators that are up-regulated post-TBI (i.e. IL-1 $\beta$ ,<sup>221</sup> IL-6,<sup>222</sup> and TNF- $\alpha$ <sup>223</sup>) that are known to activate osteoclasts.<sup>135, 139, 224-226</sup> In addition, the migration of oxidants post-TBI may suppress bone formation and promote osteoclastic differentiation.<sup>165, 166</sup> Further, post-TBI hypothalamic-pituitary dysfunction can cause a deficiency in GH and IGF-1, which may cause a reduction in bone density.<sup>4</sup> TBI has also been shown to induce sympathetic hyperactivity.<sup>5</sup> Increased sympathetic outflow results in increased activation of  $\beta$ 2 adrenergic receptors on osteoblasts. The activation of these receptors has been found to stimulate bone resorption and suppress bone formation.<sup>160, 162</sup> While TBI may have detrimental effects on bone via the abovementioned pathways, there is also initial evidence that TBI may increase heterotopic ossification (the formation of bone in extraskeletal soft tissue) and accelerate fracture healing. Specifically, *in vitro* studies have demonstrated that serum from rats that have undergone TBI increases proliferation of mesenchymal stem cells,<sup>170</sup> and that serum and CSF from TBI patients increases osteoblastic proliferation.<sup>171, 172</sup> A number of factors are up-regulated in serum post-TBI that might contribute to enhanced fracture healing. These factors include leptin, NGF and basic fibroblast growth factor.<sup>181, 227-229</sup> Whether enhanced fracture healing occurs *in vivo*, and the exact mechanisms responsible, however have yet to be conclusively determined.

Considering that there are a number of physiological changes that are induced by TBI that may affect bone, in this study the effect of experimental TBI in the rat on the quantity and quality of two different weight-bearing bones; the femur and humerus was investigated. We hypothesized that TBI would result in systemic cortical and trabecular bone loss in the absence of any changes in locomotor activity. Male rats were given either a fluid percussion

injury (FPI) or sham-injury and assigned to either a 1 week or 12 week recovery time. Open-field testing to assess locomotion was conducted at 1, 4, and 12 weeks post-injury, and rats were killed at 1 and 12 weeks post-injury. Bone samples were subsequently collected, cortical and trabecular parameters of the femora were analysed structurally and the mechanical characteristics of the femora and humerus were assessed.

## **4.2 Methods**

### *4.2.1 Subjects*

Twelve week-old male Long-Evans hooded rats were obtained from Monash animal research services (Melbourne, Australia), and weighed 250-300 g at the time of injury. Rats were housed individually under a 12 h light/dark cycle and were given access to food and water *ad libitum* for the duration of the experiment. All experimental procedures were approved by the Melbourne Health Animal Ethics Committees (AEC#1112173).

### *4.2.2 Experimental Groups*

Rats were randomly assigned to receive either sham injury or FPI and either a 1 week (Sham n = 11; FPI n = 9) or 12 week (Sham n = 15; FPI n = 14) recovery. Previous studies examining cortical and trabecular bone parameters in rat models of bone loss have established approximately 7 days post-ovariectomy is the earliest time-point at which changes in bone parameters manifest.<sup>230</sup> While 12 weeks post ovariectomy/injury is a routinely used time-point to assess chronic changes in bone parameters.<sup>230, 231</sup> There were no differences in body weight between injury groups (data not shown).

### *4.2.3 Injury procedure*

FPI and sham-injury procedures were based on a standard protocol as previously described.<sup>232, 233</sup> Briefly, under isoflurane-induced anesthesia, a craniotomy (5 mm diameter; centered 3.0 mm posterior and 4.0 mm to the right of bregma) was performed to expose the intact dura mater of the brain. A hollow plastic injury cap was sealed over the craniotomy

with cyanoacrylate and dental cement. The rat was then attached to the injury device via the head cap. At first response of hind-limb withdrawal, rats received a FPI pulse to the brain with a force of 3.0 atmospheres. Upon resumption of spontaneous breathing, the injury cap was removed and incisions were sutured. Sham-injury rats underwent the same procedures except the fluid pulse was not administered.

#### 4.2.4 *Acute assessment of injury severity*

Apnoea, unconsciousness and self-righting reflex times were monitored in all rats immediately after injury and were indicators of acute injury severity.<sup>234, 235</sup> Apnoea was the time from injury to spontaneous breathing. Loss of consciousness was the time from injury to a hind-limb withdrawal response to a toe pinch. Self-righting reflex was the time from injury to the return of an upright position.

#### 4.2.5 *Open-field testing*

Locomotion was assessed using an open-field as previously described.<sup>233, 236</sup> Rats assigned a 1 week recovery were tested on day six post-injury. Rats assigned a 12 week recovery were tested at 4 weeks and 12 weeks post-injury. Rats were placed in the centre of a circular open-field arena (100 cm diameter) enclosed by walls 20 cm high, and allowed to freely explore for 5 min. Behaviour in the open-field was recorded by an overhead camera, and *Ethovision Tracking Software* (Noldus, Netherlands) quantified the total distance travelled, as well as the number of entries and time spent in the centre area (66 cm diameter) of the arena.

#### 4.2.6 *Peripheral quantitative computed tomography (pQCT)*

Prior to histological processing, femoral length was measured using digital measuring callipers. Femora (right) were fixed in paraformaldehyde and stored as previously described.<sup>237</sup> Scans were performed using a Stratec XCT-Research SA+ scanner (Stratec Medizintechnik GmbH, Pforzheim, Germany) as previously described.<sup>238, 239</sup> Briefly, a 1 mm slice (peel mode 20, contour mode 1) was taken at the distal metaphysis (15% of total

femoral length, from upper border of distal condyle) to quantify trabecular and cortical bone, and at the midshaft (50% of total femoral length, from upper border of distal condyle) to quantify cortical bone. Tissue of a density of 280 mg/cm<sup>3</sup> or less was identified as being trabecular bone and tissue with a density of 710 mg/cm<sup>3</sup> or greater was considered cortical bone. Bone mineral content, density and thickness of femoral bone from both sham and TBI rats were analysed.

#### *4.2.7 Histological processing, staining, and histomorphometry*

Scanned femora were processed to plastic, sectioned and stained according to previous methods.<sup>240</sup> Briefly, femora were dehydrated in a graded series of ethanols and infiltrated and embedded in LR White resin (London Resin Company limited, Reading, England). Five micron thick longitudinal plastic sections were cut at the midpoint of undecalcified femur on a Leica RM 2155 Rotary Microtome (Leica, Wetzlar, Germany) with a tungsten carbide blade. Sections were stained using Goldner's modification of Masson's trichrome stain. Four sections per femur were examined and photographed on a Leica DMBRE microscope. Sections of femur were assessed both qualitatively and quantitatively. Trabecular bone measurements were obtained from a 5 mm<sup>2</sup> field, positioned 1 mm distal to the lowest point of the epiphyseal cartilage plate in the metaphysis using Leica Qwin software (Leica Microsystems, Wetzlar, Germany).

#### *4.2.8 Mechanical testing*

Biomechanical properties of the diaphysis of both the left femur (mediolateral bending) and humerus (anteroposterior bending) were compared between sham and FPI rats at 1 and 12 weeks post-injury using a three-point bending apparatus.<sup>241</sup> Load and deflection data were recorded continuously using transducers connected to an x-y plotter by preamplifiers. After testing, mechanically-fractured ends were imprinted into dental wax. Using images of each imprint, cross-sectional (CS) areas (mm<sup>2</sup>) were measured using a Leica DMRBE microscope

linked to a PC with Leica Qwin software (Leica Microsystems, Wetzlar, Germany). The overall cross-sectional area of each bone at its breaking point was then calculated by averaging the measured areas of each mechanically-fractured end. Biomechanical properties measured were: peak force to failure, stiffness, ultimate bending stress and bending modulus. Peak force is the maximum force (N) applied to the bone sample and is the highest point on the y-axis of the force-displacement curve. Stiffness ( $\text{N.m}^{-1}$ ) is a measure of the resistance offered by an elastic body to deformation and is simply measured from the gradient of the force/deflection graph, measured in the linear (elastic) region. The ultimate bending stress, ( $\text{N.m}^{-2}$ ) of the material is the relationship between the peak force and the cross sectional area of the tissue. The following formulae were used to calculate ultimate bending stress; ultimate bending stress = peak force  $\times (L A_o^{0.5} / \pi^{0.5} (A_o^2 - A_i^2))$ . Where  $\pi = 3.14$ , L is the distance between the two testing platforms (m), A is the cross-sectional area ( $\text{m}^2$ ) of bone at its breaking site,  $A_o$  is the outer area and  $A_i$  is the inner medullary cavity area. Bending modulus ( $\text{N.m}^{-2}$ ) is a measurement of the proportional relationship between applied stress and the resulting strain on the bone and indicates stiffness/rigidity. To calculate bending modulus (E) the following formulae were for used:  $E = (F/Y) \times (\pi L^3 / (12(A_o^2 - A_i^2)))$ . Where E is bending Modulus ( $\text{N.m}^{-2}$ ), F/Y is the extrinsic stiffness ( $\text{N.m}^{-1}$ ),  $\pi = 3.14$ , L is the distance between the two testing platforms (m),  $A_o^2 - A_i^2$  is the cross-sectional area of the cortical bone ( $\text{m}^2$ ) at its breaking site. All of these parameters were calculated from the load deflection data.

#### 4.2.9 Statistical analyses

Unpaired t-tests were used to compare acute injury severity measures and locomotor activity in an open-field between sham and TBI groups. pQCT bone parameters and trabecular bone volume ratio between femora of sham and TBI rats at both 1 and 12 weeks post-injury were assessed using Two-way ANOVA. Mann-Whitney U tests were used to compare mechanical

properties between femora and humeri from sham and TBI rats. All data was analysed using GraphPad Prism 6 with significance defined as  $p < 0.05$ .

### 4.3 Results

#### 4.3.1 Acute Injury Severity Measures

Fluid percussion injury resulted in worsened acute injury severity outcomes as indicated by increased apnoea (Sham: M = 0 s; TBI: M = 39.9 s, SE =  $\pm$  3.7 s), hind-limb withdrawal (Sham: M = 0 s; TBI: M = 320.1 s, SE =  $\pm$  20.9 s), and self-righting reflex times (Sham: M = 137.7 s, SE =  $\pm$  11.2 s; TBI: M = 511.8 s, SE =  $\pm$  23.2 s) compared to the sham-injured group ( $p < 0.001$ ).

#### 4.3.2 Locomotor Activity

Locomotor activity was assessed at 1, 4 and 12 weeks post-injury in the open-field. There were no differences in distance travelled in the open-field between sham and TBI rats at any of the time-points (Figure 4.1).

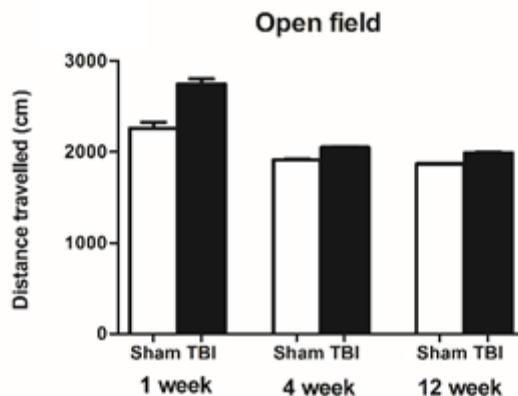


**Figure 4.1.** Distance travelled in an open-field. No difference in total distance travelled during open-field session was observed between sham and TBI rats.

#### 4.3.3 pQCT

Analysis of the distal metaphyseal region of femora from sham and TBI rats showed no difference in total bone density (Figure 4.2a) at 1 week post-injury, however, at 12 weeks post-injury this region was 6% less dense in TBI rats when compared to shams ( $p < 0.01$ ). At 1 and 12 weeks post-injury, the distal metaphyseal region of femora from TBI rats had reduced cortical thickness (Figure 4.2b, 10% decrease at 1 week, 11% decrease at 12 weeks  $p$

< 0.001) and cortical content (Figure 4.2c, 10% decrease at 1 week, 8% decrease at 12 weeks;  $p < 0.01$ ). No differences between sham and TBI animals were observed at the midshaft in any measured parameter (Figure 4.2d-f). At 1 and 12 weeks post-injury there were no between group differences in femoral length (results not shown).

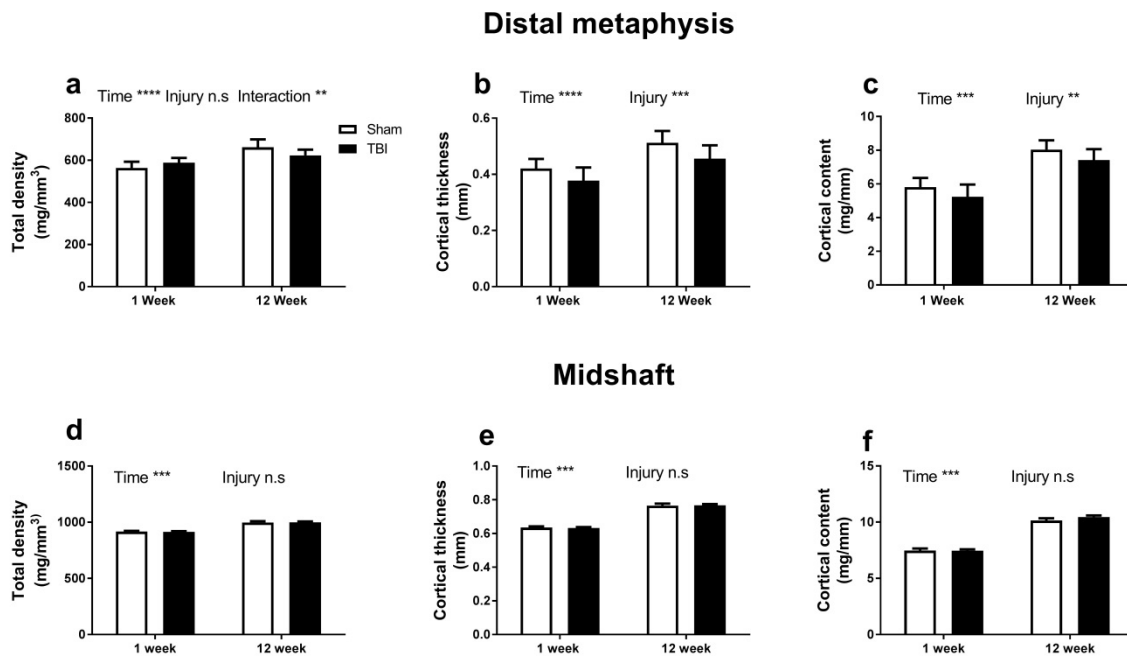


**Figure 4.2.** pQCT analysis of bone parameters of the distal metaphyseal region and midshaft of femora from sham and TBI rats. The distal metaphyseal region of femora from TBI animals had reduced total bone density at 12 weeks post-injury (a,  $**p < 0.01$ ), reduced cortical thickness (b,  $***p < 0.001$ ) and cortical content at 1 and 12 weeks post-injury (c,  $**p < 0.01$ ). No difference between sham and TBI groups was observed in total density at 1 week post-injury. At the midshaft no difference was found between sham and TBI animals in any measured parameter (d-f).

#### *4.3.4 Histologic and histomorphometric analysis*

At 1 and 12 weeks post-injury, there was a decreased proportion of trabecular bone in TBI rats compared to shams (Figure 4.3a-d). Data obtained from histomorphometric analysis (Figure 4.3e) reflected the qualitative histological assessment; as the trabecular bone volume ratio (BV/TV) was reduced by approximately 23% at 1 week post-injury and 27% at 12 weeks post-injury in FPI rats when compared to shams ( $p < 0.01$ ).

#### *4.3.5 Mechanical testing*

Mechanical properties of diaphyses of both femora and humeri from sham and TBI rats at 1 and 12 weeks post-injury are shown in Table 4.1. No differences in mechanical properties of the diaphyses of either femora or humeri were observed between the two groups in any measured parameter at any time-point.

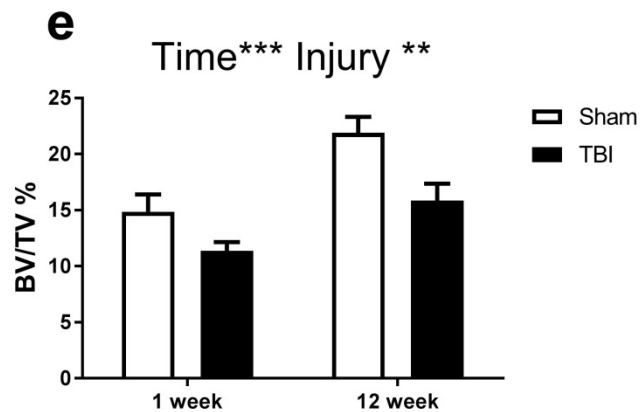
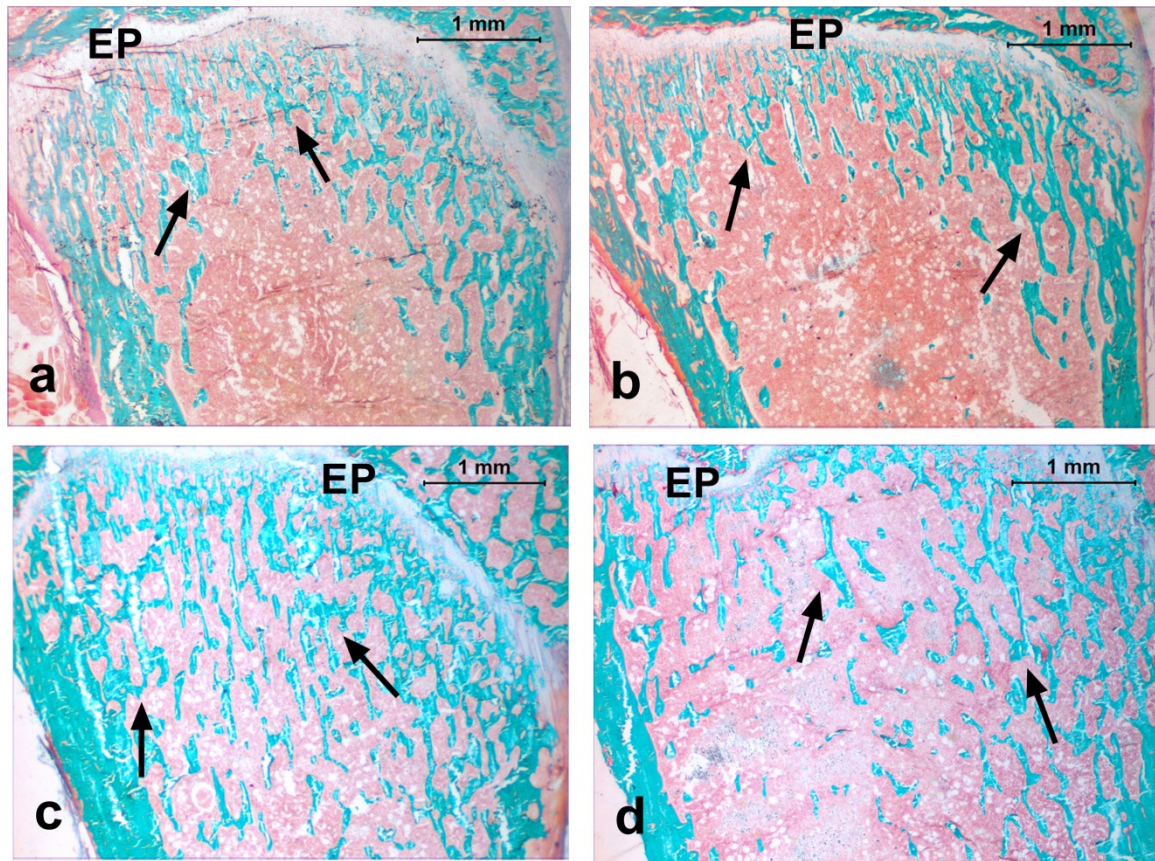


**Figure 4.3.** Longitudinal representative histological sections of distal metaphyseal region of femora from control (a, c) and TBI (b, d) animals. Histological assessment shows TBI animals (b, d) had a lower fraction of trabecular bone (arrows) compared to controls (a, c) at 1 and 12 weeks post-injury (Goldner's trichrome stain; original magnification 25 x). Histomorphometric analysis shows a decreased trabecular bone volume fraction in TBI rats compared to controls at 1 and 12 weeks post-injury (e,  $**p < 0.01$ ). Bars are means  $\pm$  SEM.

**Table 4.1.** Mechanical characteristics of sham and TBI samples at 1 and 12 weeks post-injury.

Treatment	Peak force (N)	Stiffness (x 10 <sup>4</sup> Nm <sup>2</sup> )	Cross-sectional area (x 10 <sup>-6</sup> m <sup>2</sup> )	Ultimate bending stress (x 10 <sup>6</sup> Nm <sup>-2</sup> )	Bending modulus (x 10 <sup>8</sup> Nm <sup>-2</sup> )
<b>1 week</b>					
Sham femur (n = 10)	166.6 ± 6.4	25.5 ± 2.9	5.6 ± 0.2	72.1 ± 0.2	46.7 ± 2.71
TBI femur (n = 8)	164.0 ± 6.6	25.1 ± 3.2	5.5 ± 0.1	72.1 ± 0.3	46.2 ± 2.01
<b>12 week</b>					
Sham humerus (n = 9)	153.2 ± 9.9	34.4 ± 2.7	3.5 ± 0.2	168.9 ± 14.6	225.1 ± 25.3
TBI humerus (n = 8)	140.1 ± 9.6	26.9 ± 3.9	3.4 ± 0.1	145.6 ± 10.1	180.0 ± 16.6
Sham femur (n = 15)	221.5 ± 5.8	29.5 ± 1.0	6.3 ± 0.5	68.4 ± 2.5	34.03 ± 1.57
TBI femur (n = 14)	229.5 ± 10.7	27.7 ± 2.2	7.1 ± 0.3	68.3 ± 2.2	32.44 ± 1.48

There were no differences in any measured mechanical properties at any time-point between sham and TBI groups. Values are means ± SEM.

#### 4.4 Discussion

Few studies have investigated the influence of TBI on bone homeostasis. As such, here the effect of experimental TBI in the rat on the quantity and quality of the femur and humerus at 1 and 12 weeks post-injury was assessed. pQCT analysis demonstrated that bone mineral density in TBI rats was decreased at the distal metaphyseal region of femora at 12 weeks post-injury compared to sham rats. Cortical bone thickness and content at this location was decreased at 1 and 12 weeks post-injury in TBI rats when compared to shams. Furthermore, histomorphometric analysis revealed that trabecular bone volume ratio was decreased at the distal metaphysis in femora from TBI rats at 1 and 12 weeks post-injury compared to shams. Taken together, the present findings are consistent with those from previous studies suggesting that TBI in rodents can induce bone loss remote from the site of injury.<sup>242, 243</sup> Notably, these studies speculated that bone changes post-TBI were largely due to immobilization. Human studies indicate that brain-injured patients in a vegetative or low ambulatory state have a lower bone mineral density and an increased risk of fracture.<sup>176, 215</sup> In this study, however, it was observed that there were no differences between the groups in distance travelled in the open-field at 1, 4, and 12 weeks post-injury; therefore it seems unlikely that the effects of TBI on bone were caused by immobilization.

The current findings of reduced bone post-TBI may be relevant to clinical evidence that links TBI and stroke to the later onset of osteopenia and osteoporosis,<sup>174</sup> and a long-term increased risk of fracture.<sup>175, 214</sup> It was shown that there were no differences in mechanical properties and bone volumes of the femoral midshaft between TBI and sham rats. These traits may be due to the slow remodelling rate of this region that is comprised predominantly of cortical bone.<sup>244</sup> Cortical bone has a much lower surface-to-volume ratio than trabecular bone and therefore remodels at a slower rate.<sup>245</sup> As was expected, there was a greater proportion of trabecular bone loss observed in TBI animals compared to shams, however a degree of

cortical bone loss of distal femur was evident.<sup>244</sup> It is possible that cortical bone loss may have also occurred at midshaft regions at time-points not featured in this study. In addition, although no difference in mechanical properties of the humerus were observed between TBI and sham rats, it is possible that bone loss may also have occurred in the humerus in addition to the femur. Therefore, future studies should examine bone parameters of the humerus via pQCT or  $\mu$ CT analysis.

Importantly, the reduced quantity of bone observed in TBI rats may not be the result of enhanced bone resorption. Rats used in this study were approaching skeletal maturity; growth was evident by the increases in femoral length, cortical thickness, cortical content and total density at both the femoral midshaft and distal metaphysis in 12 week when compared to 1 week recovery rats. Interestingly, TBI did not affect femoral length, which suggests TBI may not affect endochondral ossification at the growth plate and thus growth in the longitudinal axis of long bones. The current pQCT and histological findings do however indicate that TBI in rats does affect appositional growth at the femoral distal metaphysis. The reduced quantity of metaphyseal bone in TBI rats may be attributed to either a localised reduction in osteoblastic bone formation, an increase in osteoclastic bone resorption, or a combination of both.

While the current findings as well as past studies indicate that TBI can induce bone loss in the rat,<sup>242</sup> the precise cellular and molecular mechanisms through which these changes occur have yet to be elucidated. Human and animal studies indicate that microglia in the brain can be chronically activated for weeks, months and even years after the initial TBI.<sup>145-147</sup> Chronic microglia activation is associated with increased circulating levels of IL-1 $\beta$ , IL-6, IL-17 and TNF- $\alpha$ .<sup>139</sup> These inflammatory cytokines co-incidentally have a stimulatory effect on osteoclastogenesis, which potentiate bone resorption.<sup>52</sup> As BBB dysfunction can occur for months post-TBI,<sup>246</sup> it is possible that the reduction in bone volume was induced by

inflammatory cells and cytokines that migrated from the brain to the periphery. Post-TBI autonomic dysfunction may also have contributed to the reduced quantity of bone that was observed.<sup>160</sup> Specifically, autonomic dysfunction often leads to heightened adrenergic tone, and a sufficient increase in adrenergic tone can cause bone resorption by activating osteoclasts, while preventing osteoblasts from forming bone.<sup>162</sup> GH deficiency is another common abnormality following TBI that could influence bone.<sup>247</sup> Interestingly, a deficiency in GH can cause a reduction in BMD.<sup>248</sup> Furthermore, growth hormone is also known to stimulate the synthesis of IGF-1, which is required for bone growth, maturation and bone mass acquisition.<sup>249</sup> As such, decreased serum concentrations of growth hormone and IGF-1 post-TBI,<sup>158</sup> may have contributed to the reduced bone mass observed in this study.

In conclusion, the results presented in this study indicate that the FPI model of experimental TBI causes a decrease in bone mineral density, cortical thickness and trabecular bone volume ratio, in the absence of any changes in locomotion. These findings indicate that the pathological systemic effects of TBI also have a negative effect on bone.

## **5 The effect of sodium selenate treatment on traumatic brain injury-induced bone loss in rats**

The information presented in this chapter has been published prior to the completion of this thesis. Journal article: **Brady R.D.**, Grills B.L., Romano T., Wark J.D., O'Brien T.J., Shultz S.R and McDonald S.J. (Accepted) Sodium selenate treatment mitigates reduction of bone volume following traumatic brain injury in rats. *J Musculoskelet Neuronal Interact*

## 5.1 Introduction

TBI is a neurodegenerative condition induced by an external mechanical force to the brain and is a leading cause of mortality and disability worldwide.<sup>134</sup> Brain damage caused by mechanical forces at the moment of impact is often categorized as the primary injury and may involve necrotic cell death, neurovascular damage, axonal injury, oedema and ischaemia.<sup>134</sup> These primary injuries initiate a complex cascade of secondary injury pathways that may develop over the minutes, days and months that follow.<sup>139</sup> In addition to these central effects, TBI can also result in systemic changes in the immune, endocrine and sympathetic systems,<sup>139, 160, 213</sup> all of which influence bone homeostasis.<sup>52, 248, 249</sup> As such, in Chapter 4 the effect of experimental TBI on bone in the rat was assessed. Results showed that bone mineral density, trabecular bone volume ratio, cortical bone thickness and cortical bone content, were decreased in femora of rats subjected to TBI at 12 weeks post-injury compared to sham-injured rats. These findings, along with those from previous studies in rodents and humans,<sup>173, 175, 242, 243</sup> suggest that the systemic influence of TBI may also include detrimental effects on bone mass and that brain-injured patients may have an increased risk of developing osteoporosis and be more susceptible to bone fracture.<sup>175</sup> Specifically, human studies indicate that brain-injured patients have an elevated risk of hip fracture which has been associated with increased morbidity and mortality.<sup>173</sup>

There is currently no clinical pharmaceutical intervention available that improves long-term outcome following TBI.<sup>20</sup> However, the delayed and progressive nature of the neurodegenerative aftermath of TBI provides an opportunity for a pharmacological intervention to mitigate these effects.<sup>20</sup> Sodium selenate is a potent PP2A/PR55 activator that

reduces the hyperphosphorylation of tau,<sup>195, 250, 251</sup> and a 12-week sodium selenate treatment regimen was shown to be a novel TBI therapy in rats.<sup>21</sup> Sodium selenate treatment significantly increased brain tissue PP2A/PR55 and reduced tau phosphorylation, brain damage and behavioral impairments following TBI compared to saline-vehicle treatment.<sup>21</sup> These findings demonstrate that sodium selenate may be a novel therapeutic approach to improve outcome following TBI. Importantly, sodium selenate is highly water-soluble, readily crosses the blood brain barrier, and a treatment regimen similar to that used in this study has already been demonstrated to be safe in a six month Phase I trial in patients with prostate cancer,<sup>15</sup> Sodium selenate is also currently being assessed in a Phase II study for Alzheimer's disease,<sup>195</sup> Considering the lack of an effective pharmaceutical intervention for TBI patients, sodium selenate has the potential to be translated into clinical TBI trials.

Whether sodium selenate treatment and/or attenuating the brain injury affects bone mass after TBI, however, has yet to be determined. Furthermore, although there were no reported overt negative effects of sodium selenate treatment in rats in a previous TBI study,<sup>21</sup> and there were no documented serious side-effects in sodium selenate trials in Alzheimer's patients,<sup>195</sup> the potential for selenium toxicity is an important issue to consider. Though no studies have characterized the effect of prolonged sodium selenate treatment on bone, there is preliminary evidence that sodium selenate or sodium selenate metabolites may have toxic effects on skeletal cells,<sup>198</sup> and this is an important factor to consider as sodium selenate progresses towards clinical trials in TBI patients. For these reasons, here the effect of sodium selenate treatment on the quantity and quality of bone within the femur of rats subjected to TBI was investigated. Male rats were randomly assigned into either sham injury or FPI groups and administered either saline or sodium selenate for 12 weeks post-injury. Open-field testing to assess locomotion was conducted at 4 and 12 weeks post-injury and rats were killed at 12 weeks post-injury for analysis of femoral structural and mechanical properties.

## 5.2 5.2 Materials and Methods

### 5.2.1 Subjects

Fifty-four male Long-Evans hooded rats obtained from Monash animal research services (Melbourne, Australia) were 12 weeks of age and weighed 250-300 g at the time of injury. Rats were housed individually under a 12 hour light/dark cycle, and given access to food and water *ad libitum* for the duration of the experiment. Animal procedures were approved by The University of Melbourne animal ethics committee (#1112173) and all animal experiments were carried out in accordance with the guidelines of the Australian code of practice for the care and use of animals for scientific purposes by the Australian National Health and Medical Research Council.

### 5.2.2 Experimental groups

Rats were randomly assigned to one of four experimental conditions: sham-injury + saline-vehicle treatment (SHAM + VEH; n = 13), sham-injury + sodium selenate treatment (SHAM + SS; n = 15), fluid percussion injury (FPI) + saline-vehicle treatment (FPI + VEH; n = 13), or FPI + sodium selenate treatment (FPI + SS; n = 13). The assigned treatment began immediately post-injury, selenate treatment groups received 1 mg/kg/day,<sup>21</sup> delivered continuously via subcutaneously implanted mini-osmotic pump (Model 2006, Alzet, CA, USA) for the entire duration of the study.

### 5.2.3 Surgery and FPI

FPI and sham-injury procedures were administered as described in Chapter 4. Upon resumption of spontaneous breathing the head cap was removed. A transverse 1 cm incision in line with the scapulae was made and the osmotic pump was inserted subcutaneously left of the spine. The end of the cannula attached to the pump was inserted in the contralateral side. The incision was then sutured using nylon (4/0, Surgical Specialties Australia). Sham-injury rats underwent the same procedures, except the fluid pulse was not administered. Six weeks

post-injury, rats were anesthetized, the initial treatment pump was removed, and a replacement treatment pump was implanted as described above.

#### 5.2.4 *Acute injury severity*

Apnoea, unconsciousness and self-righting reflex times were monitored in all rats immediately after injury as indicators of acute injury severity.<sup>236, 252, 253</sup>

#### 5.2.4 *Open-field testing*

Locomotion was assessed using an open-field as previously described in Chapter 4.

#### 5.2.5 *pQCT*

*pQCT* scans were performed as described in Chapter 4. Bone mineral content, density and thickness of femoral bone were analysed.

#### 5.2.6 *Histological processing, staining, and histomorphometry*

Histological processing, staining, and histomorphometric analysis was performed as described in Chapter 4.

#### 5.2.7 *Mechanical testing*

Biomechanical properties of the diaphysis of the left femur (mediolateral bending) were assessed using a three-point bending apparatus as described in Chapter 4. After testing, the mechanically fractured ends were imprinted into dental wax. Using images of each imprint, cross-sectional (CS) areas (mm<sup>2</sup>) were measured using a Leica DMRBE microscope linked to a PC with Leica Qwin software (Leica Microsystems, Wetzlar, Germany). The overall cross-sectional area of each femora at its breaking point was then calculated by averaging the measured areas of each mechanically-fractured end.

#### 5.2.8 *Statistical analyses*

A two-way ANOVA, with treatment and injury as the between-subjects variables, was used to analyze all measures. Tukey post-hoc comparisons were carried out when appropriate. All

data was analyzed using GraphPad prism 6 (GraphPad software, Inc.) with significance defined as  $p < 0.05$ .

## 5.3 Results

### 5.3.1 Acute injury severity

FPI worsened apnoea ( $p < 0.001$ ), unconsciousness ( $p < 0.001$ ) and self-righting reflex times ( $p < 0.001$ ) compared to sham-injury regardless of the assigned treatment group (Table 5.1).

**Table 5.1.** Acute injury severity measures.

	SHAM + VEH	SHAM + SS	FPI + VEH	FPI + SS
Apnea	0	0	40 ± 4*	40 ± 3.0*
Unconsciousness	0	0	320 ± 30.*	335 ± 25*
Self-righting	140 ± 11	132 ± 12	512 ± 23*	528 ± 24*

FPI resulted in worsened acute injury severity outcomes as indicated by increased apnoea, hind-limb withdrawal, and self-righting reflex times compared to the sham-injured group regardless of the assigned treatment. \* = FPI significantly greater than sham-injured group,  $p < 0.001$ . Values are mean ± SEM.

### 5.3.2 Locomotor Activity

Locomotor activity was assessed at 4 and 12 weeks post-injury in the open-field. There were no differences in distance travelled in the open-field between sham and TBI rats at any of the time-points regardless of the assigned treatment group (Figure 5.1).

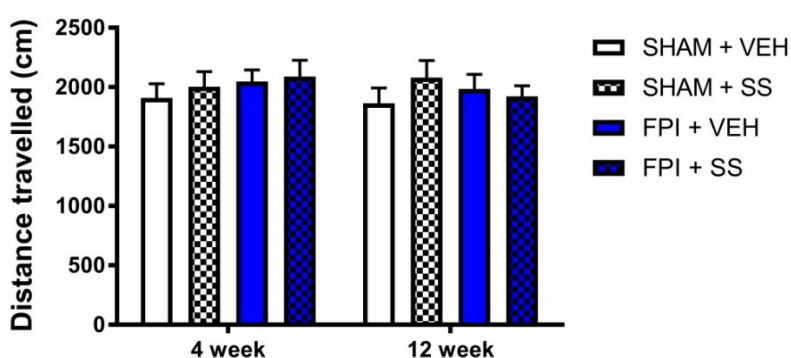


**Figure 5.1.** Distance travelled in an open-field. No difference in total distance travelled during open-field session was observed between groups. Bars are means ± SEM.

### 5.3.3 *Histologic and histomorphometric analysis*

There was a decreased proportion of trabecular bone in FPI + VEH rats compared to SHAM + VEH rats, however there was a larger proportion of trabecular bone in FPI + SS rats when compared to FPI + VEH rats ( $p < 0.01$ ; Figure 5.2a-d). Data obtained from histomorphometric analysis (Figure 5.2e) reflected the qualitative histological assessment; as two-way ANOVA revealed a significant injury x treatment interaction ( $p < 0.001$ ) on the trabecular bone volume ratio (BV/TV). Post-hoc analyses confirmed a significant decrease in the percentage of trabecular bone in FPI + VEH rats compared to both SHAM + VEH and FPI + SS groups ( $p < 0.01$ ; Figure 5.2e).

Two-way ANOVA also revealed a significant treatment effect on femoral length ( $p < 0.001$ ), with femoral length of SS-treated rats decreased by 4.3% compared to VEH-treated rats ( $p < 0.001$ ; Figure 5.2f). Growth plate width was increased by 22.1% in SS-treated rats compared to VEH-treated rats ( $p < 0.01$ ; Figure 5.2g).

### 5.3.4 *pQCT*

Two-way ANOVA revealed a significant injury x treatment interaction ( $p < 0.005$ ) on the measure of cortical thickness. Post-hoc analysis indicated that FPI + VEH rats had significantly reduced cortical thickness compared to both SHAM + VEH and FPI + SS groups ( $p < 0.05$ ; Figure 5.3a), whereas the SHAM + VEH and FPI + SS groups did not differ. Analysis of the distal metaphyseal region of femora revealed no difference in total bone density or cortical content (Figure 4.3b,c). No differences were observed at the midshaft in any measured parameter (Figure 5.3d-f).

### 5.3.5 *Mechanical testing*

There were no statistically significant differences in biomechanical measures (Table. 5.2).

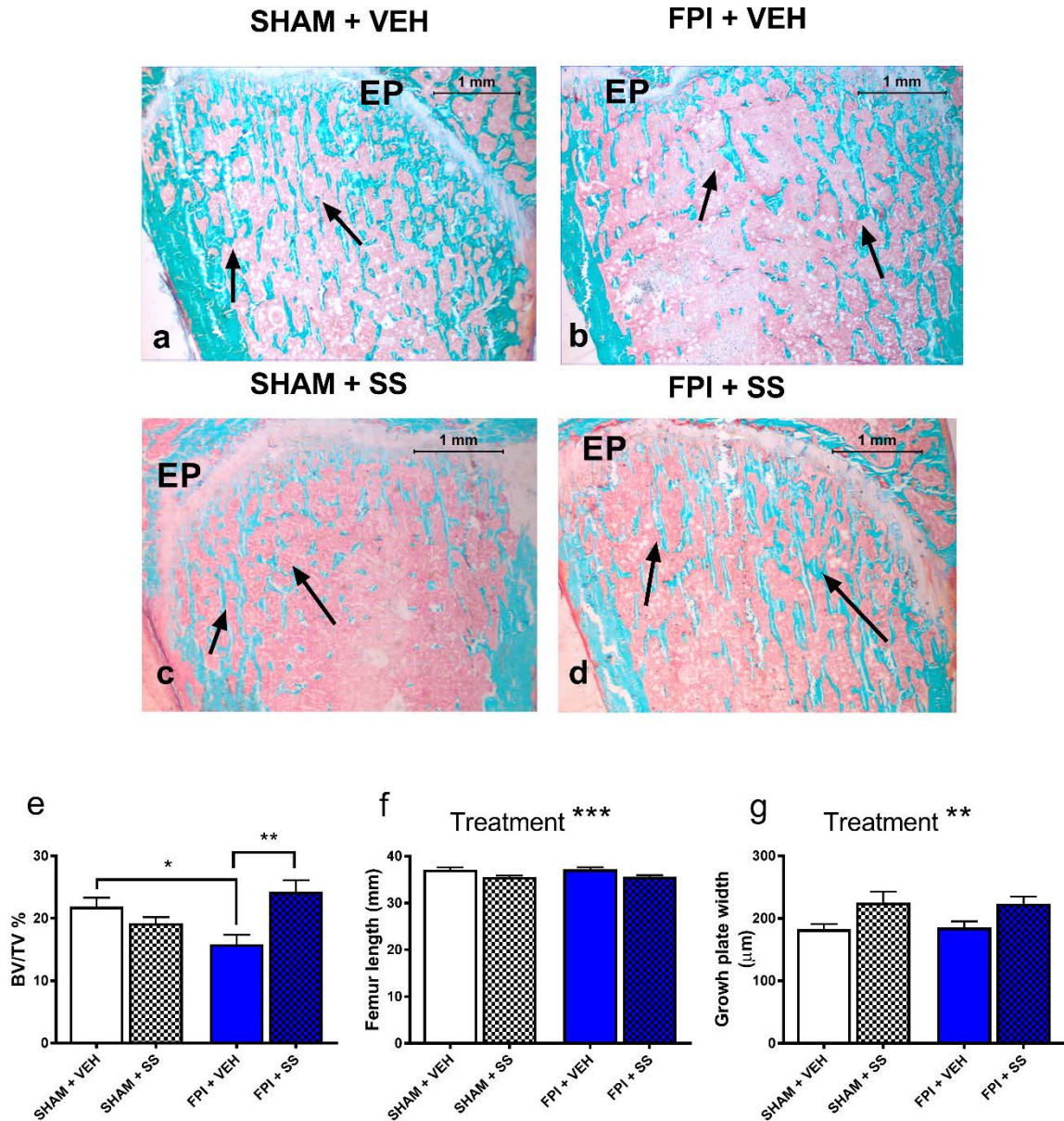


**Figure 5.2.** Longitudinal representative histological sections of the distal metaphyseal region of femora. Histological assessment shows FPI + VEH rats (a) had a lower fraction of trabecular bone (arrows) compared to SHAM + VEH rats (b). Whereas, there was a larger proportion of trabecular bone in FPI + SS rats (d) when compared to FPI + VEH rats (c; Goldner's trichrome stain; original magnification 25x). Histomorphometric analysis (e) shows a decreased trabecular bone volume fraction in FPI + VEH rats compared to SHAM + VEH rats however trabecular bone volume fraction was greater in FPI + SS rats compared to FPI + VEH rats. SS-treated rats had shorter femora (f) and wider growth plates (g) compared to VEH-treated rats. Treatment\*\* indicates a significant main treatment effect. \* $p < 0.05$ , \*\* $p < 0.01$ , \*\*\* $p < 0.001$ . Bars are means  $\pm$  SEM.

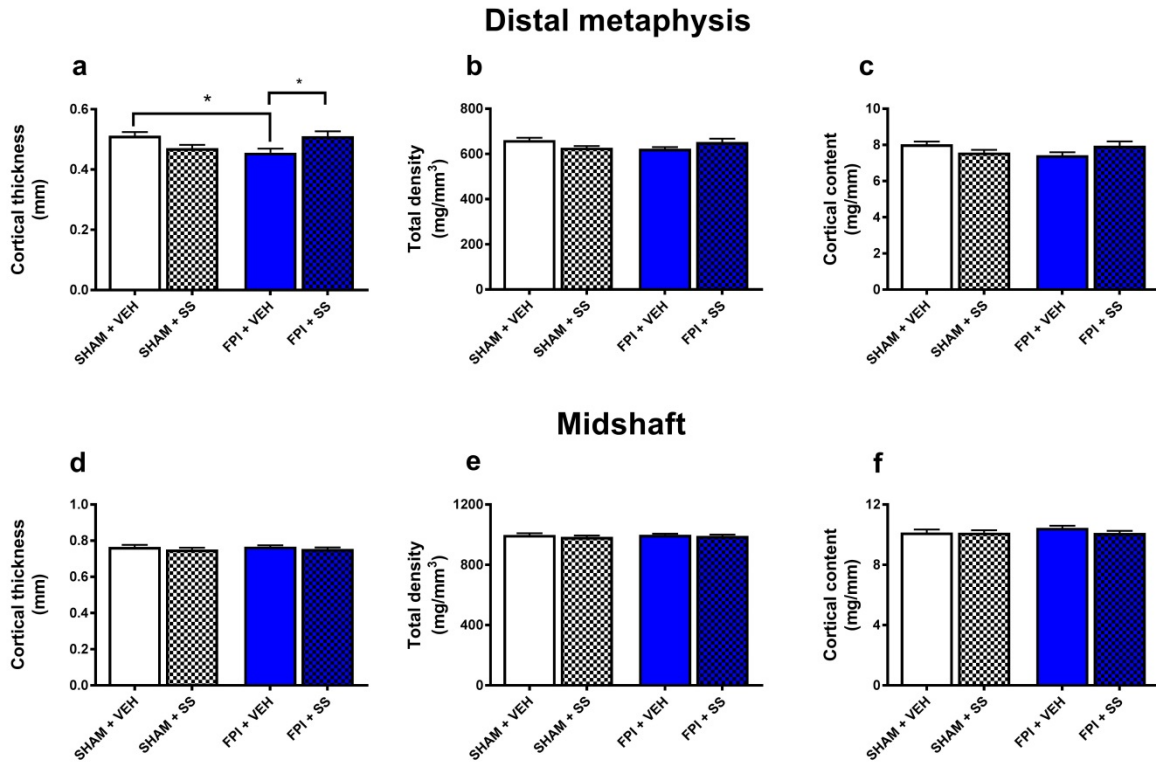


**Figure 5.3.** pQCT analysis of bone parameters of the distal metaphyseal and midshaft region of femora. The distal metaphyseal region of femora from FPI + VEH rats had reduced cortical thickness compared to both SHAM + VEH and FPI + SS groups (a). No difference in total bone density or cortical content were observed (b, c) at the distal metaphysis. Nor were there any differences observed at the midshaft in any measured parameter (d-f). \* $p < 0.05$ . Bars are means  $\pm$  SEM.

**Table 5.2.** Biomechanical characteristics of sham-vehicle, sham-selenate, FPI-vehicle and FPI-selenate femoral samples.

	SHAM + VEH (n= 15)	SHAM + SS (n = 15)	FPI + VEH (n = 14)	FPI + SS (n = 14)
Peak force (N)	222 ± 6	221 ± 7	230 ± 10.7	225 ± 11
Stiffness (x 10 <sup>4</sup> Nm <sup>2</sup> )	29.5 ± 1.0	30.1 ± 1.1	29.7 ± 1.0	29.2 ± 1.1
Cross-sectional area (x 10 <sup>-6</sup> μm <sup>2</sup> )	6.8 ± 0.2	6.8 ± 0.2	6.2 ± 0.6	6.8 ± 0.3
Ultimate bending stress (x 10 <sup>7</sup> Nm <sup>-2</sup> )	6.9 ± 0.2	6.8 ± 0.2	6.8 ± 0.2	7.0 ± 0.3
Bending modulus (x 10 <sup>9</sup> Nm <sup>-2</sup> )	3.4 ± 0.2	3.4 ± 0.2	3.2 ± 0.2	3.4 ± 0.1

There were no differences in any measured mechanical properties between any groups.  
Values are mean ± SEM.

## 5.4 Discussion

The previous chapter demonstrated that TBI is detrimental to bone microstructure in rats,<sup>254</sup> which is consistent with human findings that link brain injury to the later onset of osteopenia, osteoporosis and long-term elevated risk of fracture.<sup>174, 214</sup> It has previously been shown that sodium selenate treatment attenuates brain damage and reduces behavioural impairments following experimental TBI in rats.<sup>21</sup> The effect sodium selenate treatment has on TBI-induced reduction in bone mass is unknown, but its effect on bone is important to consider if its potential therapeutic use is to be translated to the clinical TBI setting. Therefore, here the effect of continuous sodium selenate treatment on the quantity and quality of bone within the femur of rats subjected to TBI 12 weeks post-injury was assessed. Histomorphometric analysis demonstrated that there was a larger proportion of trabecular bone in TBI rats treated with selenate compared to their vehicle treated counterparts. Furthermore, pQCT analysis revealed that cortical thickness was increased in brain-injured rats that were treated with selenate compared to brain-injured rats treated with vehicle. Interestingly, femora from selenate-treated rats were shorter in length and had increased growth plate width compared to vehicle-treated rats. Taken together, these findings suggest that selenate treatment mitigated TBI-induced reductions in bone volume, however it concomitantly reduced femoral growth. It was also shown that there were no differences between groups in distance travelled in the open-field, which suggests that the effects of TBI and selenate treatment on bone were not confounded by immobilization.

The patterns of reduced bone volume in animals given TBI in this study were similar to those described in the previous chapter,<sup>254</sup> with the effects of TBI most evident at the femoral distal metaphysis. No differences were observed in mechanical properties or bone volumes of the femoral midshaft, which is perhaps not surprising given this region is almost exclusively comprised of cortical bone, which remodels at a slower rate than trabecular bone due to a low

surface-to-volume ratio.<sup>245</sup> It is possible that changes at this region take longer to manifest and may have occurred at time-points not featured in this study. In accordance with previous findings, there were significant reductions in bone volume at the distal metaphysis, which is a metabolically active region of bone that is susceptible to bone loss.<sup>255</sup>

Brain-injured rats treated with sodium selenate did not have the reductions in distal metaphyseal bone volume of their vehicle-treated counterparts. Therefore it is possible, that the increased bone volumes observed in brain-injured selenate-treated rats was due to the attenuation of the brain injury via selenate treatment. Several of the secondary injury mechanisms of TBI have the potential to have significant catabolic effects on bone. In particular, the neuroinflammatory response that occurs post-TBI can be chronically activated post-TBI,<sup>139</sup> and can lead to persistent elevation of circulating cytokines, many of which have been shown to induce osteoclastic bone resorption.<sup>139, 224</sup> Therefore, it is possible that sodium selenate prevented loss of bone via inhibition of the neuroinflammatory response post-TBI. In addition, the increased sympathetic outflow following TBI may also contribute to TBI-induced bone loss.<sup>160</sup> Several studies have shown how sympathetic activation of  $\beta$ -adrenergic signalling in osteoblasts inhibits bone formation and triggers osteoclastogenesis and bone resorption.<sup>160, 162</sup> Therefore, sodium selenate may have reduced the extent of sympathetic signalling and thus indirectly reduced bone loss.

Though it was hypothesised that sodium selenate treatment reduced TBI severity and thereby prevented bone loss, it is possible that sodium selenate had direct influences on bone tissue that may have prevented bone loss following TBI. *In vitro* data suggest that sodium selenite, a major metabolite of sodium selenate,<sup>15</sup> can induce apoptosis of osteoclast-like cells via the mitochondrial pathway.<sup>256</sup> Furthermore, intraperitoneal injection of mice with sodium selenite was found to inhibit differentiation of bone marrow-derived monocytes into osteoclasts.<sup>256</sup> Therefore, taking these previous findings into account, it is possible that in the

current study, the metabolite sodium selenite reduced bone resorption by decreasing osteoclastic formation and increasing osteoclastic apoptosis, which thereby reduced bone loss in selenate-treated TBI rats compared to vehicle-treated TBI rats. Interestingly, however, no effects of sodium selenate treatment on distal metaphyseal bone volumes in sham animals was seen, which possibly indicates that there was no direct effect of sodium selenate treatment on metaphyseal bone turnover in uninjured animals.

Direct effects of sodium selenate treatment were however apparent at the growth plate, with treated rats displaying reduced femoral length and increased growth plate width. A previous study has reported morphological changes in epiphyseal plates of rats treated with sodium selenate.<sup>198</sup> Furthermore, sodium selenite has been shown to induce growth retardation in rats.<sup>199, 200</sup> The precise cellular and molecular mechanisms through which these above changes occur, however are not entirely understood. The reduced longitudinal bone growth and increased epiphyseal growth plate width observed in selenate-treated rats indicates that selenate treatment impaired cartilage-to-bone conversion at the growth plates. Known as endochondral ossification, this process involves the resorption of calcified cartilage matrix at the base of epiphyseal plates by osteoclasts, which then allows blood vessel invasion and bone formation by osteoblasts, which use the calcified cartilage matrix as a template on which to form bone.<sup>32</sup> Several animal studies have shown that pharmacological inhibition of osteoclastic activity with bisphosphonates markedly interferes with the endochondral ossification process, which results in widened growth plates and impaired longitudinal bone growth.<sup>257, 258</sup> These findings, along with the aforementioned associations between sodium selenate and reduced numbers of osteoclasts, suggest that the femoral growth plate deficits observed in sodium selenate-treated animals likely occurred due to impaired osteoclastic activity. A limitation of this study is the lack of dynamic bone formation parameters. For example, additional data examining bone formation rate, mineral apposition rate and

mineralizing surface may have indicated whether the observed changes occurred due to reduced osteoblastic activity, which would have been informative and should be examined in future studies. Despite the observed deficits at the epiphyseal growth plate, the underlying metaphyseal trabecular and cortical bone volumes were unaffected by sodium selenate treatment, a finding that is similar to that reported in bisphosphonate-treated animals with similarly impaired long bone growth.<sup>257, 258</sup> Further studies are necessary to determine the effects of sodium selenate on bone health in humans; however, our findings in rats suggest that sodium selenate treatment inhibits long bone growth in children and adolescents, but may not have detrimental effects on adult bone.

### **Conclusion**

These are the first findings to indicate that selenate treatment was effective at preventing reductions in bone volume post-TBI. Selenate treatment, however, also decreased long bone growth in rats that had yet to reach skeletal maturity. Therefore, the observed detrimental effects on bone growth in the current study should be carefully considered if sodium selenate treatment is to be translated in a clinical TBI setting in juveniles who experience a TBI. Further studies are needed to define the exact mechanism through which sodium selenate treatment prevented reductions in bone volume post-TBI, though the findings of this study, along with the previous rodent studies, provide strong preliminary evidence that pharmacological interventions attenuating TBI pathobiology may reduce the risk of osteoporotic development.

## **6 The effect of closed-head experimental traumatic brain injury on fracture healing in mice**

The information presented in this chapter has been published prior to the completion of this thesis. Journal article: **Brady R.D.**, Grills B.L., Church J.E., Walsh N.C., Agoston D.V., Sun M., O'Brien T.J., Shultz S.R and McDonald S.J. (In press). Closed-head experimental traumatic brain injury promotes fracture healing in mice. (2016). *Sci Reports*.

## 6.1 Introduction

Concomitant TBI and long bone fracture are present in many multitrauma and polytrauma patients as a consequence of high energy impacts that result from motor vehicle collisions, falls and warzone injuries.<sup>132, 259, 260</sup> Long bone fracture healing involves a biological sequence of four overlapping phases; an inflammatory phase, which features migration of inflammatory cells and the release of chemokines and cytokines that initiate the healing response, formation of a fibrocartilaginous soft callus to bridge the fractured bone ends, replacement of soft callus with bony hard callus in order to restore mechanical stability, and a remodelling phase that restores bone to its pre-injured state.<sup>73</sup>

TBI is a complex disease induced by external mechanical forces to the brain, and the consequent biological response results from a combination of primary injuries that occur at the moment of impact, and the subsequent complex cascade of secondary injury pathways that may develop over the hours, days, or weeks that follow.<sup>134, 139</sup> TBI is recognised to induce both central and systemic changes,<sup>133</sup> a number of which have potential to affect bone and bone fracture healing. Results from chapter 4 demonstrated that experimental TBI in the absence of fracture caused significant systemic bone loss with reductions in cortical and trabecular bone volume in rats. Clinical studies have also reported lower bone mineral density and an elevated risk of fracture in brain-injured patients.<sup>173-176</sup> Paradoxically, TBI has been associated with stimulation of osteogenesis, with heterotopic ossification (i.e. the formation of bone in soft tissues) and enhanced callus formation described in TBI patients for several decades.<sup>19, 178, 186, 261, 262</sup> Despite these associations the relationship between TBI and fracture healing remains poorly understood. Clinical data is limited by the presence of several

confounding variables and results from initial rodent studies are mixed. In addition, nearly all previous rodent studies have administered TBI using the CCI model that requires craniotomy.<sup>179-183</sup> Given that previous studies have demonstrated enhanced osteogenesis in distant skeletal sites following bone injury, possibly through release of osteogenic humoral factors via a process known as ‘systemic acceleration’,<sup>188</sup> the craniotomy performed to administer the CCI most likely represents a confounding variable.

Despite the fact that closed-skull brain injury is the most common form of TBI in humans,<sup>263,</sup><sup>264</sup> the bone healing response of rodents exposed to closed-skull TBI (i.e. without craniotomy) remains unclear. Accordingly, in order to further explore the effect of closed-skull TBI on fracture healing, a novel combined trauma mouse model was developed that involved a weight-drop TBI and concomitant tibial fracture.

## 6.2 Materials and methods

### 6.2.1 Mice

C57Bl/6 male mice were obtained from the Australian Animal Resource Centre (ARC, Western Australia) for use in this study. Mice were 12 weeks of age at the time of injury, were housed individually under a 12-hour light/dark cycle and were given access to food and water *ad libitum* for the duration of the experiment. All procedures were approved by The Florey Institute of Neuroscience and Mental Health Animal Ethics Committee (#14-006-UM), were within the guidelines of the Australian code of practice for the care and use of animals for scientific purposes by the Australian National Health and Medical Research Council and in compliance with ARRIVE guidelines for how to report animal experiments.

### 6.2.2 Experimental Groups

Mice were randomly assigned to either Fracture + Sham TBI (FX) or Fracture + TBI (MULTI) injury groups. Thirty-three mice were used for this experiment including 4 mice that died following TBI. The FX group consisted of 14 mice and the MULTI group consisted of 15 mice. Mice were either killed at 21 days post-injury (FX, n = 6; MULTI, n = 9) or at 35 days post-injury (FX, n = 8; MULTI, n = 6). Fractures were analyzed via  $\mu$ CT and histological analysis was performed on 22 of 29 fracture samples, with 7 specimens (4 MULTI, 3 FX) omitted due to complications during processing.

### 6.2.3 Tibial Fracture

Before the assigned TBI injury was given, mice received a closed tibial fracture stabilized by intramedullary fixation as previously described.<sup>265</sup> Mice were anaesthetized using a mixture of oxygen and 4% isoflurane and anesthesia was maintained using a mixture of oxygen and 2% isoflurane. A small incision was then made inferior of the right knee, an entry point into the medullary canal of the tibia was made using a 26-G needle and an intramedullary rod (000 insect pin, 0.25 mm diameter) was inserted inside the medullary canal. A fracture was

then generated in the tibial midshaft using three-point bending tweezers and the fracture was visualized using radiography for confirmation of a transverse, non-comminuted fracture supported by the intramedullary rod (Figure 6.1a). Following the fracture, the initial intramedullary rod was replaced with a new rod (00 insect pin, 0.30 mm diameter) which remained *in situ* for the remainder of the study to ensure alignment of fractured-ends (Figure 6.1b). The incision was then sutured. Sham-injury for the fracture procedure consisted of the incision and suturing, but no fracture was generated.

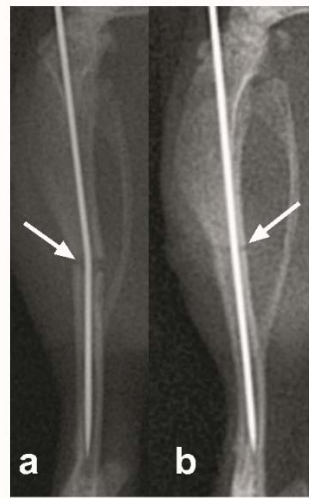


**Figure 6.1.** Tibial fracture of the mid-diaphysis. Tibial fracture was generated in the mid-diaphysis (arrow) above the fibular junction following intramedullary pinning (a) and following confirmation of the transverse, non-comminuted fracture the intramedullary rod was replaced with a new, larger rod (b).

#### 6.2.4 Closed-skull weight-drop model of TBI

Weight-drop TBI and associated sham-injury procedures were based on previously described standard protocols.<sup>253, 266</sup> Briefly, the weight-drop device consisted of a guided- and weighted-rod (215 g) with a blunt silicone-covered impact tip (4 mm diameter). A longitudinal incision was made along the midline of the scalp and following tibial fracture the mouse was stabilized on the injury device platform. The weighted rod was released from a height of 2 cm and the impact tip made contact between the sagittal and coronal suture. The TBI sham-injury procedure was identical to that described for the TBI procedure, except the

weighted rod was not released. All mice received 0.05 mg/kg of buprenorphine analgesic subcutaneously post-injuries.

### 6.2.5 Acute assessment of injury severity

Apnoea, unconsciousness and self-righting reflex times shown in table 1, were monitored in all mice immediately after injury and were indicators of acute injury severity. Apnoea was the time from injury to spontaneous breathing. Loss of consciousness was the time from injury to a hind-limb withdrawal response to a toe pinch. Self-righting reflex was the time from injury to the return of an upright position.

**Table 6.1.** Acute injury severity measures

	Apnoea	Hind-limb	Self-righting
FX	0	46.6 ± 15.6	68 ± 14.7
MULTI	19.7 ± 3.9 <sup>a</sup>	179.9 ± 43.4 <sup>b</sup>	204.4 ± 41.9 <sup>b</sup>

The MULTI group experienced significantly longer apnoea, hind-limb withdrawal, and self-righting reflex times (seconds) compared to the FX group. <sup>a</sup>Greater than FX,  $p < 0.0001$ . <sup>b</sup>Greater than FX,  $p < 0.01$ .

### 6.2.6 $\mu$ CT

Fractured tibiae were fixed overnight in 4% paraformaldehyde in 0.1M sodium cacodylate buffer (pH 7.4) and stored at 4° C in 0.1M cacodylate buffer containing 10% sucrose (pH 7.4). Images were acquired using a Skyscan 1076 scanner (Bruker-microCT) at 9  $\mu$ m voxel resolution, 0.5 mm aluminium filter, 48 kV voltage, 100  $\mu$ A current, 2400 ms exposure, rotation 0.5° across 180°, frame averaging of 1. Images were reconstructed using NRecon (version 1.6.3.1) and the following parameters: CS to image conversion, 0.0-0.11; ring artefact, 6; pixel defect mask, 5%; and beam hardening correction, 35%. Following reconstruction, the region of interest (ROI) for each bone was determined using CTAN (version 1.11.8.0, Bruker MicroCT) as being a 2 mm region longitudinally centred on the callus (i.e. 1 mm either side of the fracture line of the callus); the border of the callus was

delineated using the “shrink-wrap” function. Thresholds used for quantification of structural parameters were determined using the automatic “otsu” algorithm within CTAn, and visual inspection of images and qualitative comparison with histological sections. Once determined, a threshold of 41 was used for structural analysis of calluses at both 21 and 35 days post-fracture. 2D and 3D data were generated for all analyses and 3D models were generated using the “marching cubes” algorithm from thresholded data (in CTAn).

#### *6.2.7 Histological processing, staining, and histomorphometry*

Scanned tibial fractures were processed to plastic, sectioned and stained. Briefly, tibial fractures were dehydrated using a graded series of ethanols and infiltrated and embedded in LR White resin (London Resin Company limited, Reading, England). Samples were polymerized in LR White resin at 60°C for 24 h. Five micron thick longitudinal sections were cut at the midpoint of undecalcified callus on a Leica RM 2155 Rotary Microtome (Leica, Wetzlar, Germany) with a tungsten carbide blade. Sections were stained using Safranin O and Fast Green to examine bone and cartilage content. Additional sections were also stained for the presence of tartrate-resistant acid phosphatase (TRAP; commonly used as a cytochemical marker of osteoclasts). The total area of callus stained positive for TRAP activity was divided by the total callus area to yield the percentage of callus occupied by TRAP activity as a surrogate marker for osteoclastic area. Sections were photographed on a Leica DMBRE microscope (magnification 25x for Safranin O and Fast green stained sections and 50x for TRAP stained sections) before being assessed both qualitatively and quantitatively using Leica Qwin software.

#### *6.2.8 Statistical analyses*

All data was analyzed with GraphPad prism 6 (GraphPad software, Inc.) using Mann-Whitney-U tests with significance defined as  $p < 0.05$ .

## 6.3 Results

### 6.3.1 $\mu$ CT

Representative  $\mu$ CT reconstructions of longitudinal midpoint hemi-calluses are shown in Figure 6.2a-d.  $\mu$ CT assessment revealed that at 21 days post-fracture all calluses from both injury groups had reached union. Analysis of calluses at 21 days post-injury (Figure 6.2e-j) revealed MULTI calluses had significantly greater total volume (Figure 6.2e; 21%.  $p < 0.05$ ), bone volume (Figure 6.2f; 19%.  $p < 0.05$ ), and mean polar moment of inertia (Figure 6.2h; 40%.  $p < 0.05$ ), bone surface (Figure 6.2i; 29%.  $p < 0.05$ ) and mean tissue area (Figure 6.2j; T.Ar. 21%.  $p < 0.05$ ) when compared to calluses from FX mice, however, no difference in bone volume fraction (Figure 6.2g; BV/TV) between MULTI and FX calluses was observed. No differences between FX and MULTI calluses were observed at 35 days post-injury in any measured parameter (Figure 6.2e-j).

### 6.3.2 Histology and histomorphometric analysis

Representative histological sections are shown in Figure 6.3a-d. Qualitative histological assessment of calluses at 21 days post-injury showed an obvious increase in trabecular bone in MULTI calluses (Figure 6.3b) compared to FX calluses (Figure 6.3a). By 35 days there were no obvious qualitative differences in the histological appearance between MULTI (Figure 6.3d) and FX calluses (Figure 6.3c) in concordance with  $\mu$ CT. Histomorphometric analysis reflected the qualitative histological assessment of calluses and complemented  $\mu$ CT analysis. At 21 days post-injury, compared to FX calluses, MULTI calluses had increased total area (Figure 6.3e; 20%.  $p < 0.05$ ), bone area (Figure 6.3f; 33%.  $p < 0.01$ ) and area of newly formed trabecular bone (Figure 6.3h; 30%.  $p < 0.05$ , however, no difference in newly formed bone area fraction (Figure 6.3g; Trab.Ar/Total.Ar), or cartilage area (Figure 6.3i) was detected between MULTI and FX calluses. At 35 days post-injury no differences were found between FX and MULTI calluses in any measured parameter (Figure 6.3e-i). Representative

TRAP stained histological sections are shown in Figure 6.4a-d. Qualitative assessment of calluses shows an increase in TRAP activity in MULTI calluses (Figure 6.4b) compared to FX calluses (Figure 6.4a) at 21 days post-injury. Quantitative analysis of 21 day calluses revealed a significant increase in the TRAP activity/total callus area, which indicated a greater density of osteoclast-lineage cells in calluses from MULTI mice compared to calluses from fracture-only mice (Figure 6.4e;  $p < 0.05$ ). No difference in the extent of area stained for TRAP activity/total callus area was found at 35 days post-fracture (Figure 6.4c-e).

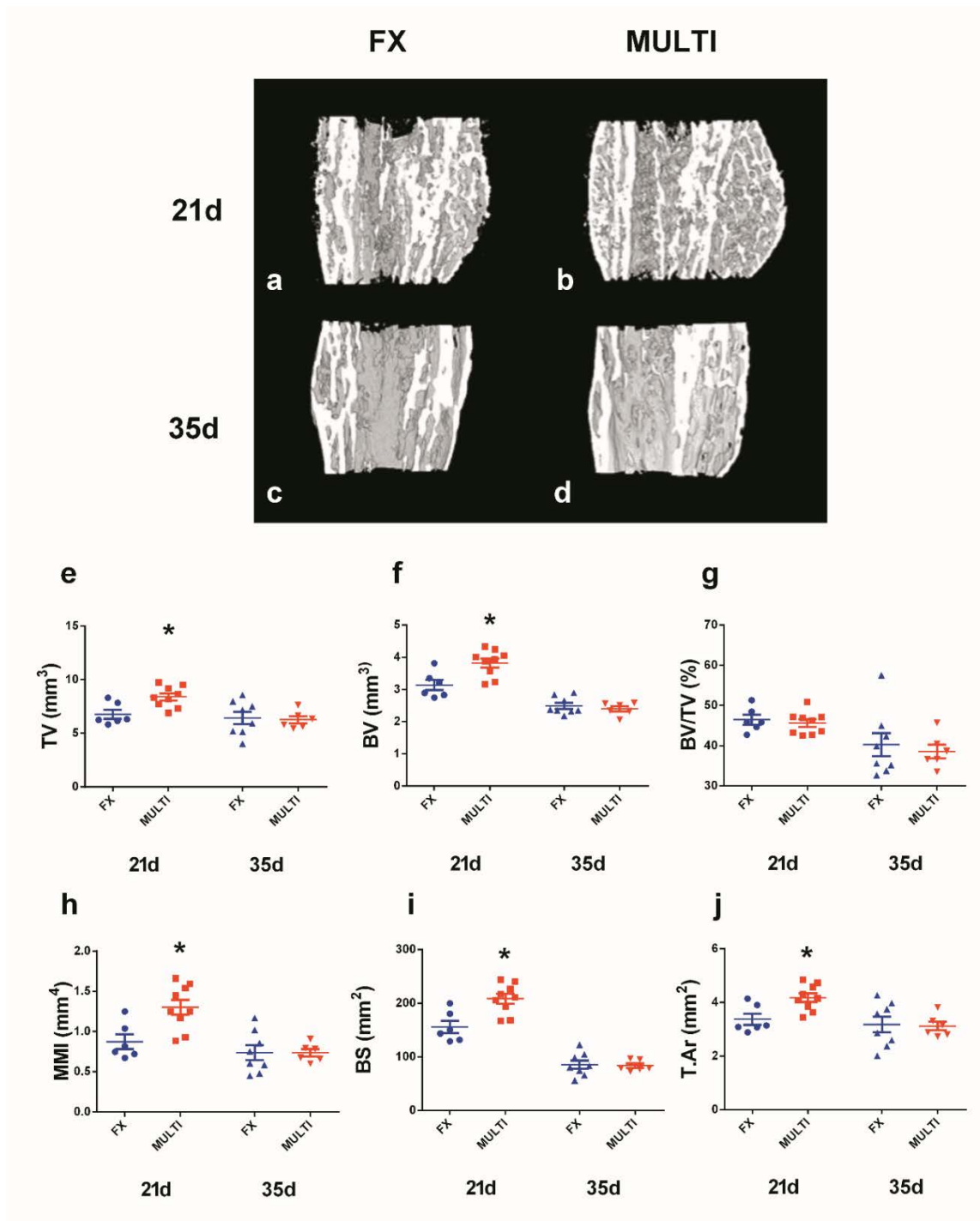


**Figure 6.2.** Longitudinal midpoint views of representative  $\mu$ CT reconstructions of hemi-calluses (a-d).  $\mu$ CT analysis of fracture calluses shows MULTI calluses ( $n = 9$ ) had increased total volume (e; TV), bone volume (f; BV), mean polar moment of inertia (h; MMI), bone surface (i; BS) and mean tissue area (j; T.Ar) at 21 days post-injury compared to FX calluses ( $n = 6$ ;  $*p < 0.05$ ). However, no difference in bone volume fraction (g; BV/TV) between MULTI and FX calluses. No differences were found between 35 day fracture calluses from FX ( $n = 8$ ) and MULTI ( $n = 6$ ) mice (e-j). Bars are means  $\pm$  SEM.

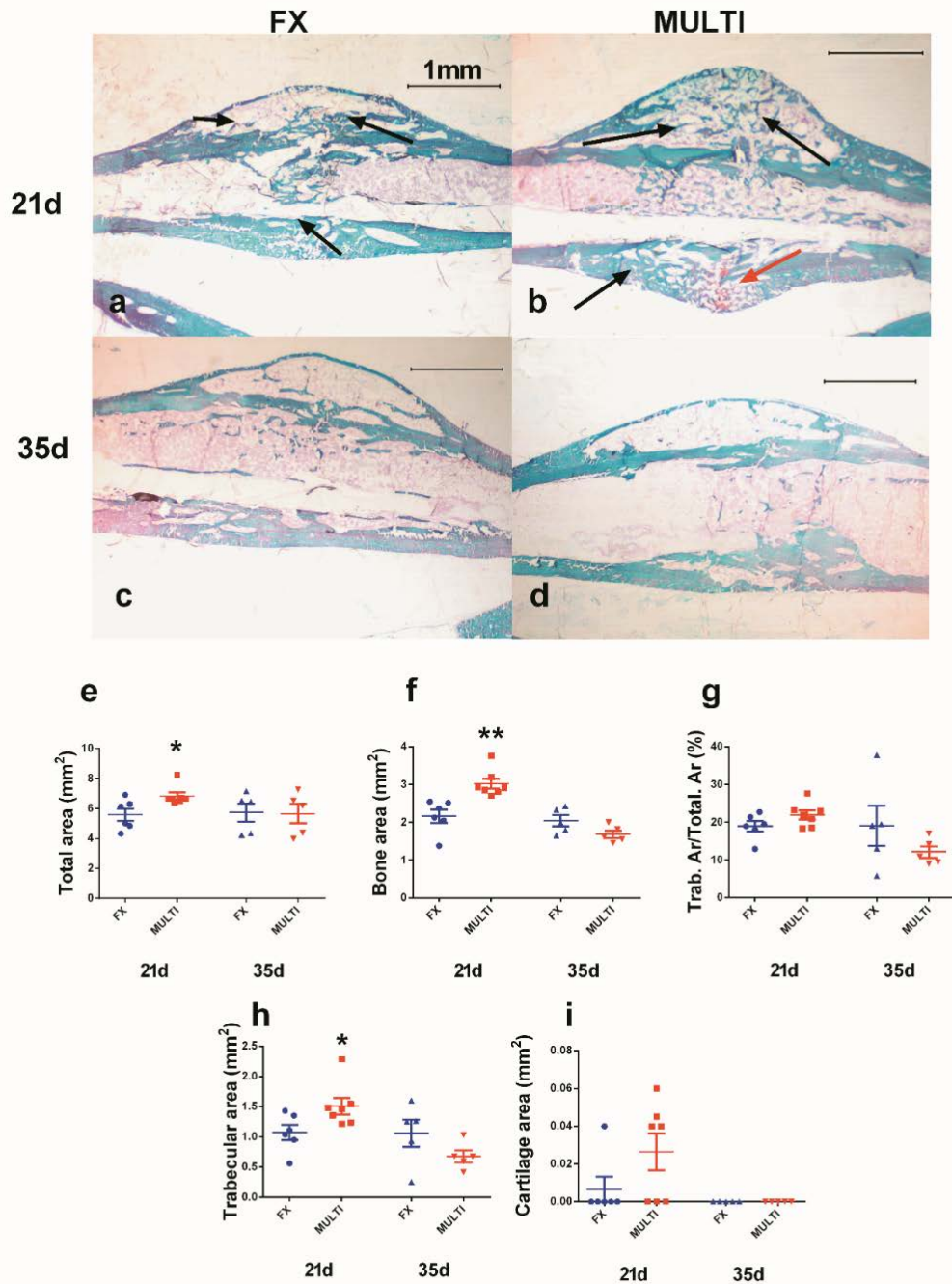


**Figure 6.3.** Representative histological sections of undecalcified calluses from FX and MULTI mice at 21 and 35 days post-injury (a-d, stained with Fast Green and Safranin O, magnification 25x). Histological assessment at 21 days post-injury shows an increased amount of newly formed mineralized trabecular bone (stained green; black arrows) and presence of non-mineralized cartilage (stained red; red arrow) in MULTI calluses (b; n = 6) compared to FX calluses (a; n = 6), however at 35 days there are no obvious differences between MULTI (d; n = 5) and FX calluses (c; n = 5). Histomorphometric analysis of fracture calluses shows MULTI calluses had increased total area (e; \* $p < 0.05$ ), bone area (f; \*\* $p < 0.01$ ) and area of newly formed trabecular bone (h; \* $p < 0.05$ ), at 21 days post-injury when compared to calluses from FX mice. However, no difference in newly formed bone area fraction (g; Trab.Ar/Total.Ar), or cartilage area (i) was detected between MULTI and FX calluses. No differences were observed in day 35 fracture calluses between FX and MULTI mice (e-i). Bars are means  $\pm$  SEM.

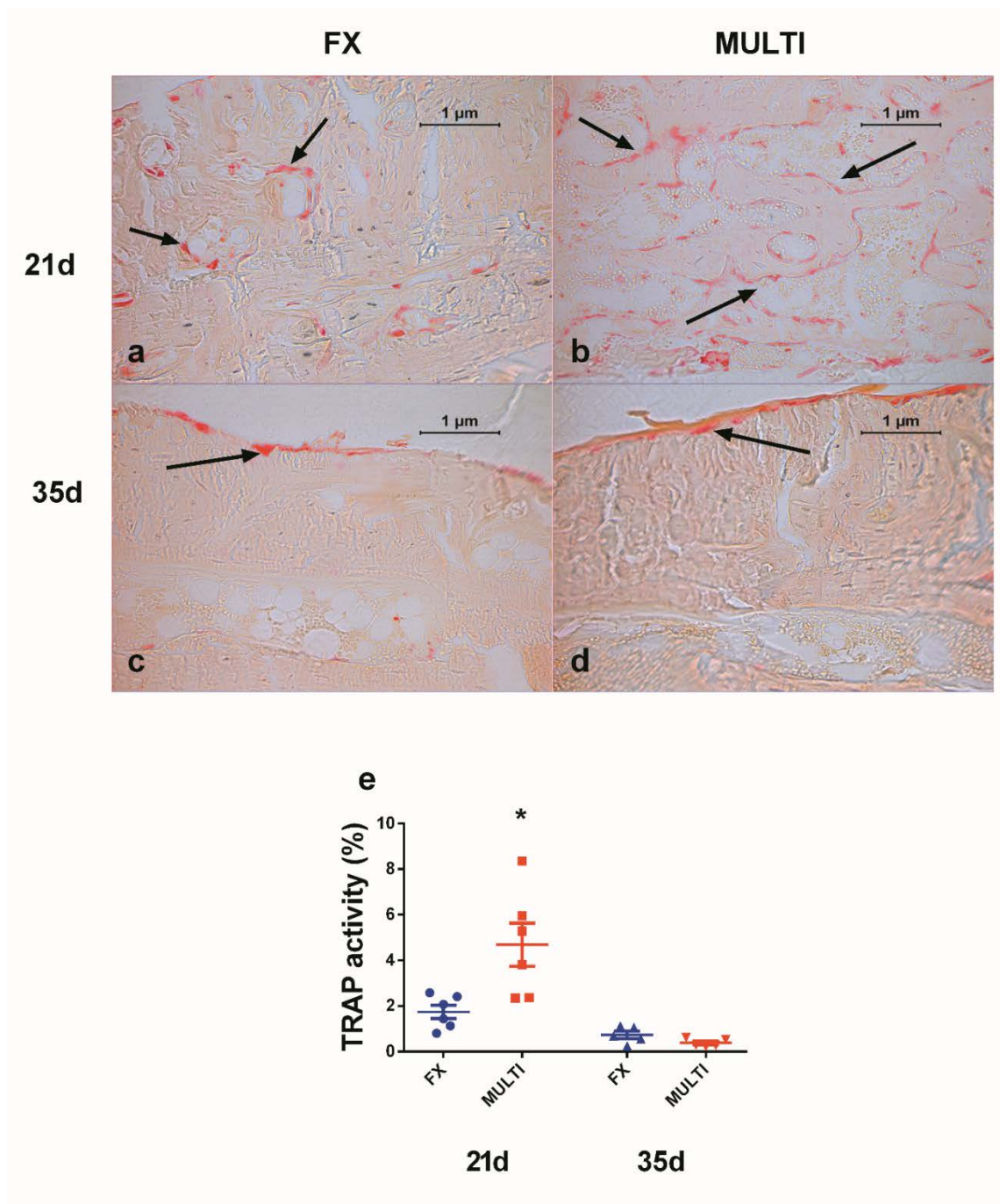


**Figure 6.4.** Representative histological sections of un-decalcified calluses from FX and MULTI mice at 21 and 35 days post-injury stained for TRAP (a-d; magnification 200x). Histological assessment at 21 days post-injury shows an increased amount of TRAP activity stained red in MULTI calluses (b; n = 6) compared to FX calluses (a; n = 6), however at 35 days there are no obvious differences between MULTI (d; n = 5) and FX calluses (c; n = 5). Analysis of fracture calluses shows MULTI calluses had increased percentage of TRAP activity (e; \*p < 0.05) compared to calluses from FX mice. However at 35 days post-fracture there were no differences between the groups (e). Bars are means ± SEM.

## 6.4 Discussion

Few studies have investigated the effect of closed-skull TBI on fracture healing, therefore here a novel mouse model that involved a closed-skull weight-drop TBI and concomitant tibial fracture was developed. In this study it was shown that in mice subjected to closed-skull TBI, fracture calluses at day 21 were larger, had a greater bone volume and displayed a higher mean polar moment of inertia when compared to calluses from fracture-only mice. By day 35 the difference in fracture callus was not evident. While several previous studies have reported that TBI increased fracture callus size and extent of mineralization, these studies all featured an open-skull TBI model using craniotomy,<sup>179-183</sup> which represents a potentially confounding factor. This study is the first to document that a closed-skull model of TBI enhanced formation of fracture callus in long bones.

The findings of this chapter findings are similar to those previously described in rodents given open-skull CCI, with several studies similarly reporting greater callus bone and total tissue volume between 2-4 weeks post-TBI.<sup>179, 180, 183</sup> In addition, the increased mean polar moment of inertia (a quantity used to predict an object's ability to resist torsion) observed in calluses from mice with TBI indicated that closed-skull TBI may have resulted in superior mechanical integrity of the fracture site. Taken together, these findings suggest that closed-skull TBI enhanced callus formation rate and/or reduced bone resorption and thereby likely resulting in a decreased risk of re-fracture at 21 days post-injury. Importantly, results from this study suggest that the heightened callus formation described in previous studies is unlikely to be primarily due to the craniotomy procedure, although in the absence of appropriate controls (i.e. craniotomy + fracture), the contribution of 'systemic acceleration' in these studies cannot be discounted.<sup>188</sup>

The results of this study provide insight into the nature of callus modelling/remodelling following TBI. Although there were no significant differences in cartilage volumes between

groups, four of the seven calluses from brain-injured mice contained non-mineralized cartilage, compared with one of the seven calluses from fracture-only mice. This finding may suggest that calluses from mice with TBI featured a relatively higher degree of cartilage formation and endochondral ossification, however further investigations are required to fully characterize the nature of callus modelling/remodelling in animals with TBI in the early stages post-injury. Structural differences in calluses from brain-injured and fracture-only mice did not persist to 35 days post-injury.<sup>181, 182</sup> This result, combined with the finding of an increased percentage of TRAP-activity in calluses from brain-injured mice at 21 days post-injury, is likely to indicate that calluses from mice with TBI underwent significant resorption between days 21 and 35 in order to remodel to the size of their fracture-only counterparts at 35 days post-fracture.

It was observed that calluses from multiply-injured mice were larger and had a greater bone volume at 21 days post-fracture compared to those from fracture only mice. These results conflict with the findings of Boes and colleagues, who reported that calluses from mice with closed-skull injury were reduced in size.<sup>170</sup> This discrepancy in findings may be attributed to differences in the nature of the weight-drop brain injury, with the model of Boes et al. inducing a highly diffuse injury and the model of the current study causing a mixed focal/diffuse injury pattern.<sup>170, 266</sup> Acute measures of injury severity in this study indicate that the TBI model was of mild-moderate severity, given that previous studies have speculated that callus size may correlate with TBI severity,<sup>267</sup> it is possible that an increased severity of experimental TBI may result in callus size remaining larger at time-points beyond 21 days post-injury. Additional studies using a variety of injury parameters, including differences in injury location, severity and mechanism, are required to provide further insights into how particular TBIs may impact callus formation.

Though several studies have reported enhanced callus volumes post-TBI,<sup>179-183</sup> the nature of callus formation following TBI is not well established. Several researchers have speculated that the enhanced callus volumes post-TBI may represent a form of heterotopic ossification about the fracture site.<sup>19, 185, 262, 267, 268</sup> In the current experiments, no gross morphological differences in healing calluses between multitrauma and fracture-only mice using high resolution  $\mu$ CT and histology, however the contribution of heterotopic ossification to an enhanced callus formation response cannot be ruled out. Notably, a recent study has provided insight into the possible pathogenesis of neurological heterotopic ossification, finding bone formation in the hamstring of mice with combined spinal cord injury and muscle injury, but not following either injury in isolation.<sup>168</sup> The authors also found depletion of phagocytic macrophages reduced heterotopic ossification volume by 90%, which suggests that localized inflammation in combination with neurological injury may drive this abnormal bone formation. Accordingly, in the current study it is possible that the inflammatory response to tibial fracture, in combination with TBI, may have provided the osteogenic conditions necessary to enhance bone formation about the fracture site.

There are several potential mechanisms through which the central and systemic changes occurring post-TBI may influence bone healing.<sup>19, 178, 186, 261, 262</sup> Growing evidence suggests a significant role for the central nervous system in regulating bone homeostasis,<sup>59, 269-273</sup> it is possible an injury-induced disturbance of these neural pathways may alter the bone modelling/remodelling response during fracture healing. Furthermore, several *in vitro* studies have demonstrated that serum from brain-injured rats increased the proliferation of mesenchymal stem cells, and that serum and CSF from TBI patients increased osteoblastic proliferation.<sup>170-172</sup> These results have led to speculation that the enhanced callus formation observed following TBI may be due to an unknown humoral mechanism.<sup>19, 178</sup> Further studies

are required to identify the possible humoral factor/s and the extracellular and intracellular signalling pathways responsible for the enhanced callus formation following TBI.

Although the current experiment provides evidence for the first time that closed head TBI results in increased callus formation; the study however has some limitations. Two defined time-points were analysed following fracture healing and the data clearly show that TBI enhanced callus size at 21 days post-fracture. These measurements are static analyses and provide a snapshot of cell activity at that given time. Further studies using *in vivo*  $\mu$ CT or serial x-ray analyses to assess changes in the fracture sites/fracture callus overtime, will provide insight into the timing of callus formation and fracture union. In addition, greater understanding of the cellular mechanism that resulted in enlarged callus formation will be possible with future studies utilising *in vivo* fluorochrome labelling to definitively determine bone formation rates and static bone histomorphometry to determine osteoclastic/osteoblastic numbers. Furthermore, analysis of serum markers for bone and cartilage formation and resorption could provide additional insight into the timing and extent of these cellular processes during callus formation and remodelling. Results presented in Chapter 4, however, revealed that TBI led to a reduction in bone volume in unfractured limbs, therefore analysis of serum bone turnover markers may not provide an accurate indication of fracture-specific remodelling. Histomorphometric analyses, combined with radiographic analyses therefore, may be more informative measures. Finally, it is important to recognize that the initial fracture healing cascade may have been influenced by any TBI-induced reductions in animal mobility in the early stages post-injury. Nonetheless, a recent study that characterised the weight-drop injury model used in this study reported no significant deficits on a neurological severity scale (of which motor function was a key outcome) by 24 hours post-injury.<sup>266</sup> Accordingly, the authors believe mobility was not reduced in mice with TBI and therefore did not influence the findings of the current study. However, future investigations should

monitor mobility/activity levels of mice in the early stages post-TBI in order to rule out a reduction in activity levels as a confounding factor.

## **Conclusions**

The findings presented in this study indicate that long bone fracture in closed head TBI results in calluses that are larger in size and have an increased bone volume compared to calluses from fracture-only mice. This finding is consistent with the notion that TBI leads to a heightened callus formation response. Although future studies are required to elucidate the mechanisms behind this phenomenon, these findings improve our understanding of the effect of TBI on bone regeneration and allow a better understanding of the complex nature of combined traumatic injuries.

## **7 Conclusions and future directions**

## 7.1 T $\beta$ <sub>4</sub> and bone healing

The first experiments of this thesis aimed to determine the effect that T $\beta$ <sub>4</sub>-treatment had on healing of murine fibular fractures. These experiments revealed that T $\beta$ <sub>4</sub>-treatment increased bone volume density (BV/TV) at 21 days post-fracture, while at 42 days post-fracture calluses from T $\beta$ <sub>4</sub>-treated mice displayed superior mechanical characteristics, specifically, elevated peak force to failure and greater stiffness, when compared to vehicle-treated mice. These findings demonstrate for the first time the therapeutic potential of T $\beta$ <sub>4</sub> for treating bone fractures. Chapter 3 of this thesis aimed to provide insights as to how T $\beta$ <sub>4</sub>-treatment may have enhanced fracture healing by examining fracture callus expression of genes associated with angiogenesis, cell differentiation and mineralization. This study found mRNA levels of VEGF $\alpha$  at 21 days post-fracture were increased in calluses from T $\beta$ <sub>4</sub>-treated mice when compared to control calluses, however no differences in mRNA expression of genes associated with cell differentiation or mineralization were observed between T $\beta$ <sub>4</sub>-treated and vehicle-treated groups. Elevated mRNA levels of VEGF $\alpha$  at 21 days post-fracture may indicate that vascularisation of the fracture site was enhanced. An additional aim was to examine the effect of treatment with T $\beta$ <sub>4</sub> and T $\beta$ <sub>4</sub>-derived fragments, 1-4, 1-15 and 17-23 on proliferation, differentiation and mineralization in an osteoprogenitor cell line, Kusa-O. Results showed that treatment of Kusa-O cells with T $\beta$ <sub>4</sub>, 1-4, 1-15 and 17-23 did not significantly affect cell proliferation, differentiation or mineralization. These findings indicate that T $\beta$ <sub>4</sub> may stimulate bone formation without directly stimulating either osteoblastic differentiation or bone mineralization. The present data therefore may indicate that T $\beta$ <sub>4</sub> enhanced angiogenesis at the injury site to stimulate fracture healing.

Although Chapter 2 provides evidence that T $\beta$ <sub>4</sub>-treatment enhanced fracture healing in a mouse model, additional experiments are required to identify if there were any differences in the rate of callus union between treated and control groups, and also to determine the cellular

mechanisms underlying the observed changes. Further studies using serial *in vivo*  $\mu$ CT or X-ray analysis to assess T $\beta$ <sub>4</sub>-induced changes in the fracture site/fracture callus overtime will provide important insights into the timing of callus formation and fracture union. These studies, combined with both dynamic and static histomorphometric analyses of the fracture site are needed to clearly identify the modelling/remodelling basis of the enhanced healing observed in T $\beta$ <sub>4</sub>-treated calluses.

In addition, further studies are required to determine the optimal dose, method of delivery,<sup>274</sup> and treatment regime (i.e. single bolus, or multiple doses per week of lesser concentration, or continuous administration via subcutaneous osmotic pump) to promote fracture healing. It is also important to determine the effect of T $\beta$ <sub>4</sub> treatment at critical time-points post-fracture, as well as the therapeutic window of this peptide, by varying the administration period of T $\beta$ <sub>4</sub> post-fracture. A greater understanding of the mechanisms through which T $\beta$ <sub>4</sub> promotes bone healing will aid in determining these above parameters. For example, as T $\beta$ <sub>4</sub> has been shown to promote angiogenesis in other healing tissues, and preliminary evidence of this thesis showed that mRNA expression of VEGF- $\alpha$  was elevated in T $\beta$ <sub>4</sub>-treated calluses; future studies should investigate the effect of T $\beta$ <sub>4</sub> on callus angiogenesis. This may be achieved by infusing animals with a contrast agent such as barium sulphate that is detectable on a  $\mu$ CT scan and would allow determination of vascular parameters. Numerous lines of evidence suggest that T $\beta$ <sub>4</sub> also promotes cell survival following injury,<sup>104, 106, 107</sup> therefore the potential anti-apoptotic actions of T $\beta$ <sub>4</sub> on osteogenic cells of the callus should also be examined, perhaps by using *in vitro* cell survival assays. A pro-survival effect of T $\beta$ <sub>4</sub> on these cells may suggest that administration with T $\beta$ <sub>4</sub> directly after fracture may lead to the most beneficial outcome. Other tissue injury models have demonstrated that the regenerative effects of T $\beta$ <sub>4</sub> may in part be attributed to the anti-inflammatory properties of the peptide,<sup>104, 105</sup> hence, the anti-inflammatory effects of T $\beta$ <sub>4</sub> within fracture callus should also be studied by determining

inflammatory cell numbers at acute time-points post-injury. Significant downregulation of inflammatory processes has, however, been shown to have an inhibitory effect on fracture healing,<sup>275</sup> therefore if T $\beta$ <sub>4</sub> is also found to significantly decrease inflammation at the fracture site, it may promote healing most efficiently if administered after the inflammatory phase of bone healing has subsided.

Moreover, future studies should further examine the actions of T $\beta$ <sub>4</sub> in other models of bone healing, particularly using models more closely resembling clinically problematic conditions that involve delayed or atrophic non-union (characterized by sparse callus formation and sclerosis of the marrow cavity with only fibrous tissue between the two fractured ends).<sup>276</sup> Such a model is seen in a femoral segmental defect (3-8 mm) in the rat, which, in the absence of intervention, leads to atrophic non-union of the fracture site.<sup>276</sup> This particular model would also allow investigation into the effect that delivery of T $\beta$ <sub>4</sub> in addition to a tissue engineering construct/bone graft may have on bone healing.

Furthermore, given that perioperative infections are a major clinical problem, the anti-microbial properties of T $\beta$ <sub>4</sub> may be of use in fracture models involving sepsis.<sup>277</sup> Finally, osteoporotic fractures represent another clinically-relevant injury that may benefit from the actions of exogenous T $\beta$ <sub>4</sub> administration. Up to 20% of osteoporotic patients die within one year post-fracture due to long-term hospitalisation,<sup>278</sup> hence there is a need for therapeutic interventions to promote healing in these situations. Osteoporosis induced by ovariectomy in rats delays bone fracture union, reduces callus cross-sectional area and decreases mechanical properties of callus.<sup>279, 280</sup> Therefore, the actions of T $\beta$ <sub>4</sub> in osteoporotic animal models of fracture healing should be examined.

In order to assess the potential of T $\beta$ <sub>4</sub> to be a clinically translatable treatment for bone injury, the efficacy of T $\beta$ <sub>4</sub> should be studied in species higher on the phylogenetic scale. Murine

bone has a large capacity to regenerate, whereas human bone has a comparatively much lower osteogenic and healing potential.<sup>274</sup> Therefore, the bone fracture healing potential of T $\beta$ <sub>4</sub> should further be explored in larger animals such as sheep. Sheep represent a viable bone healing model that, when compared to rodents, more closely resemble bone healing in humans.<sup>274</sup> In particular, ovine bone contains Haversian systems and therefore the remodelling cycle is quite similar to that of human bones.<sup>274</sup> Consequently, the healing process of fractured sheep bone is thought to closely approximate that of humans;<sup>281</sup> and therefore the therapeutic potential of T $\beta$ <sub>4</sub> may be further explored using ovine fracture models.

Additionally, as the findings of this thesis indicate that T $\beta$ <sub>4</sub> does not directly affect osteoblast-like cell differentiation and mineralization *in vitro*, treatment of fractures with T $\beta$ <sub>4</sub> in combination with a factor or factors that stimulate(s) osteoblastic activity, may further enhance healing. For example, intermittent PTH administration is an FDA-approved therapy to increase bone mass in osteoporotic patients through its actions on osteoblasts (activation of the WNT/ $\beta$ -catenin pathway),<sup>282</sup> thus the combination of T $\beta$ <sub>4</sub> and PTH may have an additive effect on fracture healing. Ultimately, clinical studies are necessary to determine the safety and efficacy of T $\beta$ <sub>4</sub> to enhance bone regeneration.

## **7.2 Influence of TBI on bone homeostasis and fracture healing**

For three decades TBI has been linked to accelerated fracture healing, however the relationship between TBI and bone turnover as well as bone fracture healing are not well understood<sup>185, 267, 268</sup>, but are important to consider, given the high incidence of TBI and multitrauma involving TBI and concomitant long bone fracture.<sup>132</sup> As such, chapters 4-6 of this thesis investigated the influence of TBI on bone homeostasis and fracture healing. Using the FPI model of TBI in the rat this thesis found that BMD was reduced at the distal metaphyseal region of femora at 12 weeks post-injury in TBI rats, when compared to shams.

Furthermore at 1 and 12 weeks post-injury, cortical content, cortical thickness and trabecular bone volume ratio was decreased at the distal metaphysis in femora from TBI rats compared to shams. In addition, distance travelled in the open-field at 1, 4 and 12 weeks post-injury was not significantly different between TBI and sham groups, which indicates that the effects of TBI on bone were not likely to be caused by immobilization. In Chapter 5, it was found that the TBI-induced bone loss was reduced by decreasing the extent of the brain injury via sodium selenate treatment. Femora from selenate-treated rats were, however, shorter in length and had an increased growth-plate width, therefore these deleterious effects on longitudinal bone growth should be considered if sodium selenate treatment is to be translated into a clinical TBI setting in juveniles who suffer a TBI. As such, further investigations are likely to be required in order to modify/optimize the duration, dose and administration of sodium selenate to possibly prevent reductions in bone growth, while still reducing brain damage post-TBI. Taken together, these findings are the first to suggest that TBI in rodents can induce bone loss remote from the site of injury in the absence of any differences in locomotion.

To extend upon the findings of Chapter 4, future studies should attempt to assess changes in bone mass at different skeletal sites over time, using *in vivo*  $\mu$ CT, to determine the timing and extent of bone loss. In order to investigate the cellular mechanisms responsible for the bone loss observed,  $\mu$ CT analysis should be combined with calcein labelling to determine bone formation rates and further histological examination of osteoclastic activity. In addition, serial analysis of serum markers of bone formation and resorption, together with investigations into the effect this serum has on osteoblastic and osteoclasts *in vitro* may unearth that possible humoral mechanism/s underlying the TBI-induced bone loss. Finally, it is also possible that the detrimental effects of TBI on bone may largely be the result of heightened sympathetic outflow, therefore future studies may combine TBI with either

sympathetic denervation or antagonism of  $\beta$ 2 adrenergic receptors to provide insights into the possible autonomic basis of bone loss following TBI.

Whether TBI-induced bone loss also occurs in humans has not yet been established, but is important to investigate given the findings of this thesis.

Human studies that have reported lower bone mineral density in brain-injured patients have attributed this bone loss to immobilization.<sup>173-176</sup> Given the findings of this thesis future studies should investigate the possibility that these changes are not solely due to reduced locomotion. Prospective randomised studies mapping changes in BMD (using pQCT) of TBI and control patients at acute, sub-acute and chronic time-points are required to determine if the bone loss observed in the rodent model of this study occurs in humans in the absence of any differences of physical locomotion. For example, in the case of severe TBI patients who are often immobilised for weeks-months post-TBI, changes in BMD could be assessed at the time of TBI (or as close to as practical) and at 1, 3, 6, 12 and 18 months post-TBI and compared to changes in BMD in appropriate controls i.e. patients without TBI who have been immobilised for a similar period of time to that of TBI individuals plus matched for other factors including age, gender and smoking status.

Having characterized the effect of TBI on un-fractured bone in Chapters 4 and 5, Chapter 6 aimed to investigate the effect of TBI on fracture healing. As discussed in Chapter 6, clinical data on TBI and bone healing is limited by confounding variables, and results from initial rodent studies are varied. In addition, the majority of rodent studies have used a TBI that requires craniotomy,<sup>179-183</sup> which may also be a confounding factor.<sup>188</sup> The novel model used in this thesis featuring a closed-skull weight-drop TBI and concomitant tibial fracture was able to control for these factors. It was found at 21 days post-fracture that calluses from TBI mice were larger, had a greater bone volume, and displayed a higher mean polar moment of

inertia when compared to calluses from fracture-only mice, which indicates that TBI induces the formation of a more robust callus that is less likely to re-fracture. At 21 days, post-fracture calluses from multi-trauma mice had an increased percentage of TRAP-activity, which likely indicates that calluses from TBI mice underwent significant resorption between days 21 and 35 to remodel towards a similar size to that of the size of fracture-only mice at 35 days post-injury.

Despite the findings of this thesis, it still remains unclear as to how TBI can alter callus formation. Future investigations in pre-clinical models are required to concurrently examine post-TBI changes in i) blood proteomics and ii) the activity of peripheral sympathetic nerves at various time-points. Specifically, analysis of plasma in order to attempt to identify possible novel humoral factors that may be stimulating bone formation. In addition to characterizing neurotransmitter release from peripheral sensory and sympathetic nerves within the callus may provide insight into possible differences in the neuronal regulation of fracture healing between multi-trauma and fracture-only groups. Such data may give insights into what factors are responsible for the increased callus size observed in multiply-injured mice. These types of investigations, will enhance our understanding of mechanisms involved in TBI stimulating early callus formation and highlight potential therapeutic targets to augment healing in delayed fracture healing and non-union fracture models.

In Chapter 6 the TBI was administered at a single anatomical location, impacts to different areas of the brain may allow determination of specific brain regions that contribute to the either TBI-induced bone loss or enhanced fracture callus size. For example, the ventromedial hypothalamic neurons have been identified as playing a key role in regulating bone metabolism, with chemical lesioning of these neurons previously shown to result in a high bone mass phenotype in mice.<sup>283</sup> In addition to examining brain regions, another factor worth investigating is the influence of injury severity. Investigating both injury severity and

anatomical locations within the brain may aid in determining the contribution of different brain regions to the enhancement of callus formation.

Although this thesis focused on the effect of TBI on bone and bone fracture healing, a common musculoskeletal complication of TBI is the development of NHO (neurological heterotopic ossification). Evidence from as early as 1968 suggests that TBI can stimulate NHO. Recent studies suggest that this debilitating condition affects 5-20% of TBI patients,<sup>168</sup><sup>169</sup> in general and up to 64% in those involved in battlefield blast injuries.<sup>284</sup> NHO commonly occurs around the hip, elbow, knee and shoulder joints, causing severe pain and joint deformation that often progresses to complete ankyloses. Currently the only intervention for this affliction is surgical resection after NHOs have matured, which is problematic as the ossifications often entrap large blood vessels and nerves. The mechanisms responsible for NHO are not yet known, however, as alluded to in Chapter 6, recent evidence suggests that localized inflammation, in combination with neurological injury, may drive this abnormal bone formation. Therefore, it is likely that the mechanisms that stimulate NHO and the heightened callus formation response are linked, hence a logical follow up study from this thesis would be to examine factors involved in the development of NHO post-TBI.

Currently, rodent models of NHO are dependent upon injection with exogenous factors that include BMP-2-4 or genetically-modified models that do not reflect the pathobiology of TBI-induced NHO. Recent work by Genet and co-workers,<sup>168</sup> demonstrated that localized inflammation, combined with central injury, may drive this abnormal bone formation. Specifically, in their experiment, spinal cord injury plus muscle injury was found to induce HO in the hamstring of mice, however, spinal cord injury and/or muscle injury alone did not.<sup>168</sup> Furthermore, ablation of phagocytic macrophages decreased the size of NHO by 90%, indicating that localized inflammation in combination with central injury may stimulate NHO.<sup>168</sup> This preliminary data may be useful in the development of a relevant rodent model

of TBI-induced NHO. Development of a rodent model of TBI-induced NHO, by combining TBI with a myotoxic injury to the periarticular tissue of the hip, the most common site of NHO formation in humans,<sup>285</sup> may allow characterisation of factors that are likely to be involved in the pathogenesis of NHO and thereby potentially validate and implement possible biomarkers and therapies for NHO.

This thesis has described for the first time that treatment of healing murine fibular fractures with T $\beta$ <sub>4</sub> enhanced fracture healing. Therefore, this pleiotropic peptide may have the potential to be a therapeutic agent to augment fracture healing. In addition, this thesis found that TBI-induced bone loss in unfractured bone in the absence of any changes in locomotion, while in fractured bones, TBI resulted in fracture calluses that were larger in size and had an increased bone volume compared to controls. It is hoped that the findings presented in this thesis may unearth new therapies to better treat both normal and problematic bone fractures, as well as interventions that may reduce or prevent bone loss following a TBI.

## References

- [1] Tzioupis C, Giannoudis PV: Prevalence of long-bone non-unions. *Injury* 2007, 38 Suppl 2:S3-9.
- [2] Watts JJA-O, J.; Sanders, K. M.: Osteoporosis costing all Australians: A new burden of disease analysis - 2012 to 2022. *Osteoporosis Australia*, 2015.
- [3] Tay WH, de Steiger R, Richardson M, Gruen R, Balogh ZJ: Health outcomes of delayed union and nonunion of femoral and tibial shaft fractures. *Injury* 2014, 45:1653-8.
- [4] Bell A, Templeman D, Weinlein JC: Nonunion of the Femur and Tibia: An Update. *The Orthopedic clinics of North America* 2016, 47:365-75.
- [5] Antonova E, Le TK, Burge R, Mershon J: Tibia shaft fractures: costly burden of nonunions. *BMC musculoskeletal disorders* 2013, 14:42.
- [6] Babhulkar S, Pande K, Babhulkar S: Nonunion of the diaphysis of long bones. *Clin Orthop Relat Res* 2005:50-6.
- [7] Garrison KR, Shemilt I, Donell S, Ryder JJ, Mugford M, Harvey I, Song F, Alt V: Bone morphogenetic protein (BMP) for fracture healing in adults. *The Cochrane database of systematic reviews* 2010:Cd006950.
- [8] Friedlaender GE, Perry CR, Cole JD, Cook SD, Cierny G, Muschler GF, Zych GA, Calhoun JH, LaForte AJ, Yin S: Osteogenic protein-1 (bone morphogenetic protein-7) in the treatment of tibial nonunions. *The Journal of bone and joint surgery American volume* 2001, 83-A Suppl 1:S151-8.
- [9] Iwata A, Kanayama M, Oha F, Hashimoto T, Iwasaki N: Effect of teriparatide (rh-PTH 1-34) versus bisphosphonate on the healing of osteoporotic vertebral compression fracture: A retrospective comparative study. *BMC musculoskeletal disorders* 2017, 18:148.

- [10] Kawaguchi H, Oka H, Jingushi S, Izumi T, Fukunaga M, Sato K, Matsushita T, Nakamura K: A local application of recombinant human fibroblast growth factor 2 for tibial shaft fractures: A randomized, placebo-controlled trial. *J Bone Miner Res* 2010, 25:2735-43.
- [11] DiGiovanni CW, Lin SS, Baumhauer JF, Daniels T, Younger A, Glazebrook M, Anderson J, Anderson R, Evangelista P, Lynch SE: Recombinant human platelet-derived growth factor-BB and beta-tricalcium phosphate (rhPDGF-BB/beta-TCP): an alternative to autogenous bone graft. *The Journal of bone and joint surgery American volume* 2013, 95:1184-92.
- [12] Aspenberg P, Genant HK, Johansson T, Nino AJ, See K, Krohn K, Garcia-Hernandez PA, Recknor CP, Einhorn TA, Dalsky GP, Mitlak BH, Fierlinger A, Lakshmanan MC: Teriparatide for acceleration of fracture repair in humans: a prospective, randomized, double-blind study of 102 postmenopausal women with distal radial fractures. *J Bone Miner Res* 2010, 25:404-14.
- [13] Peichl P, Holzer LA, Maier R, Holzer G: Parathyroid hormone 1-84 accelerates fracture-healing in pubic bones of elderly osteoporotic women. *The Journal of bone and joint surgery American volume* 2011, 93:1583-7.
- [14] Einhorn TA, Gerstenfeld LC: Fracture healing: mechanisms and interventions. *Nature reviews Rheumatology* 2015, 11:45-54.
- [15] Goldstein AL, Kleinman HK: Advances in the basic and clinical applications of thymosin beta4. *Expert opinion on biological therapy* 2015, 15 Suppl 1:S139-45.
- [16] Treadwell T, Kleinman HK, Crockford D, Hardy MA, Guarnera GT, Goldstein AL: The regenerative peptide thymosin beta4 accelerates the rate of dermal healing in preclinical animal models and in patients. *Annals of the New York Academy of Sciences* 2012, 1270:37-44.

- [17] Goldstein AL, Hannappel E, Sosne G, Kleinman HK: Thymosin beta4: a multi-functional regenerative peptide. Basic properties and clinical applications. Expert opinion on biological therapy 2012, 12:37-51.
- [18] Malinda KM, Sidhu GS, Mani H, Banaudha K, Maheshwari RK, Goldstein AL, Kleinman HK: Thymosin beta4 accelerates wound healing. J Invest Dermatol 1999, 113:364-8.
- [19] Hofman M, Koopmans G, Kobbe P, Poeze M, Andruszkow H, Brink PR, Pape HC: Improved fracture healing in patients with concomitant traumatic brain injury: proven or not? Mediators of inflammation 2015, 2015:204842.
- [20] Blennow K, Hardy J, Zetterberg H: The neuropathology and neurobiology of traumatic brain injury. Neuron 2012, 76:886-99.
- [21] Shultz SR, Wright DK, Zheng P, Stuchbery R, Liu SJ, Sashindranath M, Medcalf RL, Johnston LA, Hovens CM, Jones NC, O'Brien TJ: Sodium selenate reduces hyperphosphorylated tau and improves outcomes after traumatic brain injury. Brain : a journal of neurology 2015, 138:1297-313.
- [22] Clarke B: Normal bone anatomy and physiology. Clinical journal of the American Society of Nephrology : CJASN 2008, 3 Suppl 3:S131-9.
- [23] Ng KW, Romas E, Donnan L, Findlay DM: Bone biology. Bailliere's clinical endocrinology and metabolism 1997, 11:1-22.
- [24] Buckwalter JA, Glimcher MJ, Cooper RR, Recker R: Bone biology. I: Structure, blood supply, cells, matrix, and mineralization. Instructional course lectures 1996, 45:371-86.
- [25] Post TM, Cremers SC, Kerbusch T, Danhof M: Bone physiology, disease and treatment: towards disease system analysis in osteoporosis. Clinical pharmacokinetics 2010, 49:89-118.
- [26] Rho JY, Kuhn-Spearing L, Zioupos P: Mechanical properties and the hierarchical structure of bone. Medical engineering & physics 1998, 20:92-102.

- [27] Proff P, Romer P: The molecular mechanism behind bone remodelling: a review. *Clinical oral investigations* 2009, 13:355-62.
- [28] Einhorn TA: The cell and molecular biology of fracture healing. *Clin Orthop Rel Res* 1998:S7-21.
- [29] Pittenger MF, Mackay AM, Beck SC, Jaiswal RK, Douglas R, Mosca JD, Moorman MA, Simonetti DW, Craig S, Marshak DR: Multilineage potential of adult human mesenchymal stem cells. *Science (New York, NY)* 1999, 284:143-7.
- [30] Kalajzic Z, Li H, Wang LP, Jiang X, Lamothe K, Adams DJ, Aguila HL, Rowe DW, Kalajzic I: Use of an alpha-smooth muscle actin GFP reporter to identify an osteoprogenitor population. *Bone* 2008, 43:501-10.
- [31] Sommerfeldt DW, Rubin CT: Biology of bone and how it orchestrates the form and function of the skeleton. *European spine journal : official publication of the European Spine Society, the European Spinal Deformity Society, and the European Section of the Cervical Spine Research Society* 2001, 10 Suppl 2:S86-95.
- [32] Mackie EJ, Ahmed YA, Tatarczuch L, Chen KS, Mirams M: Endochondral ossification: how cartilage is converted into bone in the developing skeleton. *The international journal of biochemistry & cell biology* 2008, 40:46-62.
- [33] Long F: Building strong bones: molecular regulation of the osteoblast lineage. *Nature reviews Molecular cell biology* 2012, 13:27-38.
- [34] Florencio-Silva R, Sasso GR, Sasso-Cerri E, Simoes MJ, Cerri PS: Biology of Bone Tissue: Structure, Function, and Factors That Influence Bone Cells. *BioMed research international* 2015, 2015:421746.
- [35] Yoshiko Y, Candelieri GA, Maeda N, Aubin JE: Osteoblast autonomous Pi regulation via Pit1 plays a role in bone mineralization. *Molecular and cellular biology* 2007, 27:4465-74.

- [36] Komori T, Yagi H, Nomura S, Yamaguchi A, Sasaki K, Deguchi K, Shimizu Y, Bronson RT, Gao YH, Inada M, Sato M, Okamoto R, Kitamura Y, Yoshiki S, Kishimoto T: Targeted disruption of *Cbfa1* results in a complete lack of bone formation owing to maturational arrest of osteoblasts. *Cell* 1997, 89:755-64.
- [37] Zhao Z, Zhao M, Xiao G, Franceschi RT: Gene transfer of the Runx2 transcription factor enhances osteogenic activity of bone marrow stromal cells in vitro and in vivo. *Molecular therapy : the journal of the American Society of Gene Therapy* 2005, 12:247-53.
- [38] Zhang YW, Yasui N, Ito K, Huang G, Fujii M, Hanai J, Nogami H, Ochi T, Miyazono K, Ito Y: A RUNX2/PEBP2alpha A/CBFA1 mutation displaying impaired transactivation and Smad interaction in cleidocranial dysplasia. *Proceedings of the National Academy of Sciences of the United States of America* 2000, 97:10549-54.
- [39] Nakashima K, Zhou X, Kunkel G, Zhang Z, Deng JM, Behringer RR, de Crombrughe B: The novel zinc finger-containing transcription factor osterix is required for osteoblast differentiation and bone formation. *Cell* 2002, 108:17-29.
- [40] Zhou X, Zhang Z, Feng JQ, Dusevich VM, Sinha K, Zhang H, Darnay BG, de Crombrughe B: Multiple functions of Osterix are required for bone growth and homeostasis in postnatal mice. *Proceedings of the National Academy of Sciences of the United States of America* 2010, 107:12919-24.
- [41] Bonewald LF: The amazing osteocyte. *J Bone Miner Res* 2011, 26:229-38.
- [42] Mikuni-Takagaki Y, Kakai Y, Satoyoshi M, Kawano E, Suzuki Y, Kawase T, Saito S: Matrix mineralization and the differentiation of osteocyte-like cells in culture. *J Bone Miner Res* 1995, 10:231-42.
- [43] You J, Yellowley CE, Donahue HJ, Zhang Y, Chen Q, Jacobs CR: Substrate deformation levels associated with routine physical activity are less stimulatory to bone cells

relative to loading-induced oscillatory fluid flow. *Journal of biomechanical engineering* 2000, 122:387-93.

[44] Schaffler MB, Cheung WY, Majeska R, Kennedy O: Osteocytes: master orchestrators of bone. *Calcified tissue international* 2014, 94:5-24.

[45] Teitelbaum SL: Bone resorption by osteoclasts. *Science (New York, NY)* 2000, 289:1504-8.

[46] Boyle WJ, Simonet WS, Lacey DL: Osteoclast differentiation and activation. *Nature* 2003, 423:337-42.

[47] Xu F, Teitelbaum SL: Osteoclasts: New Insights. *Bone research* 2013, 1:11-26.

[48] Xiong J, Piemontese M, Onal M, Campbell J, Goellner JJ, Dusevich V, Bonewald L, Manolagas SC, O'Brien CA: Osteocytes, not Osteoblasts or Lining Cells, are the Main Source of the RANKL Required for Osteoclast Formation in Remodeling Bone. *PloS one* 2015, 10:e0138189.

[49] Teitelbaum SL: The osteoclast and its unique cytoskeleton. *Annals of the New York Academy of Sciences* 2011, 1240:14-7.

[50] Nakahama K: Cellular communications in bone homeostasis and repair. *Cellular and molecular life sciences : CMLS* 2010, 67:4001-9.

[51] Wada T, Nakashima T, Hiroshi N, Penninger JM: RANKL-RANK signaling in osteoclastogenesis and bone disease. *Trends Mol Med* 2006, 12:17-25.

[52] Hardy R, Cooper MS: Bone loss in inflammatory disorders. *The Journal of endocrinology* 2009, 201:309-20.

[53] Parfitt AM: The coupling of bone formation to bone resorption: a critical analysis of the concept and of its relevance to the pathogenesis of osteoporosis. *Metabolic bone disease & related research* 1982, 4:1-6.

- [54] Sims NA, Martin TJ: Coupling the activities of bone formation and resorption: a multitude of signals within the basic multicellular unit. *BoneKEy reports* 2014, 3:481.
- [55] Ushiku C, Adams DJ, Jiang X, Wang L, Rowe DW: Long bone fracture repair in mice harboring GFP reporters for cells within the osteoblastic lineage. *Journal of orthopaedic research : official publication of the Orthopaedic Research Society* 2010, 28:1338-47.
- [56] Courpron P, Meunier P, Vignon G: [Dynamics of bone remodeling explained by Harold Frost. Theory of the B. M.U. (basic multicellular unit)]. *La Nouvelle presse medicale* 1975, 4:421-4.
- [57] Kristensen HB, Andersen TL, Marcussen N, Rolighed L, Delaisse JM: Increased presence of capillaries next to remodeling sites in adult human cancellous bone. *J Bone Miner Res* 2013, 28:574-85.
- [58] Takeda S, Karsenty G: Central control of bone formation. *Journal of bone and mineral metabolism* 2001, 19:195-8.
- [59] Takeda S: Central control of bone remodelling. *Journal of neuroendocrinology* 2008, 20:802-7.
- [60] Takeda S, Karsenty G: Molecular bases of the sympathetic regulation of bone mass. *Bone* 2008, 42:837-40.
- [61] Yadav VK, Oury F, Suda N, Liu ZW, Gao XB, Confavreux C, Klemenhagen KC, Tanaka KF, Gingrich JA, Guo XE, Tecott LH, Mann JJ, Hen R, Horvath TL, Karsenty G: A serotonin-dependent mechanism explains the leptin regulation of bone mass, appetite, and energy expenditure. *Cell* 2009, 138:976-89.
- [62] Reseland JE, Syversen U, Bakke I, Qvigstad G, Eide LG, Hjertner O, Gordeladze JO, Drevon CA: Leptin is expressed in and secreted from primary cultures of human osteoblasts and promotes bone mineralization. *J Bone Miner Res* 2001, 16:1426-33.

- [63] Gordeladze JO, Drevon CA, Syversen U, Reseland JE: Leptin stimulates human osteoblastic cell proliferation, de novo collagen synthesis, and mineralization: Impact on differentiation markers, apoptosis, and osteoclastic signaling. *J Cell Biochem* 2002, 85:825-36.
- [64] Baldock PA, Lee NJ, Driessler F, Lin S, Allison S, Stehrer B, Lin EJ, Zhang L, Enriquez RF, Wong IP, McDonald MM, During M, Pierroz DD, Slack K, Shi YC, Yulyaningsih E, Aljanova A, Little DG, Ferrari SL, Sainsbury A, Eisman JA, Herzog H: Neuropeptide Y knockout mice reveal a central role of NPY in the coordination of bone mass to body weight. *PloS one* 2009, 4:e8415.
- [65] Baldock PA, Sainsbury A, Allison S, Lin EJ, Couzens M, Boey D, Enriquez R, During M, Herzog H, Gardiner EM: Hypothalamic control of bone formation: distinct actions of leptin and y2 receptor pathways. *J Bone Miner Res* 2005, 20:1851-7.
- [66] Feng X, McDonald JM: Disorders of bone remodeling. *Annual review of pathology* 2011, 6:121-45.
- [67] Leali PT, Muresu F, Melis A, Ruggiu A, Zachos A, Doria C: Skeletal fragility definition. *Clinical cases in mineral and bone metabolism : the official journal of the Italian Society of Osteoporosis, Mineral Metabolism, and Skeletal Diseases* 2011, 8:11-3.
- [68] Office of the Surgeon G: Reports of the Surgeon General. Bone Health and Osteoporosis: A Report of the Surgeon General. Rockville (MD): Office of the Surgeon General (US), 2004.
- [69] Tilg H, Moschen AR, Kaser A, Pines A, Dotan I: Gut, inflammation and osteoporosis: basic and clinical concepts. *Gut* 2008, 57:684-94.
- [70] Kronenberg HM: Developmental regulation of the growth plate. *Nature* 2003, 423:332-6.

- [71] Yang L, Tsang KY, Tang HC, Chan D, Cheah KS: Hypertrophic chondrocytes can become osteoblasts and osteocytes in endochondral bone formation. *Proceedings of the National Academy of Sciences of the United States of America* 2014, 111:12097-102.
- [72] Gerstenfeld LC, Cullinane DM, Barnes GL, Graves DT, Einhorn TA: Fracture healing as a post-natal developmental process: Molecular, spatial, and temporal aspects of its regulation. *J Cell Biochem* 2003, 88:873-84.
- [73] Schindeler A, McDonald MM, Bokko P, Little DG: Bone remodeling during fracture repair: The cellular picture. *Semin Cell Dev Biol* 2008, 19:459-66.
- [74] Einhorn TA, Majeska RJ, Rush EB, Levine PM, Horowitz MC: The expression of cytokine activity by fracture callus. *J Bone Miner Res* 1995, 10:1272-81.
- [75] Kolar P, Schmidt-Bleek K, Schell H, Gaber T, Toben D, Schmidmaier G, Perka C, Buttgerit F, Duda GN: The early fracture hematoma and its potential role in fracture healing. *Tissue engineering Part B, Reviews* 2010, 16:427-34.
- [76] Marsell R, Einhorn TA: The biology of fracture healing. *Injury* 2011, 42:551-5.
- [77] Stegen S, van Gastel N, Carmeliet G: Bringing new life to damaged bone: the importance of angiogenesis in bone repair and regeneration. *Bone* 2015, 70:19-27.
- [78] Henle P, Zimmermann G, Weiss S: Matrix metalloproteinases and failed fracture healing. *Bone* 2005, 37:791-8.
- [79] Oryan A, Monazzah S, Bigham-Sadegh A: Bone injury and fracture healing biology. *Biomedical and environmental sciences : BES* 2015, 28:57-71.
- [80] Wan C, Gilbert SR, Wang Y, Cao X, Shen X, Ramaswamy G, Jacobsen KA, Alaql ZS, Eberhardt AW, Gerstenfeld LC, Einhorn TA, Deng L, Clemens TL: Activation of the hypoxia-inducible factor-1alpha pathway accelerates bone regeneration. *Proceedings of the National Academy of Sciences of the United States of America* 2008, 105:686-91.

- [81] Li R, Stewart DJ, von Schroeder HP, Mackinnon ES, Schemitsch EH: Effect of cell-based VEGF gene therapy on healing of a segmental bone defect. *Journal of Orthopaedic Research* 2009, 27:8-14.
- [82] Histing T, Marciniak K, Scheuer C, Garcia P, Holstein JH, Klein M, Matthys R, Pohlemann T, Menger MD: Sildenafil accelerates fracture healing in mice. *Journal of Orthopaedic Research* 2011, 29:867-73.
- [83] Beamer B, Hettrich C, Lane J: Vascular Endothelial Growth Factor: An Essential Component of Angiogenesis and Fracture Healing. *HSS journal* 2009.
- [84] McDonald MM, Dulai S, Godfrey C, Amanat N, Szynda T, Little DG: Bolus or weekly zoledronic acid administration does not delay endochondral fracture repair but weekly dosing enhances delays in hard callus remodeling. *Bone* 2008, 43:653-62.
- [85] Huff T, Muller CS, Otto AM, Netzker R, Hannappel E: beta-Thymosins, small acidic peptides with multiple functions. *The international journal of biochemistry & cell biology* 2001, 33:205-20.
- [86] Low TL, Hu SK, Goldstein AL: Complete amino acid sequence of bovine thymosin beta 4: a thymic hormone that induces terminal deoxynucleotidyl transferase activity in thymocyte populations. *Proceedings of the National Academy of Sciences of the United States of America* 1981, 78:1162-6.
- [87] Inzitari R, Cabras T, Pisano E, Fanali C, Manconi B, Scarano E, Fiorita A, Paludetti G, Manni A, Nemolato S, Faa G, Castagnola M, Messana I: HPLC-ESI-MS analysis of oral human fluids reveals that gingival crevicular fluid is the main source of oral thymosins beta(4) and beta(10). *Journal of separation science* 2009, 32:57-63.
- [88] Bodendorf S, Born G, Hannappel E: Determination of thymosin beta4 and protein in human wound fluid after abdominal surgery. *Annals of the New York Academy of Sciences* 2007, 1112:418-24.

- [89] Badamchian M, Damavandy AA, Damavandy H, Wadhwa SD, Katz B, Goldstein AL: Identification and quantification of thymosin beta4 in human saliva and tears. *Annals of the New York Academy of Sciences* 2007, 1112:458-65.
- [90] Mannherz HG, Hannappel E: The beta-thymosins: intracellular and extracellular activities of a versatile actin binding protein family. *Cell motility and the cytoskeleton* 2009, 66:839-51.
- [91] Goldstein AL, Hannappel E, Kleinman HK: Thymosin beta4: actin-sequestering protein moonlights to repair injured tissues. *Trends Mol Med* 2005, 11:421-9.
- [92] Sosne G, Qiu P, Goldstein AL, Wheeler M: Biological activities of thymosin beta4 defined by active sites in short peptide sequences. *Faseb J* 2010, 24:2144-51.
- [93] Sosne G, Chan CC, Thai K, Kennedy M, Szliter EA, Hazlett LD, Kleinman HK: Thymosin beta 4 promotes corneal wound healing and modulates inflammatory mediators in vivo. *Exp Eye Res* 2001, 72:605-8.
- [94] Cavasin MA: Therapeutic potential of thymosin-beta4 and its derivative N-acetyl-seryl-aspartyl-lysyl-proline (Ac-SDKP) in cardiac healing after infarction. *American journal of cardiovascular drugs : drugs, devices, and other interventions* 2006, 6:305-11.
- [95] Chopp M, Zhang ZG: Thymosin beta4 as a restorative/regenerative therapy for neurological injury and neurodegenerative diseases. *Expert opinion on biological therapy* 2015, 15 Suppl 1:S9-12.
- [96] Bock-Marquette I, Saxena A, White MD, Dimaio JM, Srivastava D: Thymosin beta4 activates integrin-linked kinase and promotes cardiac cell migration, survival and cardiac repair. *Nature* 2004, 432:466-72.
- [97] Sosne G, Qiu P, Christopherson PL, Wheeler MK: Thymosin beta 4 suppression of corneal NFkappaB: a potential anti-inflammatory pathway. *Exp Eye Res* 2007, 84:663-9.

- [98] Philp D, St-Surin S, Cha HJ, Moon HS, Kleinman HK, Elkin M: Thymosin beta 4 induces hair growth via stem cell migration and differentiation. *Annals of the New York Academy of Sciences* 2007, 1112:95-103.
- [99] Ehrlich HP, Hazard SW, 3rd: Thymosin beta4 enhances repair by organizing connective tissue and preventing the appearance of myofibroblasts. *Annals of the New York Academy of Sciences* 2010, 1194:118-24.
- [100] Philp D, Huff T, Gho YS, Hannappel E, Kleinman HK: The actin binding site on thymosin beta4 promotes angiogenesis. *Faseb J* 2003, 17:2103-5.
- [101] Ho JH, Chuang CH, Ho CY, Shih YR, Lee OK, Su Y: Internalization is essential for the antiapoptotic effects of exogenous thymosin beta-4 on human corneal epithelial cells. *Investigative ophthalmology & visual science* 2007, 48:27-33.
- [102] Sosne G, Qiu P, Kurpakus-Wheater M: Thymosin beta 4: A novel corneal wound healing and anti-inflammatory agent. *Clinical ophthalmology (Auckland, NZ)* 2007, 1:201-7.
- [103] Sosne G, Christopherson PL, Barrett RP, Fridman R: Thymosin-beta4 modulates corneal matrix metalloproteinase levels and polymorphonuclear cell infiltration after alkali injury. *Investigative ophthalmology & visual science* 2005, 46:2388-95.
- [104] Peng H, Xu J, Yang XP, Dai X, Peterson EL, Carretero OA, Rhaleb NE: Thymosin-beta4 prevents cardiac rupture and improves cardiac function in mice with myocardial infarction. *American journal of physiology Heart and circulatory physiology* 2014, 307:H741-51.
- [105] Sopko N, Qin Y, Finan A, Dadabayev A, Chigurupati S, Qin J, Penn MS, Gupta S: Significance of thymosin beta4 and implication of PINCH-1-ILK-alpha-parvin (PIP) complex in human dilated cardiomyopathy. *PloS one* 2011, 6:e20184.

- [106] Morris DC, Zhang ZG, Zhang J, Xiong Y, Zhang L, Chopp M: Treatment of neurological injury with thymosin beta4. *Annals of the New York Academy of Sciences* 2012, 1269:110-6.
- [107] Sosne G, Siddiqi A, Kurpakus-Wheater M: Thymosin-beta4 inhibits corneal epithelial cell apoptosis after ethanol exposure in vitro. *Investigative ophthalmology & visual science* 2004, 45:1095-100.
- [108] Santra M, Chopp M, Santra S, Nallani A, Vyas S, Zhang ZG, Morris DC: Thymosin beta 4 up-regulates miR-200a expression and induces differentiation and survival of rat brain progenitor cells. *Journal of neurochemistry* 2015.
- [109] Xiong Y, Zhang Y, Mahmood A, Meng Y, Zhang ZG, Morris DC, Chopp M: Neuroprotective and neurorestorative effects of thymosin beta4 treatment initiated 6 hours after traumatic brain injury in rats. *Journal of neurosurgery* 2012, 116:1081-92.
- [110] Morris DC, Chopp M, Zhang L, Lu M, Zhang ZG: Thymosin beta4 improves functional neurological outcome in a rat model of embolic stroke. *Neuroscience* 2010, 169:674-82.
- [111] Malinda KM, Goldstein AL, Kleinman HK: Thymosin beta 4 stimulates directional migration of human umbilical vein endothelial cells. *Faseb J* 1997, 11:474-81.
- [112] Sosne G, Xu L, Prach L, Mrock LK, Kleinman HK, Letterio JJ, Hazlett LD, Kurpakus-Wheater M: Thymosin beta 4 stimulates laminin-5 production independent of TGF-beta. *Experimental cell research* 2004, 293:175-83.
- [113] Freeman KW, Bowman BR, Zetter BR: Regenerative protein thymosin beta-4 is a novel regulator of purinergic signaling. *Faseb J* 2011, 25:907-15.
- [114] Sosne G, Chan CC, Thai K, Kennedy M, Szliter EA, Hazlett LD, Kleinman HK: Thymosin beta 4 promotes corneal wound healing and modulates inflammatory mediators in vivo. *Exp Eye Res* 2001, 72:605-8.

- [115] Sosne G, Szliter EA, Barrett R, Kernacki KA, Kleinman H, Hazlett LD: Thymosin beta 4 promotes corneal wound healing and decreases inflammation in vivo following alkali injury. *Exp Eye Res* 2002, 74:293-9.
- [116] Grant DS, Kinsella JL, Kibbey MC, LaFlamme S, Burbelo PD, Goldstein AL, Kleinman HK: Matrigel induces thymosin beta 4 gene in differentiating endothelial cells. *Journal of cell science* 1995, 108 ( Pt 12):3685-94.
- [117] Grant DS, Rose W, Yaen C, Goldstein A, Martinez J, Kleinman H: Thymosin beta4 enhances endothelial cell differentiation and angiogenesis. *Angiogenesis* 1999, 3:125-35.
- [118] Smart N, Rossdeutsch A, Riley PR: Thymosin beta4 and angiogenesis: modes of action and therapeutic potential. *Angiogenesis* 2007, 10:229-41.
- [119] Lv S, Cheng G, Zhou Y, Xu G: Thymosin beta4 induces angiogenesis through Notch signaling in endothelial cells. *Molecular and cellular biochemistry* 2013, 381:283-90.
- [120] Philp D, Scheremeta B, Sibliss K, Zhou M, Fine EL, Nguyen M, Wahl L, Hoffman MP, Kleinman HK: Thymosin beta4 promotes matrix metalloproteinase expression during wound repair. *Journal of cellular physiology* 2006, 208:195-200.
- [121] Peng H, Carretero OA, Rajj L, Yang F, Kapke A, Rhaleb NE: Antifibrotic effects of N-acetyl-seryl-aspartyl-Lysyl-proline on the heart and kidney in aldosterone-salt hypertensive rats. *Hypertension* 2001, 37:794-800.
- [122] Xiong Y, Mahmood A, Meng Y, Zhang Y, Zhang ZG, Morris DC, Chopp M: Neuroprotective and neurorestorative effects of thymosin beta4 treatment following experimental traumatic brain injury. *Annals of the New York Academy of Sciences* 2012, 1270:51-8.
- [123] Morris DC, Cui Y, Cheung WL, Lu M, Zhang L, Zhang ZG, Chopp M: A dose-response study of thymosin beta4 for the treatment of acute stroke. *Journal of the neurological sciences* 2014, 345:61-7.

- [124] Santra M, Zhang ZG, Yang J, Santra S, Santra S, Chopp M, Morris DC: Thymosin beta4 up-regulation of microRNA-146a promotes oligodendrocyte differentiation and suppression of the Toll-like proinflammatory pathway. *The Journal of biological chemistry* 2014, 289:19508-18.
- [125] Matsuo K, Akasaki Y, Adachi K, Zhang M, Ishikawa A, Jimi E, Nishihara T, Hosokawa R: Promoting effects of thymosin beta4 on granulation tissue and new bone formation after tooth extraction in rats. *Oral surgery, oral medicine, oral pathology and oral radiology* 2012, 114:17-26.
- [126] Adachi K, Matsuo K, Akasaki Y, Kanao M, Maeda T, Ishikawa A, Hosokawa R: Effects of thymosin beta4 on the bone formation of calvarial defects in rats. *Journal of prosthodontic research* 2013, 57:162-8.
- [127] Lee SI, Kim DS, Lee HJ, Cha HJ, Kim EC: The role of thymosin beta 4 on odontogenic differentiation in human dental pulp cells. *PloS one* 2013, 8:e61960.
- [128] Lee SI, Lee DW, Yun HM, Cha HJ, Bae CH, Cho ES, Kim EC: Expression of thymosin beta-4 in human periodontal ligament cells and mouse periodontal tissue and its role in osteoblastic/cementoblastic differentiation. *Differentiation; research in biological diversity* 2015.
- [129] Ho JH, Ma WH, Su Y, Tseng KC, Kuo TK, Lee OK: Thymosin beta-4 directs cell fate determination of human mesenchymal stem cells through biophysical effects. *Journal of orthopaedic research : official publication of the Orthopaedic Research Society* 2010, 28:131-8.
- [130] Cha HJ, Philp D, Lee SH, Moon HS, Kleinman HK, Nakamura T: Over-expression of thymosin beta 4 promotes abnormal tooth development and stimulation of hair growth. *The International journal of developmental biology* 2010, 54:135-40.

- [131] Lee SI, Yi JK, Bae WJ, Lee S, Cha HJ, Kim EC: Thymosin Beta-4 Suppresses Osteoclastic Differentiation and Inflammatory Responses in Human Periodontal Ligament Cells. *PloS one* 2016, 11:e0146708.
- [132] McDonald SJ, Sun M, Agoston DV, Shultz SR: The effect of concomitant peripheral injury on traumatic brain injury pathobiology and outcome. *Journal of neuroinflammation* 2016, 13:90.
- [133] Masel BE, DeWitt DS: Traumatic brain injury: a disease process, not an event. *Journal of neurotrauma* 2010, 27:1529-40.
- [134] Xiong Y, Mahmood A, Chopp M: Animal models of traumatic brain injury. *Nature reviews Neuroscience* 2013, 14:128-42.
- [135] Chauhan NB: Chronic neurodegenerative consequences of traumatic brain injury. *Restorative neurology and neuroscience* 2014, 32:337-65.
- [136] Bramlett HM, Dietrich WD: Long-Term Consequences of Traumatic Brain Injury: Current Status of Potential Mechanisms of Injury and Neurological Outcomes. *Journal of neurotrauma* 2015, 32:1834-48.
- [137] Lu J, Goh SJ, Tng PY, Deng YY, Ling EA, Moochhala S: Systemic inflammatory response following acute traumatic brain injury. *Frontiers in bioscience (Landmark edition)* 2009, 14:3795-813.
- [138] Gupta R, Sen N: Traumatic brain injury: a risk factor for neurodegenerative diseases. *Reviews in the neurosciences* 2016, 27:93-100.
- [139] Kumar A, Loane DJ: Neuroinflammation after traumatic brain injury: opportunities for therapeutic intervention. *Brain, behavior, and immunity* 2012, 26:1191-201.
- [140] Maas AI, Stocchetti N, Bullock R: Moderate and severe traumatic brain injury in adults. *The Lancet Neurology* 2008, 7:728-41.

- [141] Luo P, Fei F, Zhang L, Qu Y, Fei Z: The role of glutamate receptors in traumatic brain injury: implications for postsynaptic density in pathophysiology. *Brain research bulletin* 2011, 85:313-20.
- [142] Faden AI, Demediuk P, Panter SS, Vink R: The role of excitatory amino acids and NMDA receptors in traumatic brain injury. *Science (New York, NY)* 1989, 244:798-800.
- [143] Loane DJ, Byrnes KR: Role of microglia in neurotrauma. *Neurotherapeutics : the journal of the American Society for Experimental NeuroTherapeutics* 2010, 7:366-77.
- [144] Block ML, Zecca L, Hong JS: Microglia-mediated neurotoxicity: uncovering the molecular mechanisms. *Nature reviews Neuroscience* 2007, 8:57-69.
- [145] Bendlin BB, Ries ML, Lazar M, Alexander AL, Dempsey RJ, Rowley HA, Sherman JE, Johnson SC: Longitudinal changes in patients with traumatic brain injury assessed with diffusion-tensor and volumetric imaging. *NeuroImage* 2008, 42:503-14.
- [146] Bramlett HM, Dietrich WD: Quantitative structural changes in white and gray matter 1 year following traumatic brain injury in rats. *Acta neuropathologica* 2002, 103:607-14.
- [147] Maxwell WL, MacKinnon MA, Smith DH, McIntosh TK, Graham DI: Thalamic nuclei after human blunt head injury. *Journal of neuropathology and experimental neurology* 2006, 65:478-88.
- [148] Gentleman SM, Leclercq PD, Moyes L, Graham DI, Smith C, Griffin WS, Nicoll JA: Long-term intracerebral inflammatory response after traumatic brain injury. *Forensic science international* 2004, 146:97-104.
- [149] Alves JL: Blood-brain barrier and traumatic brain injury. *Journal of neuroscience research* 2014, 92:141-7.
- [150] Wilson EH, Weninger W, Hunter CA: Trafficking of immune cells in the central nervous system. *The Journal of clinical investigation* 2010, 120:1368-79.

- [151] Stamatovic SM, Keep RF, Andjelkovic AV: Brain endothelial cell-cell junctions: how to "open" the blood brain barrier. *Current neuropharmacology* 2008, 6:179-92.
- [152] Shlosberg D, Benifla M, Kaufer D, Friedman A: Blood-brain barrier breakdown as a therapeutic target in traumatic brain injury. *Nature reviews Neurology* 2010, 6:393-403.
- [153] Wolburg H, Wolburg-Buchholz K, Engelhardt B: Involvement of tight junctions during transendothelial migration of mononuclear cells in experimental autoimmune encephalomyelitis. *Ernst Schering Research Foundation workshop* 2004:17-38.
- [154] Keel M, Trentz O: Pathophysiology of polytrauma. *Injury* 2005, 36:691-709.
- [155] Masel BE, Urban R: Chronic Endocrinopathies in Traumatic Brain Injury Disease. *Journal of neurotrauma* 2015, 32:1902-10.
- [156] Reed ML, Merriam GR, Kargi AY: Adult growth hormone deficiency - benefits, side effects, and risks of growth hormone replacement. *Frontiers in endocrinology* 2013, 4:64.
- [157] Kristensen E, Hallgrimsson B, Morck DW, Boyd SK: Microarchitecture, but not bone mechanical properties, is rescued with growth hormone treatment in a mouse model of growth hormone deficiency. *International journal of endocrinology* 2012, 2012:294965.
- [158] Ozdemir D, Baykara B, Aksu I, Kiray M, Sisman AR, Cetin F, Dayi A, Gurpinar T, Uysal N, Arda MN: Relationship between circulating IGF-1 levels and traumatic brain injury-induced hippocampal damage and cognitive dysfunction in immature rats. *Neuroscience letters* 2012, 507:84-9.
- [159] Patel MB, McKenna JW, Alvarez JM, Sugiura A, Jenkins JM, Guillamondegui OD, Pandharipande PP: Decreasing adrenergic or sympathetic hyperactivity after severe traumatic brain injury using propranolol and clonidine (DASH After TBI Study): study protocol for a randomized controlled trial. *Trials* 2012, 13:177.
- [160] Hinson HE, Sheth KN: Manifestations of the hyperadrenergic state after acute brain injury. *Current opinion in critical care* 2012, 18:139-45.

- [161] Di Battista AP, Rhind SG, Hutchison MG, Hassan S, Shiu MY, Inaba K, Topolovec-Vranic J, Neto AC, Rizoli SB, Baker AJ: Inflammatory cytokine and chemokine profiles are associated with patient outcome and the hyperadrenergic state following acute brain injury. *Journal of neuroinflammation* 2016, 13:40.
- [162] Nagao M, Feinstein TN, Ezura Y, Hayata T, Notomi T, Saita Y, Hanyu R, Hemmi H, Izu Y, Takeda S, Wang K, Rittling S, Nakamoto T, Kaneko K, Kurosawa H, Karsenty G, Denhardt DT, Vilardaga JP, Noda M: Sympathetic control of bone mass regulated by osteopontin. *Proceedings of the National Academy of Sciences of the United States of America* 2011, 108:17767-72.
- [163] van der Poll T, Lowry SF: Lipopolysaccharide-induced interleukin 8 production by human whole blood is enhanced by epinephrine and inhibited by hydrocortisone. *Infection and immunity* 1997, 65:2378-81.
- [164] Liao Y, Liu P, Guo F, Zhang ZY, Zhang Z: Oxidative burst of circulating neutrophils following traumatic brain injury in human. *PloS one* 2013, 8:e68963.
- [165] Garrett IR, Boyce BF, Oreffo RO, Bonewald L, Poser J, Mundy GR: Oxygen-derived free radicals stimulate osteoclastic bone resorption in rodent bone in vitro and in vivo. *The Journal of clinical investigation* 1990, 85:632-9.
- [166] Kondo H, Takeuchi S, Togari A: beta-Adrenergic signaling stimulates osteoclastogenesis via reactive oxygen species. *American journal of physiology Endocrinology and metabolism* 2013, 304:E507-15.
- [167] Galindo LT, Filippo TR, Semedo P, Ariza CB, Moreira CM, Camara NO, Porcionatto MA: Mesenchymal stem cell therapy modulates the inflammatory response in experimental traumatic brain injury. *Neurology research international* 2011, 2011:564089.
- [168] Genet F, Kulina I, Vaquette C, Torossian F, Millard S, Pettit AR, Sims NA, Anginot A, Guerton B, Winkler IG, Barbier V, Lataillade JJ, Le Bousse-Kerdiles MC, Hutmacher DW,

Levesque JP: Neurological heterotopic ossification following spinal cord injury is triggered by macrophage-mediated inflammation in muscle. *The Journal of pathology* 2015, 236:229-40.

[169] Genet F, Jourdan C, Schnitzler A, Lautridou C, Guillemot D, Judet T, Poiraudou S, Denormandie P: Troublesome heterotopic ossification after central nervous system damage: a survey of 570 surgeries. *PloS one* 2011, 6:e16632.

[170] Boes M, Kain M, Kakar S, Nicholls F, Cullinane D, Gerstenfeld L, Einhorn TA, Tornetta P, 3rd: Osteogenic effects of traumatic brain injury on experimental fracture-healing. *The Journal of bone and joint surgery American volume* 2006, 88:738-43.

[171] Gautschi OP, Toffoli AM, Joesbury KA, Skirving AP, Filgueira L, Zellweger R: Osteoinductive effect of cerebrospinal fluid from brain-injured patients. *Journal of neurotrauma* 2007, 24:154-62.

[172] Bidner SM, Rubins IM, Desjardins JV, Zukor DJ, Goltzman D: Evidence for a humoral mechanism for enhanced osteogenesis after head injury. *The Journal of bone and joint surgery American volume* 1990, 72:1144-9.

[173] Beaupre GS, Lew HL: Bone-density changes after stroke. *American journal of physical medicine & rehabilitation / Association of Academic Physiatrists* 2006, 85:464-72.

[174] Smith EM, Comiskey CM, Carroll AM: A study of bone mineral density in adults with disability. *Archives of physical medicine and rehabilitation* 2009, 90:1127-35.

[175] Smith E, Comiskey C, Carroll A: Prevalence of and risk factors for osteoporosis in adults with acquired brain injury. *Irish journal of medical science* 2016, 185:473-81.

[176] Oppl B, Michitsch G, Misof B, Kudlacek S, Donis J, Klaushofer K, Zwerina J, Zwettler E: Low bone mineral density and fragility fractures in permanent vegetative state patients. *J Bone Miner Res* 2014, 29:1096-100.

- [177] Zhao XG, Zhao GF, Ma YF, Jiang GY: Research progress in mechanism of traumatic brain injury affecting speed of fracture healing. Chinese journal of traumatology = Zhonghua chuang shang za zhi / Chinese Medical Association 2007, 10:376-80.
- [178] Morley J, Marsh S, Drakoulakis E, Pape HC, Giannoudis PV: Does traumatic brain injury result in accelerated fracture healing? Injury 2005, 36:363-8.
- [179] Locher RJ, Lunnemann T, Garbe A, Schaser K, Schmidt-Bleek K, Duda G, Tsitsilonis S: Traumatic brain injury and bone healing: radiographic and biomechanical analyses of bone formation and stability in a combined murine trauma model. Journal of musculoskeletal & neuronal interactions 2015, 15:309-15.
- [180] Tsitsilonis S, Seemann R, Misch M, Wichlas F, Haas NP, Schmidt-Bleek K, Kleber C, Schaser KD: The effect of traumatic brain injury on bone healing: an experimental study in a novel in vivo animal model. Injury 2015, 46:661-5.
- [181] Wang L, Yuan JS, Zhang HX, Ding H, Tang XG, Wei YZ: Effect of leptin on bone metabolism in rat model of traumatic brain injury and femoral fracture. Chinese journal of traumatology = Zhonghua chuang shang za zhi / Chinese Medical Association 2011, 14:7-13.
- [182] Wei Y, Wang L, Clark JC, Dass CR, Choong PF: Elevated leptin expression in a rat model of fracture and traumatic brain injury. The Journal of pharmacy and pharmacology 2008, 60:1667-72.
- [183] Liu X, Zhou C, Li Y, Ji Y, Xu G, Wang X, Yan J: SDF-1 promotes endochondral bone repair during fracture healing at the traumatic brain injury condition. PloS one 2013, 8:e54077.
- [184] Huang W, Li Z, Li Z, Yang R: Does traumatic brain injury result in accelerated mandibular fracture healing? Journal of oral and maxillofacial surgery : official journal of the American Association of Oral and Maxillofacial Surgeons 2012, 70:2135-42.

- [185] Perkins R, Skirving AP: Callus formation and the rate of healing of femoral fractures in patients with head injuries. *The Journal of bone and joint surgery British* volume 1987, 69:521-4.
- [186] Wildburger R, Zarkovic N, Tonkovic G, Skoric T, Frech S, Hartleb M, Loncaric I, Zarkovic K: Post-traumatic hormonal disturbances: prolactin as a link between head injury and enhanced osteogenesis. *Journal of endocrinological investigation* 1998, 21:78-86.
- [187] Zhuang YF, Li J: Serum EGF and NGF levels of patients with brain injury and limb fracture. *Asian Pacific journal of tropical medicine* 2013, 6:383-6.
- [188] Mueller M, Schilling T, Minne HW, Ziegler R: A systemic acceleratory phenomenon (SAP) accompanies the regional acceleratory phenomenon (RAP) during healing of a bone defect in the rat. *J Bone Miner Res* 1991, 6:401-10.
- [189] Maas AI, Roozenbeek B, Manley GT: Clinical trials in traumatic brain injury: past experience and current developments. *Neurotherapeutics : the journal of the American Society for Experimental NeuroTherapeutics* 2010, 7:115-26.
- [190] Morris M, Maeda S, Vossel K, Mucke L: The many faces of tau. *Neuron* 2011, 70:410-26.
- [191] Wang JZ, Grundke-Iqbal I, Iqbal K: Restoration of biological activity of Alzheimer abnormally phosphorylated tau by dephosphorylation with protein phosphatase-2A, -2B and -1. *Brain research Molecular brain research* 1996, 38:200-8.
- [192] Wang JZ, Grundke-Iqbal I, Iqbal K: Kinases and phosphatases and tau sites involved in Alzheimer neurofibrillary degeneration. *The European journal of neuroscience* 2007, 25:59-68.
- [193] Liu F, Grundke-Iqbal I, Iqbal K, Gong CX: Contributions of protein phosphatases PP1, PP2A, PP2B and PP5 to the regulation of tau phosphorylation. *The European journal of neuroscience* 2005, 22:1942-50.

- [194] Bolognin S, Blanchard J, Wang X, Basurto-Islas G, Tung YC, Kohlbrenner E, Grundke-Iqbal I, Iqbal K: An experimental rat model of sporadic Alzheimer's disease and rescue of cognitive impairment with a neurotrophic peptide. *Acta neuropathologica* 2012, 123:133-51.
- [195] Corcoran NM, Martin D, Hutter-Paier B, Windisch M, Nguyen T, Nheu L, Sundstrom LE, Costello AJ, Hovens CM: Sodium selenate specifically activates PP2A phosphatase, dephosphorylates tau and reverses memory deficits in an Alzheimer's disease model. *Journal of clinical neuroscience : official journal of the Neurosurgical Society of Australasia* 2010, 17:1025-33.
- [196] Jones NC, Nguyen T, Corcoran NM, Velakoulis D, Chen T, Grundy R, O'Brien TJ, Hovens CM: Targeting hyperphosphorylated tau with sodium selenate suppresses seizures in rodent models. *Neurobiology of disease* 2012, 45:897-901.
- [197] van Eersel J, Ke YD, Liu X, Delerue F, Kril JJ, Gotz J, Ittner LM: Sodium selenate mitigates tau pathology, neurodegeneration, and functional deficits in Alzheimer's disease models. *Proceedings of the National Academy of Sciences of the United States of America* 2010, 107:13888-93.
- [198] Campo RD, Bielen RJ: Acute toxic effects of sodium selenate on the epiphyseal plate of the rat. *Calcified tissue research* 1971, 7:318-30.
- [199] Gronbaek H, Frystyk J, Orskov H, Flyvbjerg A: Effect of sodium selenite on growth, insulin-like growth factor-binding proteins and insulin-like growth factor-I in rats. *The Journal of endocrinology* 1995, 145:105-12.
- [200] Thorlacius-Ussing O, Flyvbjerg A, Esmann J: Evidence that selenium induces growth retardation through reduced growth hormone and somatomedin C production. *Endocrinology* 1987, 120:659-63.

- [201] Smart N, Bollini S, Dube KN, Vieira JM, Zhou B, Davidson S, Yellon D, Riegler J, Price AN, Lythgoe MF, Pu WT, Riley PR: De novo cardiomyocytes from within the activated adult heart after injury. *Nature* 2011, 474:640-4.
- [202] Huang LC, Jean D, Proske RJ, Reins RY, McDermott AM: Ocular surface expression and in vitro activity of antimicrobial peptides. *Current eye research* 2007, 32:595-609.
- [203] Smart N, Risebro CA, Melville AA, Moses K, Schwartz RJ, Chien KR, Riley PR: Thymosin beta4 induces adult epicardial progenitor mobilization and neovascularization. *Nature* 2007, 445:177-82.
- [204] Kellum E, Starr H, Arounleut P, Immel D, Fulzele S, Wenger K, Hamrick MW: Myostatin (GDF-8) deficiency increases fracture callus size, Sox-5 expression, and callus bone volume. *Bone* 2009, 44:17-23.
- [205] Zhang J, Zhang ZG, Morris D, Li Y, Roberts C, Elias SB, Chopp M: Neurological functional recovery after thymosin beta4 treatment in mice with experimental auto encephalomyelitis. *Neuroscience* 2009, 164:1887-93.
- [206] Raftopoulos DD, Qassem W: Three-dimensional curved beam stress analysis of the human femur. *Journal of biomedical engineering* 1987, 9:356-66.
- [207] Mulder L, Koolstra JH, den Toonder JM, van Eijden TM: Relationship between tissue stiffness and degree of mineralization of developing trabecular bone. *Journal of biomedical materials research Part A* 2008, 84:508-15.
- [208] Follet H, Boivin G, Rumelhart C, Meunier PJ: The degree of mineralization is a determinant of bone strength: a study on human calcanei. *Bone* 2004, 34:783-9.
- [209] Allan EH, Ho PW, Umezawa A, Hata J, Makishima F, Gillespie MT, Martin TJ: Differentiation potential of a mouse bone marrow stromal cell line. *J Cell Biochem* 2003, 90:158-69.

- [210] Stanford CM, Jacobson PA, Eanes ED, Lembke LA, Midura RJ: Rapidly forming apatitic mineral in an osteoblastic cell line (UMR 106-01 BSP). *The Journal of biological chemistry* 1995, 270:9420-8.
- [211] Gregory CA, Gunn WG, Peister A, Prockop DJ: An Alizarin red-based assay of mineralization by adherent cells in culture: comparison with cetylpyridinium chloride extraction. *Analytical biochemistry* 2004, 329:77-84.
- [212] Green RE: Editorial: Brain Injury as a Neurodegenerative Disorder. *Frontiers in human neuroscience* 2015, 9:615.
- [213] Mundy GR: Inflammatory mediators and the destruction of bone. *Journal of periodontal research* 1991, 26:213-7.
- [214] Lin HL, Lin HC, Tseng YF, Liao HH, Worly JA, Pan CY, Hsu CY: Hip fracture after first-ever stroke: a population-based study. *Acta neurologica Scandinavica* 2015, 131:158-63.
- [215] Jorgensen L, Jacobsen BK, Wilsgaard T, Magnus JH: Walking after stroke: does it matter? Changes in bone mineral density within the first 12 months after stroke. A longitudinal study. *Osteoporosis international : a journal established as result of cooperation between the European Foundation for Osteoporosis and the National Osteoporosis Foundation of the USA* 2000, 11:381-7.
- [216] Campbell SJ, Hughes PM, Iredale JP, Wilcockson DC, Waters S, Docagne F, Perry VH, Anthony DC: CINC-1 is an acute-phase protein induced by focal brain injury causing leukocyte mobilization and liver injury. *Faseb J* 2003, 17:1168-70.
- [217] Campbell SJ, Perry VH, Pitossi FJ, Butchart AG, Chertoff M, Waters S, Dempster R, Anthony DC: Central nervous system injury triggers hepatic CC and CXC chemokine expression that is associated with leukocyte mobilization and recruitment to both the central nervous system and the liver. *The American journal of pathology* 2005, 166:1487-97.

- [218] Gris D, Hamilton EF, Weaver LC: The systemic inflammatory response after spinal cord injury damages lungs and kidneys. *Experimental neurology* 2008, 211:259-70.
- [219] Perry VH, Newman TA, Cunningham C: The impact of systemic infection on the progression of neurodegenerative disease. *Nature reviews Neuroscience* 2003, 4:103-12.
- [220] Wilcockson DC, Campbell SJ, Anthony DC, Perry VH: The systemic and local acute phase response following acute brain injury. *Journal of cerebral blood flow and metabolism : official journal of the International Society of Cerebral Blood Flow and Metabolism* 2002, 22:318-26.
- [221] Knoblach SM, Faden AI: Cortical interleukin-1 beta elevation after traumatic brain injury in the rat: no effect of two selective antagonists on motor recovery. *Neuroscience letters* 2000, 289:5-8.
- [222] Devoto C, Arcurio L, Fetta J, Ley M, Rodney T, Kanefsky R, Gill J: Inflammation Relates to Chronic Behavioral and Neurological Symptoms in Military with Traumatic Brain Injuries. *Cell transplantation* 2016.
- [223] Oshima T, Lee S, Sato A, Oda S, Hirasawa H, Yamashita T: TNF-alpha contributes to axonal sprouting and functional recovery following traumatic brain injury. *Brain research* 2009, 1290:102-10.
- [224] Lee SH, Kim TS, Choi Y, Lorenzo J: Osteoimmunology: cytokines and the skeletal system. *BMB reports* 2008, 41:495-510.
- [225] Niesman IR, Schilling JM, Shapiro LA, Kellerhals SE, Bonds JA, Kleschevnikov AM, Cui W, Voong A, Krajewski S, Ali SS, Roth DM, Patel HH, Patel PM, Head BP: Traumatic brain injury enhances neuroinflammation and lesion volume in caveolin deficient mice. *Journal of neuroinflammation* 2014, 11:39.
- [226] Ciucci T, Ibanez L, Boucoiran A, Birgy-Barelli E, Pene J, Abou-Ezzi G, Arab N, Rouleau M, Hebuterne X, Yssel H, Blin-Wakkach C, Wakkach A: Bone marrow Th17

TNF $\alpha$  cells induce osteoclast differentiation, and link bone destruction to IBD. *Gut* 2015, 64:1072-81.

[227] Beeton CA, Chatfield D, Brooks RA, Rushton N: Circulating levels of interleukin-6 and its soluble receptor in patients with head injury and fracture. *The Journal of bone and joint surgery British volume* 2004, 86:912-7.

[228] Wildburger R, Zarkovic N, Egger G, Petek W, Zarkovic K, Hofer HP: Basic fibroblast growth factor (BFGF) immunoreactivity as a possible link between head injury and impaired bone fracture healing. *Bone and mineral* 1994, 27:183-92.

[229] Grills BL, Schuijers JA, Ward AR: Topical application of nerve growth factor improves fracture healing in rats. *Journal of orthopaedic research : official publication of the Orthopaedic Research Society* 1997, 15:235-42.

[230] Laib A, Kumer JL, Majumdar S, Lane NE: The temporal changes of trabecular architecture in ovariectomized rats assessed by MicroCT. *Osteoporosis international : a journal established as result of cooperation between the European Foundation for Osteoporosis and the National Osteoporosis Foundation of the USA* 2001, 12:936-41.

[231] Ito M, Nishida A, Nakamura T, Uetani M, Hayashi K: Differences of three-dimensional trabecular microstructure in osteopenic rat models caused by ovariectomy and neurectomy. *Bone* 2002, 30:594-8.

[232] Bao F, Shultz SR, Hepburn JD, Omana V, Weaver LC, Cain DP, Brown A: A CD11d monoclonal antibody treatment reduces tissue injury and improves neurological outcome after fluid percussion brain injury in rats. *Journal of neurotrauma* 2012, 29:2375-92.

[233] Shultz SR, Cardamone L, Liu YR, Hogan RE, Maccotta L, Wright DK, Zheng P, Koe A, Gregoire MC, Williams JP, Hicks RJ, Jones NC, Myers DE, O'Brien TJ, Boulleret V: Can structural or functional changes following traumatic brain injury in the rat predict epileptic outcome? *Epilepsia* 2013, 54:1240-50.

- [234] Gurkoff GG, Giza CC, Hovda DA: Lateral fluid percussion injury in the developing rat causes an acute, mild behavioral dysfunction in the absence of significant cell death. *Brain research* 2006, 1077:24-36.
- [235] Shultz SR, Bao F, Omana V, Chiu C, Brown A, Cain DP: Repeated mild lateral fluid percussion brain injury in the rat causes cumulative long-term behavioral impairments, neuroinflammation, and cortical loss in an animal model of repeated concussion. *Journal of neurotrauma* 2012, 29:281-94.
- [236] Shultz SR, Tan XL, Wright DK, Liu SJ, Semple BD, Johnston L, Jones NC, Cook AD, Hamilton JA, O'Brien TJ: Granulocyte-macrophage colony-stimulating factor is neuroprotective in experimental traumatic brain injury. *Journal of neurotrauma* 2014, 31:976-83.
- [237] McDonald SJ, Dooley PC, McDonald AC, Djouma E, Schuijers JA, Ward AR, Grills BL: alpha(1) adrenergic receptor agonist, phenylephrine, actively contracts early rat rib fracture callus ex vivo. *Journal of orthopaedic research : official publication of the Orthopaedic Research Society* 2011, 29:740-5.
- [238] Romano T, Wark JD, Wlodek ME: Calcium supplementation does not rescue the programmed adult bone deficits associated with perinatal growth restriction. *Bone* 2010, 47:1054-63.
- [239] Romano T, Wark JD, Wlodek ME: Physiological skeletal gains and losses in rat mothers during pregnancy and lactation are not observed following uteroplacental insufficiency. *Reproduction, Fertility and Development* 2014, 26:385-94.
- [240] Brady RD, Grills BL, Schuijers JA, Ward AR, Tonkin BA, Walsh NC, McDonald SJ: Thymosin beta4 administration enhances fracture healing in mice. *Journal of orthopaedic research : official publication of the Orthopaedic Research Society* 2014, 32:1277-82.

- [241] Leppanen O, Sievanen H, Jokihaara J, Pajamaki I, Jarvinen TL: Three-point bending of rat femur in the mediolateral direction: introduction and validation of a novel biomechanical testing protocol. *J Bone Miner Res* 2006, 21:1231-7.
- [242] Lee JI, Kim JH, Kim HW, Choi ES, Lim SH, Ko YJ, Han YM: Changes in bone metabolism in a rat model of traumatic brain injury. *Brain injury* 2005, 19:1207-11.
- [243] Yu H, Watt H, Mohan S: The negative impact of traumatic brain injury (TBI) on bone in a mouse model. *Brain injury* 2014, 28:244-51.
- [244] Fonseca H, Moreira-Goncalves D, Coriolano HJ, Duarte JA: Bone quality: the determinants of bone strength and fragility. *Sports medicine (Auckland, NZ)* 2014, 44:37-53.
- [245] Szulc P, Seeman E: Thinking inside and outside the envelopes of bone: dedicated to PDD. *Osteoporosis international : a journal established as result of cooperation between the European Foundation for Osteoporosis and the National Osteoporosis Foundation of the USA* 2009, 20:1281-8.
- [246] Pop V, Sorensen DW, Kamper JE, Ajao DO, Murphy MP, Head E, Hartman RE, Badaut J: Early brain injury alters the blood-brain barrier phenotype in parallel with beta-amyloid and cognitive changes in adulthood. *Journal of cerebral blood flow and metabolism : official journal of the International Society of Cerebral Blood Flow and Metabolism* 2013, 33:205-14.
- [247] Kasturi BS, Stein DG: Traumatic brain injury causes long-term reduction in serum growth hormone and persistent astrocytosis in the cortico-hypothalamo-pituitary axis of adult male rats. *Journal of neurotrauma* 2009, 26:1315-24.
- [248] Holmes SJ, Economou G, Whitehouse RW, Adams JE, Shalet SM: Reduced bone mineral density in patients with adult onset growth hormone deficiency. *The Journal of clinical endocrinology and metabolism* 1994, 78:669-74.

- [249] Giustina A, Mazziotti G, Canalis E: Growth hormone, insulin-like growth factors, and the skeleton. *Endocrine reviews* 2008, 29:535-59.
- [250] Zheng P, Shultz SR, Hovens CM, Velakoulis D, Jones NC, O'Brien TJ: Hyperphosphorylated tau is implicated in acquired epilepsy and neuropsychiatric comorbidities. *Molecular neurobiology* 2014, 49:1532-9.
- [251] Corcoran NM, Hovens CM, Michael M, Rosenthal MA, Costello AJ: Open-label, phase I dose-escalation study of sodium selenate, a novel activator of PP2A, in patients with castration-resistant prostate cancer. *British journal of cancer* 2010, 103:462-8.
- [252] Johnstone VP, Shultz SR, Yan EB, O'Brien TJ, Rajan R: The acute phase of mild traumatic brain injury is characterized by a distance-dependent neuronal hypoactivity. *Journal of neurotrauma* 2014, 31:1881-95.
- [253] Shultz SR, Sun M, Wright DK, Brady RD, Liu S, Beynon S, Schmidt SF, Kaye AH, Hamilton JA, O'Brien TJ, Grills BL, McDonald SJ: Tibial fracture exacerbates traumatic brain injury outcomes and neuroinflammation in a novel mouse model of multitrauma. *Journal of cerebral blood flow and metabolism : official journal of the International Society of Cerebral Blood Flow and Metabolism* 2015, 35:1339-47.
- [254] Brady RD, Shultz S, Sun M, Romano T, van der Poel C, Wright DK, Wark JD, O'Brien TJ, Grills BL, McDonald SJ: Experimental traumatic brain injury induces bone loss in rats. *Journal of neurotrauma* 2015.
- [255] Glatt V, Canalis E, Stadmeier L, Bouxsein ML: Age-related changes in trabecular architecture differ in female and male C57BL/6J mice. *J Bone Miner Res* 2007, 22:1197-207.
- [256] Chung YW, Kim TS, Lee SY, Lee SH, Choi Y, Kim N, Min BM, Jeong DW, Kim IY: Selenite-induced apoptosis of osteoclasts mediated by the mitochondrial pathway. *Toxicology letters* 2006, 160:143-50.

- [257] Evans KD, Lau ST, Oberbauer AM, Martin RB: Alendronate affects long bone length and growth plate morphology in the oim mouse model for Osteogenesis Imperfecta. *Bone* 2003, 32:268-74.
- [258] Evans KD, Sheppard LE, Grossman DI, Rao SH, Martin RB, Oberbauer AM: Long Term Cyclic Pamidronate Reduces Bone Growth by Inhibiting Osteoclast Mediated Cartilage-to-Bone Turnover in the Mouse. *The open orthopaedics journal* 2008, 2:121-5.
- [259] Menetrez JS: Inpatient multitrauma rehabilitation in a U.S. military hospital. *Physical medicine and rehabilitation clinics of North America* 2002, 13:67-83.
- [260] Al-Thani H, El-Menyar A, Abdelrahman H, Zarour A, Consunji R, Peralta R, Asim M, El-Hennawy H, Parchani A, Latifi R: Workplace-related traumatic injuries: insights from a rapidly developing Middle Eastern country. *Journal of environmental and public health* 2014, 2014:430832.
- [261] Zhang L, Zhang L, Mao Z, Tang P: Semaphoring 3A: an association between traumatic brain injury and enhanced osteogenesis. *Medical hypotheses* 2013, 81:713-4.
- [262] Wildburger R, Zarkovic N, Leb G, Borovic S, Zarkovic K, Tatzber F: Post-traumatic changes in insulin-like growth factor type 1 and growth hormone in patients with bone fractures and traumatic brain injury. *Wiener klinische Wochenschrift* 2001, 113:119-26.
- [263] Masson F, Thicoipe M, Aye P, Mokni T, Senjean P, Schmitt V, Dessalles PH, Cazaugade M, Labadens P: Epidemiology of severe brain injuries: a prospective population-based study. *The Journal of trauma* 2001, 51:481-9.
- [264] Myburgh JA, Cooper DJ, Finfer SR, Venkatesh B, Jones D, Higgins A, Bishop N, Higlett T: Epidemiology and 12-month outcomes from traumatic brain injury in australia and new zealand. *The Journal of trauma* 2008, 64:854-62.
- [265] Schindeler A, Morse A, Harry L, Godfrey C, Mikulec K, McDonald M, Gasser JA, Little DG: Models of tibial fracture healing in normal and Nf1-deficient mice. *Journal of*

orthopaedic research : official publication of the Orthopaedic Research Society 2008, 26:1053-60.

[266] Flierl MA, Stahel PF, Beauchamp KM, Morgan SJ, Smith WR, Shohami E: Mouse closed head injury model induced by a weight-drop device. *Nature protocols* 2009, 4:1328-37.

[267] Spencer RF: The effect of head injury on fracture healing. A quantitative assessment. *The Journal of bone and joint surgery British volume* 1987, 69:525-8.

[268] Smith R: Head injury, fracture healing and callus. *The Journal of bone and joint surgery British volume* 1987, 69:518-20.

[269] Baldock PA, Lin S, Zhang L, Karl T, Shi Y, Driessler F, Zengin A, Horner B, Lee NJ, Wong IP, Lin EJ, Enriquez RF, Stehrer B, During MJ, Yulyaningsih E, Zolotukhin S, Ruohonen ST, Savontaus E, Sainsbury A, Herzog H: Neuropeptide y attenuates stress-induced bone loss through suppression of noradrenaline circuits. *J Bone Miner Res* 2014, 29:2238-49.

[270] Rosen CJ: Bone remodeling, energy metabolism, and the molecular clock. *Cell metabolism* 2008, 7:7-10.

[271] Swift JM, Hogan HA, Bloomfield SA: beta-1 adrenergic agonist mitigates unloading-induced bone loss by maintaining formation. *Medicine and science in sports and exercise* 2013, 45:1665-73.

[272] Baldock PA, Allison S, McDonald MM, Sainsbury A, Enriquez RF, Little DG, Eisman JA, Gardiner EM, Herzog H: Hypothalamic regulation of cortical bone mass: opposing activity of Y2 receptor and leptin pathways. *J Bone Miner Res* 2006, 21:1600-7.

[273] Baldock PA, Sainsbury A, Couzens M, Enriquez RF, Thomas GP, Gardiner EM, Herzog H: Hypothalamic Y2 receptors regulate bone formation. *The Journal of clinical investigation* 2002, 109:915-21.

- [274] Martini L, Fini M, Giavaresi G, Giardino R: Sheep model in orthopedic research: a literature review. *Comparative medicine* 2001, 51:292-9.
- [275] Simon AM, Manigrasso MB, O'Connor JP: Cyclo-Oxygenase 2 Function Is Essential for Bone Fracture Healing. *Journal of Bone and Mineral Research* 2002, 17:963-76.
- [276] Garcia P, Histing T, Holstein JH, Klein M, Laschke MW, Matthys R, Ignatius A, Wildemann B, Lienau J, Peters A, Willie B, Duda G, Claes L, Pohlemann T, Menger MD: Rodent animal models of delayed bone healing and non-union formation: a comprehensive review. *European cells & materials* 2013, 26:1-12; discussion -4.
- [277] Pollard TC, Newman JE, Barlow NJ, Price JD, Willett KM: Deep wound infection after proximal femoral fracture: consequences and costs. *The Journal of hospital infection* 2006, 63:133-9.
- [278] Boyle P, Leon ME, Autier P: Epidemiology of osteoporosis. *Journal of epidemiology and biostatistics* 2001, 6:185-92.
- [279] Namkung-Matthai H, Appleyard R, Jansen J, Hao Lin J, Maastricht S, Swain M, Mason RS, Murrell GA, Diwan AD, Diamond T: Osteoporosis influences the early period of fracture healing in a rat osteoporotic model. *Bone* 2001, 28:80-6.
- [280] Egermann M, Goldhahn J, Schneider E: Animal models for fracture treatment in osteoporosis. *Osteoporosis international : a journal established as result of cooperation between the European Foundation for Osteoporosis and the National Osteoporosis Foundation of the USA* 2005, 16 Suppl 2:S129-38.
- [281] Pearce AI, Richards RG, Milz S, Schneider E, Pearce SG: Animal models for implant biomaterial research in bone: a review. *European cells & materials* 2007, 13:1-10.
- [282] Tashjian AH, Jr., Gagel RF: Teriparatide [human PTH(1-34)]: 2.5 years of experience on the use and safety of the drug for the treatment of osteoporosis. *J Bone Miner Res* 2006, 21:354-65.

[283] Takeda S, Elefteriou F, Levasseur R, Liu X, Zhao L, Parker KL, Armstrong D, Ducy P, Karsenty G: Leptin regulates bone formation via the sympathetic nervous system. *Cell* 2002, 111:305-17.

[284] Forsberg JA, Pepek JM, Wagner S, Wilson K, Flint J, Andersen RC, Tadaki D, Gage FA, Stojadinovic A, Elster EA: Heterotopic ossification in high-energy wartime extremity injuries: prevalence and risk factors. *The Journal of bone and joint surgery American volume* 2009, 91:1084-91.

[285] Garland DE, Blum CE, Waters RL: Periarticular heterotopic ossification in head-injured adults. Incidence and location. *The Journal of bone and joint surgery American volume* 1980, 62:1143-6.

## 8 Appendices

### 8.1 Appendix A, Declaration of contribution

In the case of Chapter 2, the nature and extent of my contribution to the work was the following:

Contributor	Statement of Contribution
Rhys D. Brady	Drafted the manuscript, collected tissue, cut sections, scanned bones and completed histomorphometric and $\mu$ CT analysis, performed and analysed mechanical tests.
Brian L. Grills	Administered the fractures, conceptualised and designed the experiment.
Johannes A. Schuijers	Conceptualised and designed the experiment
Alex R. Ward	Assisted with analysis of mechanical tests
Brett A. Tonkin,	Assisted with $\mu$ CT scans
Nicole C. Walsh	Assisted with $\mu$ CT analysis and edited the manuscript
Stuart J. McDonald	Conceptualised and designed the experiment.

In the case of Chapter 4, the nature and extent of my contribution to the work was the following:

Contributor	Statement of Contribution
Rhys D. Brady	Collected tissue, cut sections, completed histomorphometric and pQCT analysis, completed biomechanical tests and analysis drafted the manuscript.
Sandy R. Shultz	Administered the TBI, conceptualised and designed the experiment, edited the manuscript
Mujun Sun	Conducted open field test
Tania Romano	Conducted pQCT
Chris van der Poel	Edited the manuscript
David K. Wright,	Conceptualised and designed the experiment, edited the manuscript
John D. Wark	Provided pQCT scanner
Terence J. O'Brien	Conceptualised and designed the experiment, edited the manuscript,
Brian L. Grills	Conceptualised and designed the experiment, edited the manuscript, assisted with histomorphometric analysis
Stuart J. McDonald	Conceptualised and designed the experiment, edited the manuscript, assisted with pQCT analysis, assisted with biomechanical tests and analysis.

In the case of Chapter 5, the nature and extent of my contribution to the work was the following:

Contributor	Statement of Contribution
Rhys D. Brady	Collected tissue, cut sections, completed histomorphometric and pQCT analysis, completed biomechanical tests and analysis, drafted the manuscript
Brian L. Grills	Conceptualised and designed the experiment, edited the manuscript, assisted with histomorphometric analysis
Tania Romano	Conducted pQCT
John D. Wark	Provided pQCT scanner
Terence J. O'Brien	Conceptualised and designed the experiment, edited the manuscript
Sandy R. Shultz	Administered the TBI, conceptualised and designed the experiment conducted open field, edited the manuscript
Stuart J. McDonald	Conceptualised and designed the experiment, edited the manuscript, assisted with pQCT analysis, assisted with biomechanical tests and analysis

In the case of Chapter 6, the nature and extent of my contribution to the work was the following:

Contributor	Statement of Contribution
Rhys D. Brady	Administered the fracture and TBI, collected tissue, cut sections, scanned bones and completed histomorphometric and $\mu$ CT analysis, drafted the manuscript.
Brian L. Grills	Conceptualised and designed the experiment, edited the manuscript, assisted with histomorphometric analysis
Jarrold E. Church	Conceptualised and designed the experiment, edited the manuscript
Nicole C. Walsh	Assisted with $\mu$ CT analysis.
Aaron C. McDonald	Assisted with TRAP stain
Denes V Agoston	Conceptualised and designed the experiment, edited the manuscript
Mujun Sun	Assisted with tissue collection
Terence J. O'Brien	Conceptualised and designed the experiment, edited the manuscript
Sandy R. Shultz	Conceptualised and designed the experiment, edited the manuscript, assisted in administering TBI.
Stuart J. McDonald	Conceptualised and designed the experiment, edited the manuscript